



**Doctorate program  
Milan  
EXPERIMENTAL  
MEDICINE**



# **Università degli Studi di Milano**

**PhD Course in  
Experimental Medicine**

**CYCLE XXXIV**

**PhD thesis**

---

**ATR controls the excitatory/inhibitory ratio in the  
central nervous system and its inhibition leads  
to anticonvulsant effects**

---

**Candidate: Dr. Clara Maria Cambria**

**Matr. R12365**

**Tutor: Prof. Flavia Antonucci**

**Director: Prof. Nicoletta Landsberger**

**Academic Year 2020-2021**

# TABLE OF CONTENTS

<b>TABLE OF CONTENTS</b> .....	<b>2</b>
<b>ABSTRACT</b> .....	<b>4</b>
<b>DISCLOSURE FOR RESEARCH INTEGRITY</b> .....	<b>7</b>
<b>ABBREVIATIONS</b> .....	<b>8</b>
<b>INTRODUCTION</b> .....	<b>11</b>
<b>ATR protein and Seckel Syndrome</b> .....	<b>12</b>
The structure of ATR .....	12
Atr gene mutations cause Seckel Syndrome .....	13
<b>Classical function of ATR</b> .....	<b>17</b>
ATR is responsible for ss-breaks repair .....	17
ATR controls cell-cycle checkpoints .....	20
Other nuclear functions of ATR.....	22
<b>Cytoplasmic functions of ATR</b> .....	<b>25</b>
Identification of novel ATR targets.....	25
Cytoplasmic ATR associate to synaptic vesicles .....	26
<b>Therapeutic ATR inhibition</b> .....	<b>29</b>
<b>Excitatory/inhibitory imbalance and epilepsy</b> .....	<b>32</b>
<b>AIM OF THE THESIS</b> .....	<b>34</b>
<b>EXPERIMENTAL PROCEDURES</b> .....	<b>36</b>
<b>Animals</b> .....	<b>37</b>
<b>Cell Cultures</b> .....	<b>37</b>
Primary cultures of neurons.....	37
Dissection and cultures of hippocampal neurons .....	37
In vitro AZD6738 treatment .....	38
<b>Cell cultures staining and analysis</b> .....	<b>38</b>
Immunocytochemical experiments.....	38
Tunel imaging assay .....	39
Image acquisition and analysis.....	39
<b>Western Blotting</b> .....	<b>40</b>
<b>Calcium Imaging</b> .....	<b>41</b>
<b>Cell culture electrophysiology</b> .....	<b>42</b>
Miniature post-synaptic currents (mPSCs) analysis .....	42
Multi-unit (MU) analysis .....	43
Long term potentiation (LTP) and depression (LTD) analysis.....	43
<b>Quantitative Real-time PCR</b> .....	<b>44</b>
RNA extraction and quantification.....	44
Reverse transcription and real-time PCR .....	44
<b>In vivo procedures</b> .....	<b>45</b>
In vivo AZD6738 injection .....	45
Behavioral analysis after systemic kainic acid.....	45

<b>RNA sequencing .....</b>	<b>46</b>
RNA Extraction and Library Preparation .....	46
RNA-seq analysis .....	46
<b>Statistical analysis .....</b>	<b>47</b>
<b>RESULTS.....</b>	<b>48</b>
<b>Characterization of the ATR kinase inhibitor .....</b>	<b>49</b>
<b>in neuronal primary cultures .....</b>	<b>49</b>
AZD6738 in vitro duration of action.....	49
AZD6738 safety profile.....	50
<b>Evaluation of acute effects induced by AZD6738 on neuronal development .....</b>	<b>52</b>
<b>Evaluation of functional changes induced by ATR inhibition in mature neurons.....</b>	<b>56</b>
Acute treatment in mature neurons .....	56
Chronic treatment in mature neurons.....	61
<b>Assessment of in vivo action of AZD6738.....</b>	<b>71</b>
AZD6738 in vivo duration of action.....	71
AZD6738 acts a master downregulator.....	72
ATR is involved in the control of transcriptional factors.....	76
<b>Evaluation of AZD6738 applicability as anticonvulsant drug .....</b>	<b>78</b>
AZD6738 anticonvulsant effects in the kainate mouse model.....	78
Controlled Egr1 levels in AZD6738 treated mice and related consequences .....	80
<b>Evaluation of possible ATR involvement during aging .....</b>	<b>84</b>
<b>DISCUSSION .....</b>	<b>87</b>
<b>ACKNOWLEDGMENTS .....</b>	<b>94</b>
<b>REFERENCES.....</b>	<b>95</b>
<b>LIST OF FIGURES.....</b>	<b>116</b>
<b>DISSEMINATION OF RESULTS.....</b>	<b>124</b>

## **ABSTRACT**

ATR (ATM and Rad-3 related) is a kinase protein of approximately 301 KDa, mainly known for its nuclear function played in proliferating cells. Indeed, in these cells it is recruited and activated at the site of DNA damage, promoting the phosphorylation of numbers of substrates directly involved in the cell cycle regulation and DNA damage repair, such as CHK1, p53 and BRCA1. Mutations in the *Atr* gene are responsible for the onset of the Seckel Syndrome (SS), an autosomal recessive disorder mainly characterized by intrauterine growth retardation, craniofacial abnormalities, dwarfism, chromosomal instability and mental retardation. Recent studies have revealed a much wider role of ATR, in particular it is present into the neuronal cytoplasm participating in the regulation of the synaptic vesicles trafficking; also, genetic deletion of the protein seems to be responsible for an increased excitatory activity and subsequently for the onset of sporadic non-lethal epileptic seizures in 12 months-old mice. Therefore, the abnormal synaptic transmission due to ATR mutations could partially explain the neurological dysfunctions found in SS patients. Despite the evidence related to the genetic deletion of ATR, up to now, no data regarding the pharmacological inhibition of ATR kinase activity have been provided. Thus, in this thesis, we aimed at filling this scientific gap investigating the impact mediated by a specific ATR kinase activity blocker on hippocampal function and neuronal transmission. This drug can penetrate inside the brain and it is currently involved in oncological pre-clinical studies, indeed it prevents the ATR-mediated signaling and inhibit the DNA damage checkpoint activation, promoting cancer cells apoptosis. Hence, hippocampal neuronal cultures have been treated with the ATR inhibitor in the attempt to block the ATR pathway and study related consequences at different stages of neuronal maturation. The treatment was administered both in acute, a single day treatment, and in chronic, one-week protocol. First of all, Ca<sup>2+</sup> imaging experiments in 7 DIV neurons demonstrated that reduced ATR activity in immature neurons has no impact on the GABAergic development. Subsequently, electrophysiological and immunofluorescence experiments in mature hippocampal neurons revealed that both acute and chronic ATR inhibition are responsible for neuronal transmission defects, inducing a marked imbalance between excitation and inhibition, thus favoring the establishment of a more inhibited tone. Also, synaptic plasticity was found affected, resulting in defective long term potentiation and depression. Real time PCR experiments performed in vitro and RNA

sequencing in vivo were useful to investigate the molecular mechanism at the basis of the defects here described. In particular, data collected by both these approaches suggest the immediate early gene *Egr1* as one of the main factors deregulated by ATR inhibition. Importantly, several findings describe *Egr1* as a key transcriptional regulator of genes contributing to the development of hyperexcitability during epileptogenesis. Also, increased *Egr1* expression levels have been detected in hippocampal biopsies collected from epileptic individuals. Thus, we evaluated the effect mediated by pharmacological ATR inhibition in a mouse model of acute seizures and, coherently, we found a strong anticonvulsant effect. These results highlight ATR as a novel target in acute seizures onset and the ATR inhibitor as an innovative therapeutic tool in neurological disorders characterized by increased excitability. As a matter of fact, RNA profiling also unveiled similarity with other conventional antiepileptic drugs. Altogether, our data demonstrating that ATR kinase inhibition prevents the hyperactivity-induced *Egr1* expression nicely fall with the recent theory of “master regulators candidates” in epilepsy, given that among the transcriptional activators and repressors suggested there is *Egr1*.

On the other hand, we performed biochemical investigations of the active ATR levels in the attempt to monitor changes of ATR activity along life. Data obtained from mouse and human hippocampal tissues collected at increasing age display a reduction of the phosphorylated ATR (the active form of the protein) suggesting that ATR levels variations participate in the establishment of cognitive defects during the physiological aging. It remains to investigate the role of *Egr1* in this field. Overall, the results collected in this thesis suggest a novel role of ATR in the maintenance of the proper neuronal transmission and plasticity in mature hippocampal neurons and highlight ATR inhibition as an important therapeutic tool for neurological disorders characterized by hyperexcitability.

## **DISCLOSURE FOR RESEARCH INTEGRITY**

I certify that during my PhD project all the procedures have been conducted according to the European Code of Conduct for Research Integrity.

All the research procedures have been designed, carried out and analysed carefully, in an adequate design frame and in a rigorous and accurate fashion. The results obtained have been presented in this thesis in an open, honest and transparent manner and the methodologies performed explained to be reproducible.

Animals used in this research have been handled with respect and care, applying the 3Rs principles (replacement, reduction and refinement) and relieving excessive suffering, in accordance with legal and ethical provisions.

The supervisor reviewed the final draft of this thesis and is aware of its submission for examination.

## **ABBREVIATIONS**



ADD: ATR-activation domain  
AED: anti-epileptic drug  
AMPAr: AMPA receptor  
ANOVA: analysis of variance  
ASD: autism spectrum disorder  
ATM: Ataxia Telangiectasia Mutated  
ATR: ATM and Rad-3 related  
ATRIP: ATR interacting protein  
BCA: bicinchoninic acid  
CDC-: cell division cycle -  
CDK-: cyclin-dependent kinase -  
CHK1: checkpoint kinase 1  
CNS: central nervous system  
DDR: DNA damage response  
DEG: differentially expressed genes  
DIV: days in vitro  
DNA-PKcs/DNA-PK: DNA-dependent protein kinase catalytic subunit  
DSB: DNA double strand breaks  
dsDNA: double-stranded DNA  
E/I: excitatory/inhibitory  
ETAA1: Ewing tumor-associated antigen 1  
FANCD2: Fanconi-anemia protein  
FAT: Frap/Atm/Trrap  
FATC: FAT-carboxyl terminal  
GSDB: goat serum dilution buffer  
HEAT: Huntington, elongation factor 3, protein phosphatase 2A, TOR1  
Hz: hertz  
IP: intraperitoneal  
IQ: intelligence quotient  
KA: kainic acid  
KRH: Krebs'-Ringer's-Hepes  
LAD: lamina-associated domain  
LTD: long term depression  
LTP: long term potentiation

mEPSC: miniature excitatory post-synaptic current  
mIPSC: miniature inhibitory post-synaptic current  
MRN: MRE11 – RAD50 – NBS1  
MU: multi-unit  
ND: neurodevelopmental disorder  
NGS: next generation sequencing  
NPC: neuronal progenitor cell  
P90: post-natal day 90  
PARP: poly ADP-ribose polymerase  
pATR: phospho-ATR  
PCA: principal component analysis  
PIKK: phosphoinositide 3-kinase-related kinase  
Pol  $\alpha$ : DNA polymerase  $\alpha$   
Pol  $\epsilon$ : DNA polymerase  $\epsilon$   
PRD: PIKK regulatory domain  
PROT: sodium-dependent proline transporter  
RHINO: RAD9, RAD1, HUS1 interacting nuclear orphan  
RPA: replication protein A  
SD: standard deviation  
SDS-PAGE: Sodium Dodecyl Sulphate - PolyAcrylamide Gel Electrophoresis  
SLE: seizure-like event  
SNARE: Snap Receptor  
SS: Seckel Syndrome  
SSB: DNA single strand breaks  
ssDNA: single-stranded DNA  
SYT1: synaptotagmin-1  
SYT2: synaptotagmin-2  
TERT: telomerase reverse transcriptase  
TOPBP1: Topoisomerase II Binding Protein 1  
TTX: tetrodotoxin  
UV: ultraviolet radiation  
VAMP2: vesicle-associated membrane protein 2  
VOCC: voltage operated calcium channels

# **INTRODUCTION**

## Chapter 1

### ATR protein and Seckel Syndrome

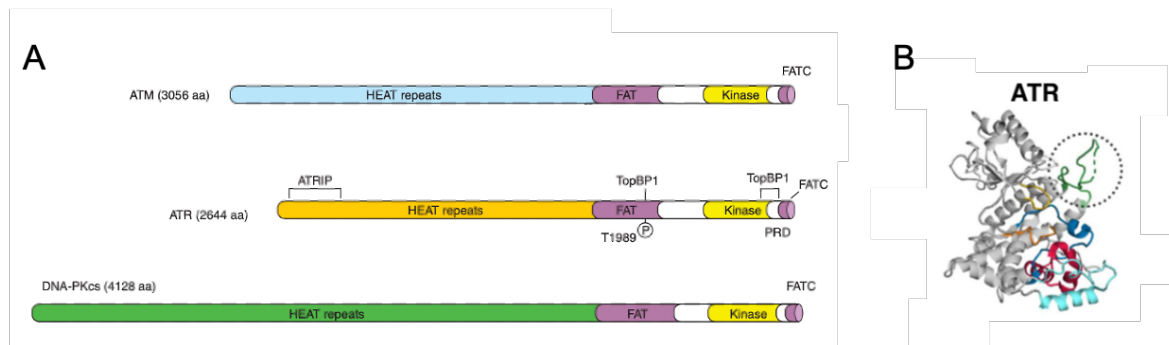
#### **The structure of ATR**

The ATR (ATM and Rad-3 related) protein is encoded by the gene *Atr*, localized on the chromosome 3 (3q23) [1].

ATR is a serine-threonine kinase of high molecular weight of approximately 301 kDa, mainly found in big protein complexes. This protein is well conserved during development and indeed it has been found in all eukaryotes examined for now, such as *Saccharomyces cerevisiae*, *S. pombe*, *D. melanogaster* and *A. thaliana* [2]. The discovery of ATR date back to 1996, when two different groups [3, 4] successfully described the cloning of the total protein; this allowed to identify the last of the three vertebrate proteins establishing the DNA damage response (DDR) belonging to the phosphoinositide 3-kinase-related kinases (PIKKs) family, with principal roles in activating the DDR [5]. The ATR structural organization is very similar to the structural sequence of the other members of this group, the proteins ATM (Ataxia Telangiectasia Mutated) and DNA-PKcs (DNA-dependent protein kinase catalytic subunit). Thus, the catalytic domain (about 300 aa) is located in proximity of the carboxyl termini and flanked by two conserved domains: FAT (Frap/Atm/Trrap) and FATC (FAT-carboxyl terminal); both these two domains play significant regulatory functions: during ATR activation, FAT is phosphorylated on the Thr-1989, whereas FATC is fundamental for the proper ATR kinase activity. The internal region is composed by numerous  $\alpha$ -helical HEAT (Huntington elongation factor 3 protein phosphatase 2A- TOR1) repeats, responsible for protein-protein interactions and so for the correct protein functioning. As an example, the  $\alpha$ -helical HEAT repeats are involved in the ATR-ATRIP (ATR interacting protein) bond, fundamental in the DDR pathways [6]. Finally, located in between the catalytic domain and the FATC region, it is present the PRD (PIKK regulatory domain) domain, which is also involved in the modulation of ATR activation. These kinases transfer phosphate groups preferentially to protein rather than lipid substrates. In particular, the catalytic domain phosphorylates SQ and/or

TQ motif: serine or threonine followed by a glutamine; these motifs are recognized as consensus motif by the kinases [7].

ATR displays the important function of checkpoint signaling activator upon genotoxic stress or DNA replication stalling, thereby it acts as DNA damage sensor [8]. Indeed, its structure presents amino-terminal substrate-binding domains, which recognize and bind the substrate consensus sequence (SQ/TQ motifs) in proteins such as BRCA1, RAD17 and p53 [9, 10]. Deletion of *Atr* in mice results lethal, indicating that it is an essential gene and indeed loss of ATR protein or function compromises the DNA damage repair, fragile site stability and centrosome duplication [11, 12]. Defects in the *Atr* gene cause Seckel Syndrome [13]. This is a developmental disorder characterized by primordial dwarfism, microcephaly, craniofacial abnormalities and mental retardation.



**Figure 1:** a) ATR, ATM and DNA-PKcs are large proteins belonging to the PI3K superfamily. They are characterized by the presence of similar domains: FAT, the catalytic domain and FATC, all located near the carboxyl termini. Here are also shown the ATR regions recognized by the proteins ATRIP and TOPBP1, fundamental during modulation of ATR activation. Image from Marechal and Zou, 2013. b) Three-dimensional structure of ATR; the kinase domain is green colored and circled. Image from Williams et al., 2020.

### ***Atr* gene mutations cause Seckel Syndrome**

Genes involved in the DNA damage response are essential for the maintenance of genomic integrity: indeed numerous disorders associated with failures in development have been linked to DDR genes mutations [14]; classical examples are represented by BLM in the Bloom's syndrome, NBS in the Nijmegen breakage

syndrome, ATM in the Ataxia-Telangiectasia and ATR responsible for the onset of the Seckel Syndrome [15].

Seckel Syndrome (SS) is a rare autosomal recessive disorder that belongs to a group of microcephalic primordial dwarfism syndrome [16]. It is characterized by a wide range of symptoms, among which: intrauterine growth retardation, microcephaly, unique facial features (large eyes, beak-like nose and receding lower jaw), proportionate dwarfism, mental retardation, brain abnormalities and chromosome instability at fragile site [17]. It is characterized by genotypic and phenotypic heterogeneity and, for this reason, some patients can show additional clinical findings, such as cleft palate, pancytopenia, ocular manifestations, abnormalities in dentition and limb anomalies [18]. Indeed, ultimately, in 2020 the Matos-Rodrigues et al. [16] showed how the ATR-ATRIP complex is essential for the maintenance of retinal integrity and so for a proper visual function, suggesting a causal relationship between the death of progenitor cells due to a defective replication stress response and a central nervous system (CNS) dysfunction and in turn elucidating the neurodevelopmental defects in a model of Seckel Syndrome. SS patients, differently from those affected by other DNA repair-deficiency disorders, do not present ataxia or immunodeficiency, while the characteristic intellectual disability is usually moderate to severe, with full-scale IQ scores below 50 in 50% of affected individuals [19]. Brains of SS patients are often characterized by morphological alterations, such as agenesis of corpus callosum with depletion of astrocytes, presence of cysts, dysgenetic cerebral cortex and hypoplasia of the cerebellar vermis, suggesting that neural migration abnormalities could be responsible for the mental retardation [18, 19].

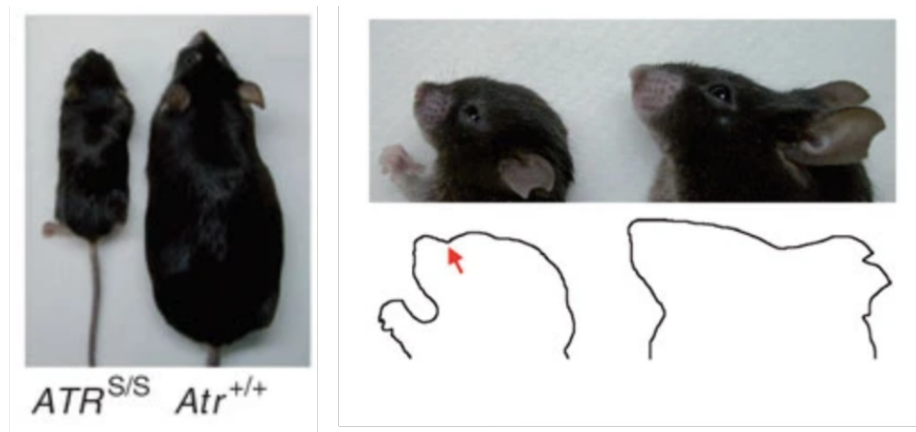
This syndrome was firstly described as “dwarfism bird head” in 1892 by Rudolf Virchow, but only in 1960 Seckel, based on 2 cases studies in Chicago and 13 cases of microcephaly dwarfs, properly characterized it as it is currently described in literature. Diagnosis is mainly based on clinical findings and precocious brain imaging that shows a reduced brain volume with grossly normal architecture, in fact the microcephaly is characterized by onset during the second trimester of gestation. Prenatal diagnosis is still extremely rare, even though few cases of Seckel Syndrome had been diagnosed via combination of two- and three-dimensional sonography at 21 weeks’ gestation [22]. This approach seems able to prenatally unveil the classical signs characteristic of the syndrome, such as

abnormal fetal head appearance, fetal growth restriction and microcephaly [22–24]. The clinical delineation of this disorder has been for now contradictory and, as a result, SS is overdiagnosed and probably fewer than one-third of reported case are truly affected with the syndrome and appear to fulfil the criteria originally set by Seckel [26].

The classical Seckel phenotype is caused by mutations in genes involved in basic processes controlling the DNA integrity and the cell cycle checkpoints [27]. The phenotypic heterogeneity is generated by the variety of factors and genes involved in the onset of the disease. Among causative genes, the first identified and one of the most important is *Atr*. Patients in which *Atr* is found mutated are characterized by a severe form of microcephaly (head circumference -12 SD; height -5 SD) due to deficiency in signaling and damage responses mediated by the protein ATR [28]. In particular, the pathological phenotype is associated to reduced level of the protein whereas its total absence is responsible for early embryonic lethality and thus it is inconsistent with life [11]. A synonymous mutation responsible for a single base change (2101A>G) has been discovered to determine the loss of exon 9 and aberrant splicing of the gene *Atr*, in turn resulting in a severe ATR hypomorphism, although can also be found homozygous mutations that reduce the ATR translation due to premature termination of the mRNA [28].

Cell lines obtained from SS-ATR mutated patients display characteristic abnormalities, such as lower level of the protein ATR, impaired DNA damage response and phosphorylation of ATR substrates and defects in the ATR-dependent G2/M checkpoint arrest. In addition, those cells also exhibit a range of aberrant responses to agents that cause replication stalling, such as nuclear fragmentation and supernumerary centrosomes in mitotic cells [13, 26]. It was also possible to differentiate SS-iPSCs into neuronal progenitor cells (NPC) in order to better understand the pathophysiology of the syndrome. Indeed, it was found that ATR mutation causes different patterns of exon 9 splicing in a cell type-specific manner, with a prevalence of abnormal mitotic events in SS-NPC which could be responsible for the impaired structural organization during brain development [29]. Recently, also mouse models of the syndrome have been developed and the animals well recapitulates the human disease. In addition to the overall appearance, they are characterized by chromosomal instability, senile appearance, pancytopenia and microcephaly [20, 29]. These models result very

practical for genetic studies of the ATR function in mammals and, more importantly, refocused the attention on an aspect of the syndrome which is often set aside, but still it is present in many of SS patients. Indeed,  $ATR^{SS}$  mouse models - obtained either inducing the exon 9 skipping [30] or through lentitransgenesis [14] - show, in addition to the classical Seckel symptomatology, also signs of premature aging: cachexic appearance, hair graying, kyphosis, osteoporosis, accumulation of fat in the bone marrow, pancytopenia, decreased density of hair follicles, thinner epidermis and shorter life expectancy. Altogether, these phenotypes indicate the development of a progeroid symptoms and, accordingly, the Seckel Syndrome can be accounted both as a neurodevelopmental and as a progeroid disorder. In support of this further definition of the Seckel Syndrome, it was found that in vitro  $ATR^{SS}$  fibroblast show a reduced replicative capacity, a typically aged morphology and activate the MAPK p38 pathway [31], which is known to be responsible for the premature senescence present in the Werner syndrome, one of the most studied progeroid disease [31, 32]. One possible explanation of this progeroid phenomenon is that loss of cells during embryogenesis due to ATR deficiency can compromise the stem cell niche and that additional exposure to DNA damage could initiate a progeroid program that drives young animals into senescence [14, 29].



**Figure 2:** Representative pictures of  $Atr^{S/S}$  and  $Atr^{+/+}$  mice at three months of age. The SS mouse model well recapitulate all the classic features characteristic of the human syndrome: severe dwarfism and disproportionate decrease in the dimension of the head are evident in  $Atr^{S/S}$  mouse in contrast to control mouse. Image from Murga et al., 2009.



## **Chapter 2**

### **Classical function of ATR**

#### **ATR is responsible for ss-breaks repair**

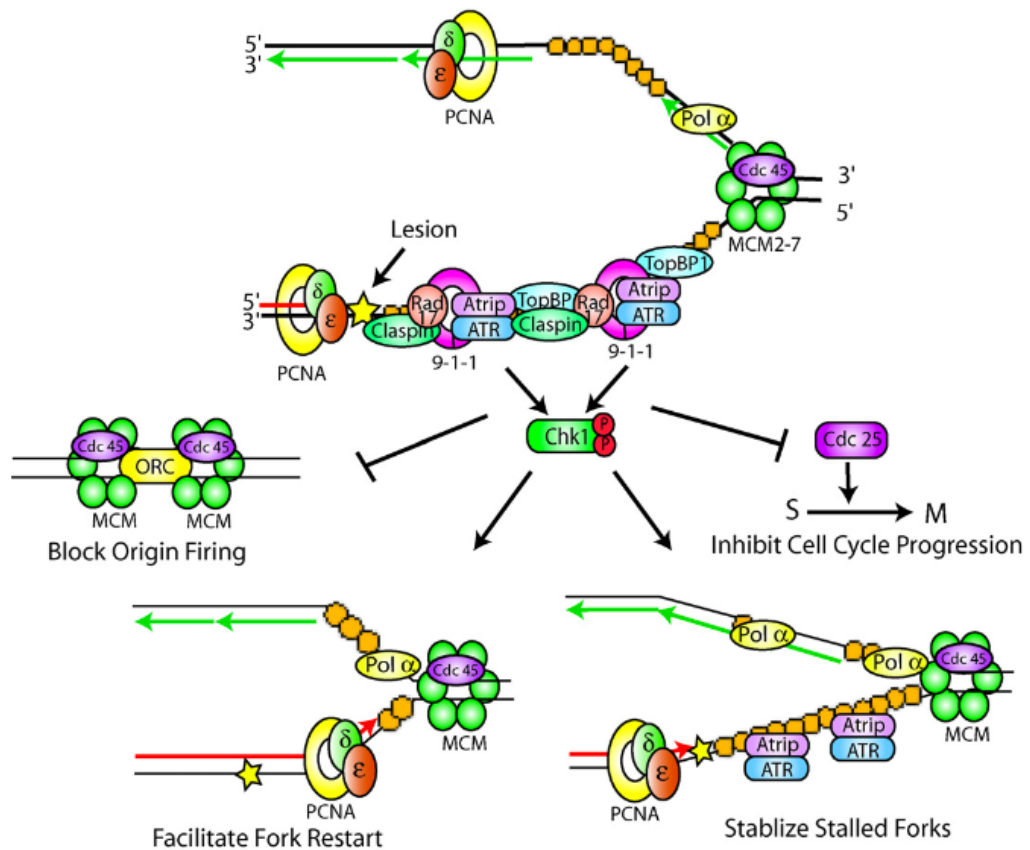
A fundamental role and one of the most described function played by the ATR protein is its involvement in the response against replication stress and DNA damage. In particular ATR responds to DNA single strand breaks (SSB) that occur mainly during the S and the G<sub>2</sub>/M phase of the cell cycle [34]. In addition, the protein takes part to other important pathways: in collaboration with the kinase protein ATM, which repairs DNA double strand breaks [34, 35]; ATR is also involved in the meiosis and inter-strand crosslink repair, in the long-term maintenance of telomeres and in the response to mechanical and osmotic stress [36–38]. Since ATR plays these important functions for the proper conservation of DNA, loss of this protein leads to accumulation of SSBs, replication fork collapse, chromosomal rearrangements and gene loss. Different type of genotoxic stress are responsible for activation of the ATR protein, as the ultraviolet radiation (UV), ionizing radiation (X-rays and  $\gamma$ -rays), hypoxia, dNTPs depletion, hydroxyurea, DNA polymerase inhibitors and chemotherapeutic drugs [34]. These stress agents induce slowing or even stalling of the DNA polymerase and thus collapse of the replication fork.

In case of fork stalling, ATR is recruited, activated and starts the signaling cascade blocking the cell cycle progression, downregulating late origin firing, stabilizing and facilitating the restart of the collapsed replication fork [1]. Activation of the ATR signaling cascade occurs consequentially to different type of DNA lesion or to the formation of protein-DNA structures that are responsible for the fork progression arrest; thus, ATR must be able to recognize all these different intermediates. Single-stranded DNA (ssDNA) is the most common structure primarily identified that triggers the amplification of an emergence signal. The ssDNA is generally formed by the continued unwinding of the DNA by the replicative helicase in case the leading and/or the lagging strand polymerase are stalled; this is a structure highly unstable and thus, in order to preserve the single filament, it is bound by the stabilizing ssDNA binding protein RPA (replication protein A) [1, 33, 39]. The

second structure RPA-coated ssDNA works as a recruiting platform for all the proteins and factors involved in the response.

Among the first proteins recognized at the DNA site there is ATRIP, the ATR-interacting protein, which mediates the recruitment of ATR at the region involving DNA damage [41]. Even if the RPA-ssDNA can recruit the ATR-ATRIP complex, to completely activate the ATR kinase it is necessary the presence of other activating proteins [42]. In vertebrates, two are the main activators already identified and studied: the topoisomerase II binding protein 1, also known as TOPBP1, and the Ewing tumor-associated antigen 1, also known as ETAA1; both these two protein present an ATR-activation domain (ADD) through which they are able to bind the ATR-ATRIP complex [42–44].

In addition to ssDNA, other anomalous structures inducing ATR activation are endogenous replication fork barriers, mainly represented by DNA-protein complexes, secondary DNA structures (i.e. hairpins of repeated DNA sequences) and fragile site, thus chromosomal regions characterized by late replication in the S phase and gaps and breaks in metaphase chromosomes [1, 45, 46, 48]. It has been observed an increased expression of fragile sites in absence of ATR or of some of its effectors. In particular, most of the downstream effects mediated by the ATR signaling cascade are controlled by the checkpoint kinase CHK1: indeed, once ATR is active and functioning, it firstly phosphorylates CHK1 on S317 and S345 [1, 45, 49]. The adaptor protein Clapsin is involved in this activating process, bringing ATR and CHK1 together and thus allowing a more efficient reaction [46, 50]. Once activated, CHK1 spreads the signal for a proper damage response to the rest of the nucleus, phosphorylating its own substrates: in particular the message mediated by this kinase is responsible for a reduced replication and cell cycle progression, thus allowing time for repair to occur [45, 49].



**Figure 3:** Model of replication checkpoint activation and function. In case of DNA lesion, the polymerase and the helicase on the opposing DNA strand will continue to unwind and synthesize new DNA, leading to ssDNA accumulation. The ssDNA recruits the ATR-ATRIP complex and immediately after several other replication checkpoint proteins for the activation of ATR and CHK1 (the ATR effector protein), promoting genomic stability by blocking the cell cycle progression and new origin firing, stabilizing and facilitating the replication fork restart. Image from Paulsen and Cimprich, 2007.

### **ATR controls cell-cycle checkpoints**

The activation of cell cycle checkpoints in case of DNA damage and replication stress is a fundamental step for the survival of the cell; in this scenario ATR is a key regulator, controlling and regulating the cellular checkpoints [46, 54]. Activation of protein belonging to this class guarantees the maintenance of genome integrity and, in case of abnormalities or errors, the promotion of a signaling cascade resulting either in the arrest of the cell cycle in order to prevent replication and fixation of potentially fatal DNA mutations or in programmed cell death, or apoptosis, when the DNA damage is too extended [47]. Interruption of the cell cycle can occur at different stages: in G<sub>1</sub> and S phase to avoid aberrant DNA replication and prior to mitosis to prevent segregation of damaged chromosomes. As a matter of fact, abortion of some of these mechanisms results in genomic instability and cancer predisposition.

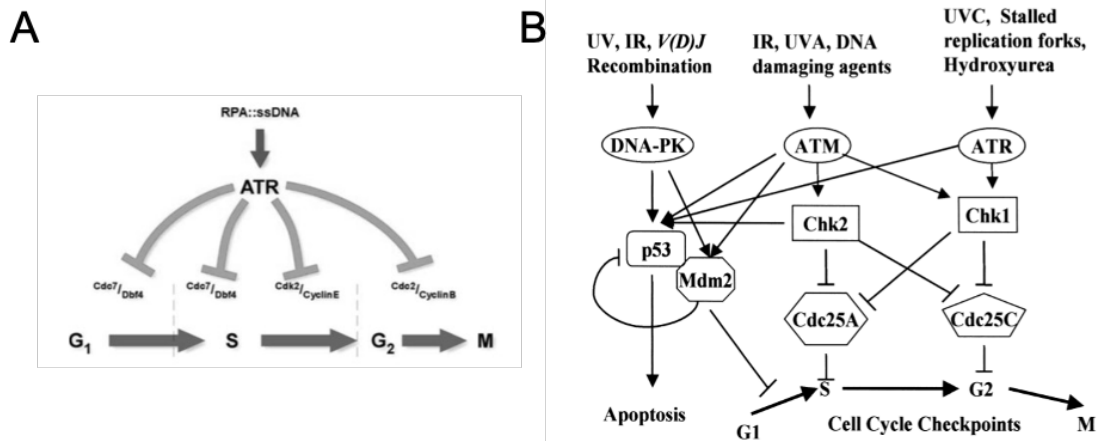
It has been shown that the ATR protein controls in particular checkpoints of the S and G<sub>2</sub> phase of the cell cycle, but also it is involved in the regulation of the G<sub>1</sub> phase in collaboration with the kinase ATM [55, 56]. Indeed, ATM belongs to the same PI3K superfamily and in particular is known to start and coordinate the signaling cascade in response to DNA double strand breaks (DSB) and, similarly to ATR, to regulate the cell cycle checkpoints. In existence of DSB, ATM is recruited at the site of DNA damage and then induces its autophosphorylation, sustained by the presence of coactivator proteins belonging to the MRN complex (Mre11, Rad50 and Nbs1) [54]. When ATM is fully activated, it phosphorylates the direct effectors responsible for the DNA damage response and regulation of the cell cycle: some of the most relevant targets to mention are represented by p53, which controls the G<sub>1</sub>-S checkpoint; NBS-1, responsible for the arrest of the cycle in the S phase; H2AX, regulating the DNA repair machinery [57, 58].

Starting from the cell cycle progression from the S phase, ATR regulates the kinase complexes Cdc7/Dbf4 and Cdk2/Cyclin E that are fundamental for the cycle transition. When these two complexes are activated, it is favored the entry of Cdc45, the Mc helicase activation and so the promotion of DNA replication [56]. During the normal progression of the cell cycle, the Cdc7 protein is active when interacting with the counterpart Dbf4; Cdk2 instead is inactive due to the presence of a phosphate group on the tyrosine-15 and only when the phosphatase CDC25A removes it Cdk2 can actually become activated. Differently, when replication stress

occurs, CHK1 (as mentioned above, the first ATR target and effector) directly phosphorylates CDC25A that is then ubiquitinated and destroyed, avoiding in this way the Cdk2 activation. In addition, ATR itself induces the detachment of Cdc7 from Dbf4. Overall, the straight results is blockage of the cell cycle progression to the G<sub>2</sub> phase [56].

In case of DNA damage during the G<sub>1</sub> or the S phase of the cycle, the promotion to mitosis is aborted through the CHK1 phosphorylation of the factor CDC25C. Indeed, this protein is sequestered from the nucleus to the cytoplasm and thus cannot dephosphorylate and activate the kinase B-Cdc2, responsible for the advancement from G<sub>2</sub> phase to mitosis [57].

Ultimately, in collaboration with the kinase ATM, ATR is also involved in the cell cycle arrest during the G<sub>1</sub> phase [56]. Extensive DNA damage is responsible for an increased expression of the tumor suppressor protein p53, which is activated by phosphorylation of both ATR and ATM. Interestingly, the activity of these two protein is time-dependent: during the early phase of the damage response it is mainly involved ATM, whereas ATR play a more significant role in the late phase. Indeed, in case of DNA double strand breaks ATM is rapidly recruited, starting the cascade which mediates the cell cycle arrest and DNA repair. Key step of the signaling cascade is the phosphorylation of the tumor suppressor protein on the serine-15. As the DNA repair is in place, it is generated an intermediate form – probably constituted in part of dsDNA and in part of ssDNA – which is better recognized by ATR; thus the kinase is recruited and phosphorylates twice again p53 on serine-15 and -37. In this way, ATR sustains and maintains active during time the response started by ATM [9]. When the tumor suppressor protein is phosphorylated and becomes active, it functions as transcription factor inducing the expression of p21. Increased p21 levels inhibit both the cyclin E and cyclin A and consequently their partner Cdk2. Taken together these changes, they are responsible for the cell cycle stall in G<sub>1</sub>, preventing progress in the S phase [7]. It is largely known that p53 controls the expression of a wide number of genes apart from p21; thus, depending on the cellular context and on the vastity of the DNA damage, it may sustain the cell cycle arrest with DNA repair or on the contrast the cell programmed death pathways [58].



**Figure 4:** a) ATR responds to RPA-bound ssDNA and regulates the cell cycle progression. Image from Gautier et al., 2004. b) The signaling pathway involving ATR, ATM and DNA-PK following DNA damage. Once activated, these kinases phosphorylates several downstream effectors leading to cell cycle arrest and in some cases also apoptosis. Image from Yang et al., 2003.

### Other nuclear functions of ATR

It has been demonstrated by several new studies that the protein ATR plays a much wider activity in the cell, in addition to its classical involvement in the signaling cascade of the DNA damage repair. The three most described unconventional roles of ATR are the meiotic silencing, the maintenance of telomeres and the perinuclear chromatin regulation [36–38].

#### Meiotic silencing

The pairing of the maternal and paternal homologous chromosomes during meiosis is a fundamental step of cellular division and importantly during this step can occur crossover of genetic material, that assure remixing and novelty in the genetic background. The presence of aneuploidy gametes is an event to be avoided in order to reduce the risk of severe life threatening mutations; thus, cells that presents defects of this process, either errors in chromosomes synapsis or recombination, must be destroyed from the germ cell pool [59]. Mechanisms of

meiotic surveillance are fundamental at this extent and one of these is represented by the meiotic silencing: a failure in the chromosomes pairing is responsible for transcriptional inactivation of the genes they carry during the whole process of meiosis [60]; if the meiotic silencing persists and the error is not corrected, germ cells result lacking of essential gene products and thus this determines their elimination.

The ATR protein has been found localizing to unpaired chromosomes, thus suggesting its involvement in the process of meiotic silencing [37, 65]. In particular, ATR cooperates with proteins such as TOPB1, BRCA1 and ATRIP and control the expression of some silencing factors, among which HORMAD1/2. Indeed, HORMAD1 and HORMAD2, during the zygotene phase, recognized the unsynapsed chromosomes through a BRCA1-dependent mechanism. ATR is then recruited at the same site and stimulates the accumulation of HORMAD1, HORMAD2, BRCA1 and other factors involved in the process at the silencing site [62]. This is a very delicate process, which must be dynamic and flexible since if the correct chromosome homologs pairing is finally achieved, all the silencing factors must rapidly remove and the meiotic silencing reverted. On the contrary, in case the unsynapse condition persists, ATR guides the establishment of repressive post-translational modifications that are responsible for irreversible gene silencing [63]. Among the targets recognized for the onset of those modifications it is present the histone H2AFX, which is phosphorylated by ATR leading to gene inactivation. [64].

### Maintenance of telomeres

Maintenance of chromosome integrity is a hallmark for the correct conservation of the genomic pool, thus it is essential that the natural end of each chromosome is not mistaken for DNA damage sites. In this context, the presence of telomeres assures the protection of the whole chromosomes integrity. Telomeric DNA is constituted by TTAGGG repeats that together with the Shelterin complex prevents the recruitment of whichever repair mechanism preserving genome integrity [65]. In order to do this, the complex arranges the telomeres in a t-loop structure that is able to hide the telomere terminus in the core of the structure. The protein ATR seems to be involved exactly in this process of t-loop formation, during replication of both lagging and leading telomeres. Unfortunately the complete mechanism is

not fully understood yet [66]. Coherently, patients affected by the Seckel Syndrome are characterized by increased telomeres instability both during and after telomeres replication [67].

#### Mechanical and osmotic stress

It has been shown that ATR directly protects the perinuclear chromatin for mechanical insults that can result as consequence to a large diversity of osmotic and mechanical stimuli [39]. A classical example is represented by the topological stress derived from the chromatin condensation and replication, which can be then converted in mechanical stimuli. In this context, ATR plays a role in the control of chromatin association to the cytoskeleton organization and the lamin A [68]. When hyperosmotic conditions are present, the whole cell and its nucleus may contract thus leading to disarrangement of the nuclear envelope and chromatin condensation. On the opposite case, hypotonic stress may be responsible for cell swelling and membrane tension and again leading to alteration of the chromatin structure and potentially to DNA breaks [69]. In turn, both the hypertonic and the hypotonic states lead to ATR and, then consequently, CHK1 activation. In particular, ATR recognized the nuclear envelope and activate its signaling cascade in a way that is totally independent from the DNA damage response [70]. A similar re-location of the protein is also present in case of strong mechanical stimulations that act on the plasma membrane leading to cell compression and chromatin rearrangements, such as compaction and decompaction [39]. During this process the response played by ATR does not require its kinase activity, in contrast to activation of DNA response [68]. The signaling promoted in this case facilitates processes of chromatin condensation, resolving newly formed structures such as lamina-associated domains (LADs) and avoiding cell deformation [71]. De facto, lack of ATR activity is responsible for aberrant chromatin rearrangements which could fall in severe consequences for the cell.



## **Chapter 3**

### **Cytoplasmic functions of ATR**

Mutations of ATR are responsible for the onset of the neurological disease known as Seckel Syndrome [19], as it has already been described in the chapter 1. Most of the clinical phenotypes characteristic of the disease can be ascribed to deficiencies in the DNA damage repair machinery, however neurodegeneration, neuronal dysfunctions and microcephaly cannot be totally explained [72]. This led to identification of novel additional functions of the protein ATR besides DDR, both in the nucleus and in the neuronal cytoplasm.

#### **Identification of novel ATR targets**

Up to now, the complete set of ATR targets is still largely unknown, but it has been demonstrated that most of them often contain clusters of S/TQ motifs, which constitutes the so called SCD domain [73]. Indeed, looking for proteins enriched in those domains, now researchers are trying to identify novel targets of the kinase [74]. Interestingly, ontology analysis revealed overrepresentation of conserved SCD-containing proteins in pathways related to vesicles-Golgi trafficking, actin cytoskeleton and neuronal development, of course in addition to proteins involved in the DNA damage machinery, regulation of DNA replication and control of the cell cycle [75]. Thus, this finding suggests a direct involvement of the kinase ATR in controlling these new different processes, laying the bases for a clearer explanation of neurological defects in patients affected by Seckel Syndrome.

Targets newly identified comprehend proteins responsible for the Golgi maintenance, among which GCC1, USO1 and GOLGA2, for the formation of clathrin-associated adaptor protein complex and the SNARE complex. Also, proteins involved in the anchoring of vesicles to the actin cytoskeleton have been identified [83, 84]. Taken together, these data strongly demonstrate the importance that ATR plays in the vesicles trafficking and in the neurotransmitter vesicles transport to the synapses. In addition, in the central nervous system ATR seems to regulate several transcription factors. Among the novel candidates proposed, there are DLX1, which control the forebrain development [77]; TRB1, responsible

for the cortical development [78]; POU6F1, involved in the pituitary development [79]; and BSX, which is a brain-specific homeobox protein [80]. In all these proteins, the SCD domain has been found either in the DNA-binding domain or within the transactivation domain. Furthermore, cytoplasmic portion of many receptors controlling the axon guidance process, a fundamental mechanism during the development and differentiation of the neuronal network, present the SCD domain [75]. Receptors belonging to these class are able to modulate axon attraction and repulsion and neuronal migration during the different differentiation steps because can recognize signals promoting rearrangements of the actin cytoskeleton, released by protein such as semaphorins or netrins [89; 90]. Hence, these new studies point to a much wider role of the protein kinase ATR in the control of cellular processes, proposing a strong relevance in the development and maintenance of neuronal functions.

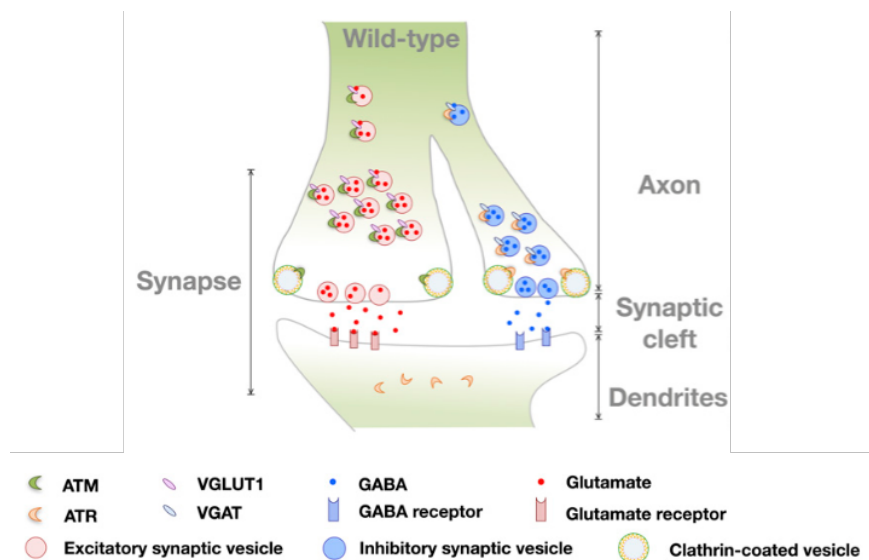
### **Cytoplasmic ATR associate to synaptic vesicles**

Recent findings describe the role of ATR into the cytoplasm of post mitotic neurons, especially in mechanisms of synaptic vesicles trafficking but, up to now, the role of this protein in the neuronal context is still under evaluation and some discrepancies about its functioning are emerged.

It was firstly described that into the neuronal cytoplasm ATR associates to a variety of vesicular proteins as  $\beta$ -adaplin and clathrin, both involved in the synaptic vesicles endocytosis, suggesting a new ATR role in the process of vesicles endocytosis [91, 92]. Indeed, knocking down ATR, the vesicle release properties are altered as displayed in cortical neurons where ATR-deficiency leads to a reduced vesicles release and lower synaptic density [83], thus demonstrating that ATR is fundamental for the maintenance of a normal functionality and density of the synaptic compartment.

According to the work of Cheng at al. (2017) the distribution of ATR at the synapse is wide and in fact it was found in close proximity both to presynaptic proteins, such as VAMP2, Synapsin-1 and Bassoon, and to postsynaptic proteins, as for example PSD95. In addition, ATR seems to associate also with chromogranin A, which is a cargo protein found in large dense core vesicles [85].

Importantly, VAMP2 (Vesicle-Associated Membrane Protein 2), also known as Synaptobrevin2, belongs to the SNARE complex for the synaptic vesicles fusion with the cellular membrane and the release of neurotransmitter at the chemical synapse [94, 95]. Synapsin-1 is instead a linker protein that maintain stable and ready releasable the reserved pool of synaptic vesicles in the cytoplasm; it mainly connects the vesicles pool to the cytoskeleton, in particular to actin [88]. In Cheng et al., authors also state that ATR is located in association with inhibitory vesicles, as suggested by its selective colocalization with the vesicular protein vGAT [83]. All these data pointed to the identification of a novel important function that ATR plays for the maintenance of the correct excitatory/inhibitory (E/I) balance in the central nervous system.



**Figure 5:** ATR is present at the neuronal synapse, in association to synaptic vesicles. In particular, ATR is found colocalizing with vGAT<sup>+</sup> inhibitory vesicles. Image modified from Cheng et al., 2017.

Further confirmations of an important ATR role in the presynaptic compartment were released on July 2021, when the group of Kirtay et al. proposed an involvement of this kinase in the regulation of neuronal activity by modulating the presynaptic firing. According to this study, the genetic deletion of ATR in both excitatory and inhibitory neurons does not affect the brain formation and

architecture, but alters their intrinsic activity. Absence of the protein in the Purkinje cells resulted in a pathologically enhanced neuronal activity and a similar increased activation was found in glutamatergic forebrains neurons of adult ATR-deleted mice. The increased excitatory activity was responsible for the onset of sporadic non-lethal epileptic seizures in 12 months-old mice [89]. Authors ascribed to these functional defects an increased vesicles release, mediated by the higher expression and localization of two presynaptic proteins: synaptotagmin-2 (SYT2) and PROT (sodium-dependent proline transporter). These proteins are both involved in the regulation of excitatory neurotransmission [89]. In particular, synaptotagmin-2 functions as a  $Ca^{2+}$  sensor for fast neurotransmitter release and it is preferentially expressed in inhibitory neurons, in contrast to its homolog SYT1 (synaptotagmin-1) majorly present in excitatory neurons [98, 99]. PROT instead is a selective L-proline transporter responsible for the proline transfer into the presynaptic compartment and for the promotion of neuronal excitation since L-proline, at high concentration, can directly activate both the AMPA and NMDA receptors [92]. Thus, when ATR is deleted in post mitotic neurons, SYT2 switches its expression profile and it is found in excitatory synapses, conferring them a rapid release kinetics. In addition, in this context, SYT2 and PROT are also found together in the same vesicles cluster promoting vesicles fusion to facilitate fast neurotransmitter release and increasing epilepsy susceptibility [89]. Finally, authors display that ATR interacts with both of them and its deletion increases their levels. Overall, these recent findings show a fundamental role of ATR in the regulation of vesicles release into the presynaptic compartments and in the maintenance of proper neuronal transmission but, unfortunately, no data regarding molecular mechanisms at the basis of these alterations have been produced. As an example, it is unclear if the interaction between cytoplasmatic ATR and SYT2/PROT either promotes their stronger stabilization, inhibits their degradation beyond the proteins mislocalization or if nuclear ATR negatively modulates SYT2/PROT transcription. Also, no data regarding the inhibition of ATR kinase activity have been provided, whose would strength the aforementioned conclusions. In this thesis, we assessed this point, exploiting a specific ATR kinase activity blocker, and our results lead to completely opposite conclusions.

## **Chapter 4**

### **Therapeutic ATR inhibition**

Since ATR plays a central role in the DNA damage response, over these past years it has become an attractive target for cancer therapy. Indeed ATR, but also its first effector CHK1, are essential for cell surviving in mammals and severe reduction of the protein level confers resistance to tumors development [101, 102]. Importantly, it has been demonstrated that an ATR signaling reduced to 10% of its normal level is sufficient to induce synthetic lethality in tumors, while the bone marrow and the intestinal homeostasis are only minimally affected [95]. All of this provides genetic support for inhibition of DNA damage repair in cancer therapy.

In this context, ATR inhibitors may act through two different mechanisms of action: the generation of replication stress, which is the main goal of most of the genotoxic agents used in cancer therapy, and the inability to activate cellular checkpoints, thus leading to mitotic catastrophe and cell death [96]. Indeed, the entrance into mitosis in presence of DNA damage and no finished replication plays an important role for the marked toxicity of selective ATR inhibitors.

Several factors made it difficult to identify and develop proper ATR inhibitors, in particular the large size of the protein and the activity mainly restricted to the S-G<sub>2</sub> phase of the cell cycle complicated the condition to study.

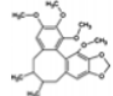
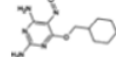
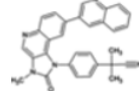

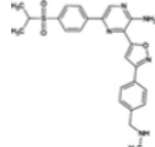
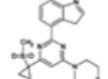
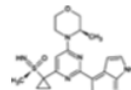
The first inhibitor ever discovered was caffeine, but its high dose usage reduces its selectivity and in fact other members of the PIKK family were affected by the treatment [105, 106]. Then, in 2009 it was identified schisandrin B, a natural compound shown to inhibit the kinase and thus the activation of the G<sub>2</sub>-M checkpoint but also this inhibitor was used at very high doses [99]. Finally in 2011, several different chemical compounds were developed through the optimization of screening methods, but still they were lacking of full target selectivity. In particular: ETP-46464 specifically inhibits ATR with no effects on ATM or DNA-PKs, but it loses this selectivity at increasing concentrations thus acting also on mTOR or PI3K; NVP-BEZ235, which inhibits PI3K and mTOR, and also ATR [100]; NU6027, a CDK2 inhibitor that can also act on ATR [101]; and Torin 2 [102].

The same year, it was generated the first real selective ATR inhibitor: VE-821 [111, 112]. It was firstly developed in 2011, but further modifications of the VE-821 compound allowed to improve its pharmacological properties and the derivative molecule M6620 is now in clinical trials for the treatment of solid tumors, in combination or not with cisplatin [113, 114]; it has >100-fold selectivity for ATR versus ATM, DNA-PKs, PI3K and mTOR and it is characterized by increased solubility, potency and pharmacodynamic properties, showing impressive results in xenograft studies [107]. In addition, a novel class of ATR inhibitors was developed by AstraZeneca in 2013: they are ATP competitors and include the chemical AZ20 [116, 117] then optimized in its derivative AZD6738 [118, 119], currently also in clinical trial for advanced solid tumor treatment [120, 121, 122]. One of the most interesting feature of this new inhibitor is its orally bioavailability and the fact that can effectively penetrate the brain barrier after systemic intraperitoneal administration. Indeed, it reaches the brain already 1 hour after a single peripheral injection at the dosage of 25 mg/kg [115], which is a concentration well tolerated also in chronic protocols [123, 124]. Another ATR inhibitor is currently under clinical evaluation and belongs to Bayer (BAY1895344). Finally, pyrazolopyrimidine was recently identified but up to now no consistent pharmacokinetic informations are available [118].

In preclinical mouse models, positive effects of ATR kinase inhibitors have been investigated as monotherapy, whereas increased toxicity occurs when other chemototoxic agents are co-administered, such as agents inducing DNA interstrand crosslinks, nucleoside analogues and PARP inhibitors [125; 126]. In contrast, although some studies have shown efficacy of ATR inhibitors in combination with radiations, it is important to underline that ATR-deficient mammalian cells are only mildly sensitive to this treatment probably because it is mainly responsible for the onset of DSBs [118].

At present, no further applications apart from the oncologic field are currently available for the ATR inhibitors.

**A**

Compound	Targets
Schisandrin B 	ATR
NU6027 	CDK2, ATR
NVP-BEZ235 	PI3K, MTOR, ATR, ATM, DNA-PKcs
VE-821 	ATR
VE-822 (VX-970) 	ATR
AZ20 	ATR
AZD6738 	ATR

**B**

ATR inhibitor	Cancer type	Combination agent	Year	Phase
M6620 (formerly VX-970)	Solid tumours	Gemcitabine, cisplatin, etoposide or carboplatin	2014	I
	Small-cell cancers	Topotecan	2015	I/II
	HNSCC	Cisplatin and radiotherapy	2015	I
	Brain metastases	Whole brain radiation	2015	I
	Ovarian, peritoneal and fallopian tube cancers	Gemcitabine	2015	II
	Solid tumours	Irinotecan	2015	I
	Ovarian, peritoneal and fallopian tube cancers	Carboplatin or gemcitabine	2015	I/II
	Solid tumours	Cisplatin	2016	I
	Urothelial	Cisplatin or gemcitabine	2015	II
	Solid tumours	Carboplatin or paclitaxel	2017	I
AZD6738	Leukaemia	Alone	2013	I
	Solid tumours	Alone or radiotherapy	2014	I
	HNSCC, NSCLC and gastric and breast cancers	Carboplatin, olaparib or MEDI4736	2014	II
	HNSCC	Alone (as an evaluation of biomarkers of immune response)	2017	I
	Refractory cancer	Paclitaxel	2015	I
	Chronic lymphocytic leukaemia	Acalabrutinib	2017	I
	Triple-negative breast cancer	Olaparib	2017	II
BAY1895344	NSCLCs that have progressed on anti-PD1 and/or anti-PDL1 therapy	Durvalumab	2017	II
	Solid tumours and lymphomas	Alone or radiotherapy	2017	I

**Figure 6:** a) List of ATR inhibitors: for each compound are shown the chemical formula and the list of targets selectively inhibited. Image modified from Weber and Ryan, 2014. b) List of ATR inhibitors currently in clinical trials: for each drug are reported the cancer type in which the molecule is tested, the agents the molecule is tested with and the year and the phase of the trial. Image from Lecona et al., 2018.

## **Chapter 5**

### **Excitatory/inhibitory imbalance and epilepsy**

The establishment and maintenance of the proper balance between excitatory and inhibitory transmission (E/I balance) is fundamental during early development to guarantee processes as circuitry formation and cortical layers distribution, but also after maturation for the correct activity-dependent tuning of neuronal networks and neuronal plasticity. Thus, it must be preserved throughout life. Interestingly, *in vitro* and *in vivo* models for the study of neurodevelopmental and psychiatric diseases (NDs) revealed the presence of important dysfunctions in GABAergic signaling and only limited effective therapy acting on GABAergic system are available.

The structure and organization of inhibitory synapses are carefully regulated during early development to precisely match the function, strength and organization of excitatory synapses [120]; they represent about 20-30% of all cortical neurons and generally are considered a brake for excitatory neurotransmission and excitability [121]. If the excitatory transmission is mainly driven by glutamatergic synapses, the inhibitory one involves GABAergic and glycinergic signaling [122]. Altogether, these systems provide the spatial and temporal framework for the physiological transfer of information in the brain. In particular, the early brain development is characterized by a strong interplay of gene expression, intrinsic neuronal activity and molecular guidance [131–134], combined with a good amount of external and environmental stimuli [128, 135]. This process is time-limited and developmental stages involving neuronal migration, circuitry formation and synaptic refinement are fundamental for generation of a working adult brain. Impairments during this specific time-window, defined as critical or sensitive period, are indeed linked to neurodevelopmental brain disorders [120]. Other balanced factors that must be present for a correct brain development are the equilibrium between cell growth and differentiation, oxidant and anti-oxidant compounds, pro-inflammatory and anti-inflammatory molecules and neurotrophins production [136–139]. Moreover, the process of circuitry formation at the basis of neuronal plasticity involves the right production and release of neurotransmitter, which are thus responsible for the excitatory/inhibitory balance [132]. Accordingly, deregulation of the E/I ratio has



been associated with a variety of human neurodevelopmental disorders such as intellectual disabilities, autism spectrum disorders (ASDs) and schizophrenia. Among the chronic neurological diseases linked to aberrant E/I ratio, there is also epilepsy [128, 142, 144, 145].

It represents one of the most common neurological disorders that affects about 65 million people worldwide [136]. Importantly, even though different classes of drugs exist since long time, still about the 30% of epileptic patients fail to respond to anti-epileptic drugs (AEDs) [137]. It is described as a dynamical disorder characterized by the occurrence of recurrent epileptic seizures, which are due to excessive or abnormal synchronicity of neural activity [138]. Epilepsy etiology is vast and seizures can be triggered by different stimuli [139], but the classic understanding of this pathology relies on disruption of the E/I balance in the brain [140]. Indeed, hyperexcitable epileptic tissues have been characterized either by an increased excitatory synaptic conductance or by a decreased inhibitory synaptic conductance [141]. In particular, during different stages of seizure-like events (SLEs) – initiation, body and termination – are observed different E/I conductance ratio [142]. Recent interpretations suggest that the initial synchronized theta rhythms can be due to increased local inhibitory inputs, which are then overcompensated by runaway excitation responsible for seizures generation [142]. Indeed, the role of GABAergic transmission in this context is much more complex than what was initially suggested: tonic GABA-mediated inhibition, regulation of chloride ion homeostasis and the activity-dependent regulation of GABAergic and glutamatergic synaptic function all occur for the proper network excitability establishment [153, 154].

Of course, ascribing epilepsy generation only to disrupted E/I balance is an oversimplification and additional mechanisms, such as individual ion concentrations, intrinsic cellular properties and network dynamics concur in seizures onset [155, 156]. Also, the discovery of a vast number of genetic mutations, which bear no obvious relationship to E/I balance, clearly expands the neurobiological patho-mechanism at the base of epilepsy, opening new roads for therapy [144].

## **AIM OF THE THESIS**

Activity of the ATR protein in dividing cells has been largely investigated, however increasing evidences are demonstrating novel role of this kinase in post mitotic neurons, suggesting the lack of a complete understanding of ATR functions.

Deletion of the *Atr* gene is lethal in mice and genetic mutations lead to the expression of an unfunctional protein, unable to guarantee the DNA damage repair signaling and the response against mechanical and osmotic stress. In human, mutations in the *Atr* gene lead to Seckel Syndrome (SS), a rare pathology characterized by a complex phenotype where severe neurological alterations and a precocious aging have been described. Despite the occurrence of a neuronal symptomatology, only few studies focused their attention on the role of ATR in neuronal function. Recently, it has been showed a fundamental role of ATR in the regulation of vesicles release into the presynaptic compartments and its involvement for the maintenance of proper neuronal transmission, with no specification regarding molecular mechanisms at the basis of the alterations found in absence of the protein. Importantly, no data regarding the pharmacological inhibition of ATR kinase activity have been provided. Thus, in this thesis, we aimed at filling this scientific gap investigating the effect mediated by a specific ATR kinase activity blocker, leading to opposing conclusions that are in contrast with data obtained by genetic abolition of the protein.

We took advantage of a selective inhibitor of ATR kinase activity and then carried out functional, biochemical and molecular analysis in order to investigate the effect of the ATR kinase inhibition on neuronal transmission both in vitro and in vivo. The data presented in this thesis propose ATR as a key regulator of the proper E/I balance and highlight ATR inhibition as a novel target in the treatment of neurologic disorders characterized by hyperexcitability.

## **EXPERIMENTAL PROCEDURES**

## **Animals**

All the experimental procedures were performed following the guidelines established by the Italian Council on Animal Care and were approved by the Italian Government Decree n° 27/2010 and the Italian Legislation (L.D. n° 26/2014). All efforts were made in order to minimize the number of animals used and their suffering. The animals in question are wild type Sprague-Dawley rats and C57BL/6J mice. They were housed in standard cages (no more than 4 per cage), kept in a stable environment of 18-22 °C and 50% humidity, with a 12-hours light and dark cycle set, with food and water ad libitum. The number of animals used is the minimum to obtain statistically significant data.

## **Cell Cultures**

### **Primary cultures of neurons**

24 mm glass coverslips were placed in porcelain holders and left overnight in 100% ethanol at 37°C. Afterwards, we proceed with washes in distilled water to eliminate alcoholic residues, followed by one night in stove at 200°C in order to sterilize them. Three different slides were placed in a single 60 mm petri, which were then exposed to UV rays for 30 minutes. Finally, they were treated with poly-L-lysine (Sigma Aldrich, 1 mg/mL in borate buffer 0,1 M at pH 8,5) and the next day plating medium (89 mL di Starting Solution; 1 mL of PenStrep, Sigma Aldrich; 10 mL horse serum 10%, GIBCO; Starting Solution: 500 mL MEM, Invitrogen; 5 mL pyruvate 100X; 15 mL glucose 20%) was added to each petri.

### **Dissection and cultures of hippocampal neurons**

Characterization of AZD6738 impact on neuronal cultures was conducted on hippocampal neurons obtained from E18 wild type rats and mice embryos. Brains were withdrawn, stored in HBSS 1x (10 mL HBSS 10X, GIBCO; 3,30 mL HEPES 0,3 M at pH 7,3; 1mL PenStrep, Sigma Aldrich; 87 mL sterile water) and then hippocampi were extracted and cleared from the meninges. The hippocampi obtained were chemically digested with 0,5% trypsin in HBSS 1x for 15 minutes at

37°C, followed by a mechanical dissociation with a sterile micropipette. The dissociated cells were plated on slides previously coated with poly-L-lysine. Neuronal cultures were maintained in culture medium (100 mL Neurobasal, GIBCO; 2mL B27 Supplement 50X, GIBCO; 1 mL PenStrep, Sigma Aldrich; 250 µL Glutamine 200 nM, GIBCO; 125 µL Glutamate 10 mM, Sigma Aldrich), in incubator at the constant temperature of 37 °C and in the presence of 5% CO<sub>2</sub>. At 3 days in vitro (DIV), half of the complete medium was replaced with fresh medium lacking of glutamate in order to avoid excitotoxicity phenomena.

### **In vitro AZD6738 treatment**

In our study, hippocampal neuronal cultures were treated using the selective inhibitor of ATR kinase activity AZD6738, at the final concentration of 1 µM. The treatment was administered both in acute, a single day administration, and in chronic, one-week treatment. In the acute protocol, the drug was delivered at 6 DIV or 13 DIV neuronal cultures and then experiments carried out at 7 DIV or 14 DIV. In the chronic protocol, AZD6738 was administered twice a week, starting either at 10 DIV or at 13 DIV, considering the duration of action of AZD6738 (about 48 hours); through this paradigm we suppress ATR kinase activity for an entire week. At the end of the treatment, we performed biochemical and functional experiments among which immunocytochemical staining, western blotting, real time PCR, calcium imaging and cell culture electrophysiology.

## **Cell cultures staining and analysis**

### **Immunocytochemical experiments**

Primary hippocampal neurons were fixed in 4% paraformaldehyde and 4% sucrose for 8 minutes and washed three times for 5 minutes in phosphate buffer PSB 1X. Subsequently were performed three washes with a solution of low salts (150 mM NaCl and 10 mM phosphate buffer 240 mM at pH 7,4) and three washes with a solution of high salts (500 mM NaCl and 20 mM phosphate buffer 240 mM at pH 7,4), each wash lasted 6/7 minutes. Slices were incubated for 30 minutes with GSDB 1X (Goat Serum Dilution Buffer) for permeabilization and then incubated

overnight with the primary antibodies diluted in GSDB 1X to concentration ad hoc. The days after, they were washed with the high salts solution and then incubated with the secondary antibodies for 1 hour. At the end, slides were again washed starting with high salts solution and then with the low salts. Finally, they were assembled with Mowiol and fixed to the coverslip.

Immunofluorescence experiments were carried out using the following antibodies: anti-tubulin (rabbit, 1:80; Sigma), anti-MAP2 (mouse, 1:500; Immunological Science); anti-vGLUT (guinea pig, 1:1000; SySy), anti-vGAT (guinea pig, 1:1000; SySy), anti-PSD95 (mouse, 1:400; Neuromab) and anti-Gephyrin (mouse, 1:300; SySy). Secondary antibodies were conjugated with Alexa-488, Alexa-568 or Alexa-633 fluorophores (1:200; Alexa Fluor Invitrogen).

### **Tunel imaging assay**

Primary hippocampal neurons were fixed in 4% paraformaldehyde and 4% sucrose for 15 minutes and washed one time in phosphate buffer PBS 1X; slices were then incubated for 20 minutes at room temperature with the permeabilization reagent (0,25 % Triton X-100 in PBS). In order to detect the in situ apoptosis, the Click-iT Plus TUNEL assay (Invitrogen) was performed as described in the manufacturer's protocol. The assay utilizes EdUTP, dUTPs modified with a small alkyne moiety, which is incorporated at the 3'-OH ends of fragmented DNA by the TdT enzyme. Detection of the apoptotic cells is based on a click reaction: a copper catalyzed covalent reaction between the Alexa Fluor 488 picolyl azide dye and an alkyne.

### **Image acquisition and analysis**

Images were acquired using a LSM800 confocal microscope (ZEN system program) with 20x and 63x objectives and then analysed using ImageJ Software (National Institutes of Health). In case of immunocytochemical images, we performed an analysis of complete inhibitory synapses density, complete excitatory synapses density, v-GAT density, v-Glut density and PSD95 density per unit length of dendrite. In order to study the complete synapses density, puncta positive for the proteins of the presynaptic compartment co-localizing with the positive puncta of the respective postsynaptic compartment were counted in selected areas of neuronal branches. The density value was then obtained as ratio of the counted

co-localizing puncta over micron of dendrite. Very similarly, the density of v-GAT, v-Glut and PSD95 was calculated as ratio between the counted positive v-GAT or v-Glut puncta over micron of dendrite. In addition, it was also analysed the size and the intensity of the puncta positive for v-GAT, v-Glut, gephyrin and PSD95. In case of slices stained with the Click-iT Plus TUNEL assay kit, it was counted the number of positive apoptotic cells in each image field and expressed as percentage.

## **Western Blotting**

Western Blotting experiments were performed either on neurons scraped using a lysing buffer (15% SDS; 0,575 M sucrose; 0,325 M Tris-HCl at pH 6,8; 0,5% betamercaptoethanol and bromophenol blue, as dye to follow the electrophoretic run) or on explanted tissues homogenized in sample buffer (1% SDS; 62,5 mM Tris-HCl at pH 6,8; 290 mM sucrose). In this latter case, the protein content extracted was quantified using the bicinchoninic acid (BCA) assay, through the BCA protein assay kit (Thermo Fisher Scientific). Accordingly, the protein concentration of the sample is proportional to the absorbance at the wave length of 562 nm of a reaction product, resulting from chelation of  $\text{Cu}^+$  ions by the BCA molecules.  $\text{Cu}^+$  ions are present in the sample due to reduction of  $\text{Cu}^{++}$  by proteins when in a marked alkaline environment. Absorbance was obtained using a spectrophotometer (Victor2-1420 multilabel counter, Wallac) set to 570 nm and then the protein content extracted through the use of a standard curve, calculated on the absorbance of a protein characterized by known concentration, namely bovine serum albumin.

The samples obtained either from cell cultures or from tissue were separated by SDS-PAGE electrophoresis, transferred to nitrocellulose membrane (Whatman) and then incubated with primary antibodies for about 3 hours at room temperature or overnight at 4°C. The secondary antibodies used were either conjugated to peroxidase (Jackson ImmunoResearch) or to fluorophores that emit infrared (Li-Cor Bioscience) and thus, according to the detection method, the immunoreactive bands were visualized by exposure to the action of the reagent Pierce ECL



Western Blotting Substrate (Thermo Scientific) or acquiring the fluorescence signals with the instrument CLx Odyssey (LI-COR Biosciences). The quantization of the signal was performed using ImageJ or Image Studio software.

Western Blotting experiments were carried out using the following antibodies: anti-calnexin (rabbit, 1:1000; Sigma), anti- $\beta$ -tubulin (mouse, 1:1000; Promega), anti-KCC2 (rabbit, 1:1000; Millipore), anti-MeCP2 (rabbit, 1:1000; Sigma), anti-actin (mouse, 1:500; Sigma), anti-ATR (mouse, 1:300; GeneTex), anti-pATR (rabbit, 1:500; GeneTex), anti-ATM (rabbit, 1:500; Millipore), anti-EGR1 (rabbit, 1:500; Cell Signaling), anti-CACNA1H (mouse, 1:1000; Invitrogen), anti-CACNA2D4 (rabbit, 1:1000; Invitrogen).

## **Calcium Imaging**

We performed calcium imaging experiments on 7 DIV and 14 DIV hippocampal neurons, treated 24h with the drug AZD6738 1  $\mu$ M. Each slide was incubated for 30 minutes at 37°C with the membrane-permeable fluorescent  $\text{Ca}^{2+}$  indicator Fura2-AM (Sigma-Aldrich) 1  $\mu$ M. After the incubation, the slide is washed from the excess of Fura-2AM in a KRH solution and loaded into the recording chamber of the microscope AxioVERT 100 in KRH and tetrodotoxin (TTX, Tocris), in correspondence of the objective 40X. The  $\text{Ca}^{2+}$  indicator was excited at 340 nm and 380 nm by Polychrom V (TILL Photonics GmbH) controlled by the acquisition software Live Acquisition FEI. Emitted light was acquired at 505 nm with a rate of 1-4 Hz and data collected by CCD Imago-QE camera (TILL Photonics GmbH). After the selection of appropriate field and of regions of interest (ROIs), different stimuli were administered and variation of the calcium transient (F340/380 fluorescence ratio) was measured.

7 DIV hippocampal neurons were subjected to “GABA switch” experiments. Firstly, neurons were stimulated through the administration of GABA 100  $\mu$ M, to evaluate the level of neurons maturation; calcium transient increment were considered valid when higher than 0,05 units. Following GABA stimulation, KRH washes were applied to restore the basal level of intracellular calcium; once neurons recovered,

they were excited with a KCl 50 mM administration. This stimulus allowed to identify vital neurons and to analyze the expression of Voltage Operated Calcium Channels (VOCC); calcium transient increments lower than 0,1 units were not considered during the experiment analysis. 14 DIV hippocampal neurons received only the KCl stimulation, to evaluate the depolarization kinetic and the VOCC expression. For each slide the imaging was achieved twice, choosing two different, but still comparable, fields.

## **Cell culture electrophysiology**

### **Miniature post-synaptic currents (mPSCs) analysis**

MINIs, miniature excitatory (mEPSCs) and inhibitory (mIPSCs) events, were recorded in whole-cell voltage-clamp configuration in presence of TTX at the concentration of 1  $\mu$ M. Tetrodotoxin is a reversible blocker of the sodium channel, thus its presence avoids the generation of action potentials. In presence of TTX, miniature post-synaptic currents occur spontaneously, by the release of single synaptic vesicles, thus are events generated from the quantal release of neurotransmitter molecules interacting with the postsynaptic receptors. Whole-cell recordings were performed in the voltage-clamp configuration on 14 DIV hippocampal neurons, after a 24 hours treatment with the drug AZD6738 1  $\mu$ M, and in 20 DIV hippocampal neurons treated chronically with AZD6738 1  $\mu$ M, using an Axopatch 200A amplifier (Axon Instruments, Forest City, CA, USA). Recording pipettes were fabricated from glass capillary (World Precision Instruments) using a two stage puller (Narishige, London, United Kingdom); they were filled with the intracellular solution Cs-gluconate (Cesium Gluconate 130 mM; CsCl 8 mM; NaCl 2 mM; HEPES 10 mM; EGTA 4 mM; MgATP 4 mM; GTP 0,3 mM; pH 7,3) and the tip resistance was 3-5 M $\Omega$ . Recording were performed using as external solution KRH (Krebs'-Ringer's-Hepes: 125 mM NaCl, 5 mM KCl, 1,2 mM MgSO<sub>4</sub>, 1,2 mM KH<sub>2</sub>PO<sub>4</sub>, 2 mM CaCl<sub>2</sub>; 6 mM glucose, 25 mM Hepes-NaOH pH 7,4). Neurons were held at holding potentials of -70 mV, to identify the excitatory miniature events, and at +10 mV for the inhibitory miniature events. Currents were sampled at 10 kHz and filtered at 2 kHz. Analysis of the recorded traces have been

performed using Clampfit-pClamp 10 software; event threshold was set at -8 pA for mEPSCs and +6 pA for mIPSCs. The E/I ratio was calculated as ratio of mEPSCs and mIPSCs frequencies measured in the same neuron.

### **Multi-unit (MU) analysis**

MU events were recorded in the cell-attached voltage-clamp configuration. The multiunit activity reflects the average spiking network activity and so the excitability state of the neuronal culture. Recordings were performed on 17 DIV hippocampal neurons, after chronic administration of the drug AZD6738 1  $\mu$ M. Recording pipettes, fabricated as described before, were filled the intracellular solution K-gluconate (130 mM K-gluconate, 10 mM KCl, 1 mM EGTA, 10 mM HEPES, 2 mM MgCl<sub>2</sub>, 4 mM ATP, 0,3 mM GTP). Recordings were performed using as external solutions complete KRH as describe previously and KRH without Mg<sup>2+</sup>, a protocol largely described to induce hyperexcitability. In both cases, to identify MU events neurons were held at holding potential of -50 mV. Currents were sampled at 10 kHz and filtered at 2 kHz and analysis of the recorded traces have been performed using Clampfit-pClamp 10 software.

### **Long term potentiation (LTP) and depression (LTD) analysis**

Prior mEPSCs recordings, we exploited a chemical protocol to induce long term potentiation and long term depression in 17 DIV hippocampal neurons treated chronically with the drug AZD6738 1  $\mu$ M. Firstly, basal mEPSCs activity was recorded as previously described at -70 mV, using as internal solution K-gluconate and as external solution KRH supplemented with TTX 0,5  $\mu$ M, Strychnine 1  $\mu$ M and Bicuculline 20  $\mu$ M. Neurons were then subjected to chemical protocols aiming either the induction of LTP or LTD: to achieve synaptic potentiation, neurons were held for 3 minutes in a medium constituted of KRH without Mg<sup>2+</sup> and with TTX 0,5  $\mu$ M, Strychnine 1  $\mu$ M, Bicuculline 20  $\mu$ M and Glycine 100  $\mu$ M; whereas in case of synaptic weakening, neurons were incubated for 10 minutes in KRH without magnesium and with TTX 0,5  $\mu$ M, Strychnine 1  $\mu$ M, Bicuculline 20  $\mu$ M and then for 3 other minutes in KRH without Mg<sup>2+</sup> and with TTX 0,5  $\mu$ M, Strychnine 1  $\mu$ M, Bicuculline 20  $\mu$ M, NMDA 20  $\mu$ M and Glycine 20  $\mu$ M. 15 minutes later the chemical induction, electrophysiological recordings of mEPSCs were performed again in the

same condition as before. Currents were sampled at 10 kHz and filtered at 2 kHz and analysis of the recorded traces have been performed using Clampfit-pClamp 10 software, as already described. In parallel, hippocampal neurons subjected to the same LTP or LTD chemical induction were fixed and then immunocytochemical staining was performed as previously described.

## **Quantitative Real-time PCR**

### **RNA extraction and quantification**

20 DIV hippocampal neurons treated chronically with the drug AZD6738 1  $\mu$ M were incubated overnight with TTX 1  $\mu$ M and the following morning a 50 mM KCl stimulus was administered to the culture. 30 minutes after, neurons were lysed using TRIzol reagent (Invitrogen). Total RNA was extracted using the Direct-zol RNA MiniPrep isolation kit (Zymo Research), as described in the manufacturer's protocol. This kit allows total RNA extraction, including small RNAs of 17-200 nt length, and take advantage of Zymo-Spin IICR Column (silica columns) for serial elution. The RNA extracted was eluted with 40  $\mu$ L of DNase/RNase-free water and then stored at  $-80^{\circ}\text{C}$ . Each sample was obtained from about  $1 \times 10^6$  cells. Before further utilization, the extracted RNA was quantified with the BioPhotometer spectrophotometer (Eppendorf) and optical density 260/280 nm and 260/230 nm ratios were determined, in order to verify RNA purity and exclude possible contaminations of proteins and organic solvents.

### **Reverse transcription and real-time PCR**

Reverse transcription was performed using 1  $\mu$ g RNA for each sample with the High Capacity cDNA RT kit (Applied Biosystem). The total volume transcribed was 14  $\mu$ L for each sample and the cDNA obtained was either involved in the real-time PCR reaction or conserved at  $-20^{\circ}\text{C}$ . Real-time PCR (qRT-PCR) was performed using a QuantStudio 5 Real-Time PCR System (ThermoFisher) thermal cycler in a final volume of 10  $\mu$ L with TaqMan probes (ThermoFisher). Each target was analysed at least in duplicate and normalized to GAPDH. Data analysis was

performed with the  $\Delta\Delta\text{Ct}$  method and expressed as fold change, supported by the use of QuantStudio 5 software.

Real-time PCR experiments were carried out using the following TaqMan probes: GAPDH Rn01775763\_g1; Egr1 Rn00561138\_m1; Fos Rn02396759\_m1; Npas4 Rn01454622\_g1; Egr4 Rn00569509\_g1; CACNA1H Rn01460348\_m1; CACNA2D4 Rn01492789\_m1; CACNA1G Rn01299126\_m1.

## **In vivo procedures**

### **In vivo AZD6738 injection**

AZD6738 (or vehicle-DMSO) was administered with intranasal delivery to P90 wild type C57BL/6J mice at the dosage of 20 mg/kg. Mice were previously anesthetized, in order to reduce the distress caused by the treatment, and the total volume was administered through single injections of 4  $\mu\text{L}$ , alternating the two nostrils. Indeed, it has been chosen the intranasal delivery because it is considered the most appropriate administration method to target the whole brain.

### **Behavioral analysis after systemic kainic acid**

Two days after in vivo AZD6738 (or vehicle) administration, P90 male mice received an intraperitoneal injection of kainic acid (KA), a known convulsant agent, at the dosage of 25 mg/kg. The control group received a similar volume of normal saline. Each animal was housed in single cage and observed for a period of 3,5 hours after KA administration. Animal behavior was scored every 5 minutes according to the Racine scale: stage 0, normal behavior; stage 1, immobility; stage 2, head bobbing and stereotypies; stage 3, forelimb and/or tail extension, rigid posture; stage 4, sporadic clonus with rearing and falling; stage 5, generalized clonus with continuous rearing and falling; stage 6, severe whole-body convulsions; stage 7, death. After the monitoring, all the animals were sacrificed through cervical dislocation and cerebral tissues collected and stored at  $-20^{\circ}\text{C}$  for Western Blotting analysis.

## **RNA sequencing**

### **RNA Extraction and Library Preparation**

Two days after in vivo AZD6738 (or vehicle-DMSO) administration, P90 male mice were sacrificed through cervical dislocation and cerebral tissues collected and stored at -80°C. Total RNA was extracted from the hippocampus using standard column purification according to the manufacturer's protocol (RNAeasy Mini Kit, QIAGEN). All procedures were conducted in RNAase-free conditions. RNA concentration was evaluated using Qubit RNA BR Assay Kit (Life Technologies). RNA purity was assessed by determining UV 260/280 and 260/230 absorbance ratios using a Nanodrop® ND-1000 spectrophotometer (Thermo Fisher Scientific). RNA quality was evaluated by measuring the RNA integrity number (RIN) using an Agilent RNA 6000 Nano Kit with an Agilent 2100 Bioanalyzer (Agilent Technologies, Santa Clara, CA, USA) according to the manufacturer's instructions. Only RNA with a RNA integrity number (RIN) of > 6.5 and a DV200 values (% of RNA fragments >200 nucleotides) greater than 89% were selected and used for RNA-seq library preparation.

Libraries were prepared with the TruSeq® Stranded mRNA Sample Preparation kit (Illumina, San Diego, Ca, USA) according to manufacturer's instructions. For each sample of hippocampus, 1000 ng and 500 ng were used as input quantity, respectively. The libraries were sequenced at an average read-depth of 58 million reads per sample on an Illumina NovaSeq 6000 (NovaSeq Control Software 1.7.0) with 2 ×150 bp paired-end protocol, using an SP Reagent Kit (300 cycles) in standalone mode, and libraries loaded at 2.25 nM and a volume of 100 µl. The NovaSeq 6000 sequencing was performed by the LaBSSAH/CIBIO NGS Core Facility of the University of Trento.

### **RNA-seq analysis**

Raw sequence files were subjected to quality control analysis using FastQC (v 1.3) (<http://www.bioinformatics.babraham.ac.uk/projects/fastqc/>, accessed on May, 2021). Transcript quantification was conducted with SALMON (version v1.4) using Transcriptome index for salmon, with selective alignment method that Improves quantification accuracy compared to the regular index downloaded from

<http://refgenomes.databio.org/> (accessed on May, 2021). The generated gene counts were analysed using DESeq2 package. Starting from the normalized (vst method) expression matrix, it was explored the high-dimensional property of the data using Principal Component Analysis (PCA), as dimensionality reduction algorithm implemented in stats DESeq2 package. Genes that were considered as differentially expressed (DEG), were analyzed using hierarchical clustering method (euclidian distance). An adjusted p-value cut off of 0.05 and a log fold change greater or lower than 1 were decided as threshold for detection of DEGs. Visualization of the clustering and heatmap of log2-normalized values were obtained using heatmap.2 of gplots package. Visualization of the DEGs in the volcano plot was obtained using EnhancedVolcano package. For the Functional annotations analyses we used ClusterProfiler and for visualization ggplot2 packages.

## **Statistical analysis**

The statistical analysis was performed using the Prism 8 software (GraphPad). Data were analysed by unpaired parametric or nonparametric statistics: Student t-test or Mann-Whitney test were performed in presence of two experimental groups, otherwise, in case of more groups, it was used one-way analysis of variance (ANOVA) or Kruskal-Wallis followed by post-hoc multiple comparison test. Data, unless otherwise stated, were expressed as means  $\pm$  sem for number of cells. The differences were considered significant with P value  $<0,05$  (one asterisk),  $<0,01$  (double asterisks),  $<0,005$  (triple asterisks) and  $<0,0001$  (quadruple asterisks).

## **RESULTS**



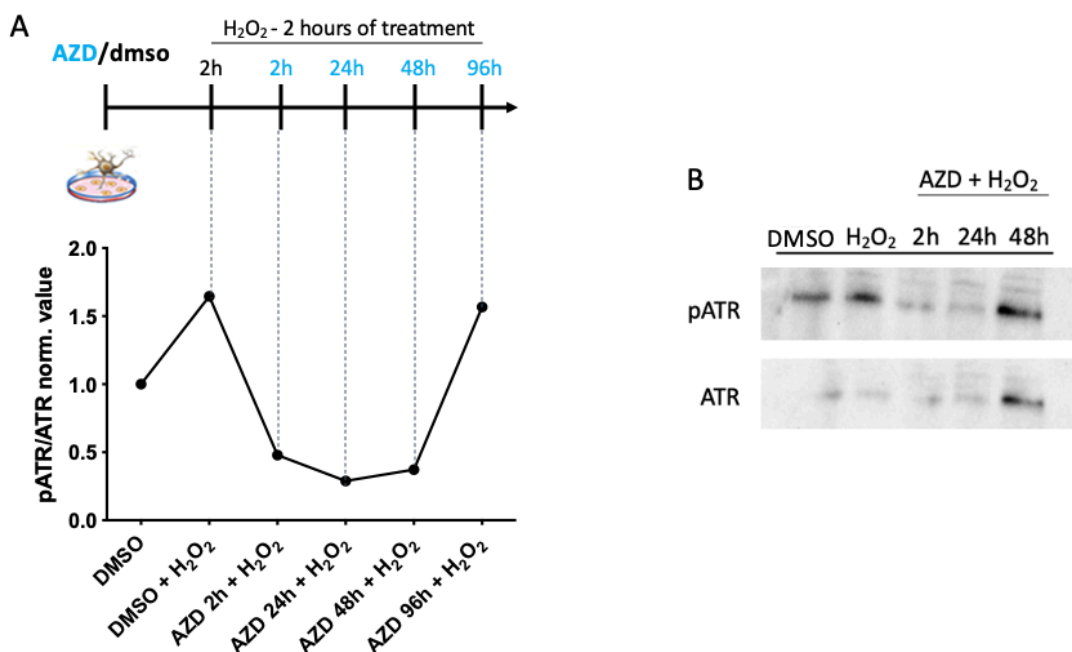
## **Characterization of the ATR kinase inhibitor in neuronal primary cultures**

### **AZD6738 in vitro duration of action**

In order to investigate how and at which extent the hippocampal neurons functionality could be impacted by the pharmacological blockade of the ATR kinase activity, we decided to take advantage of the selective ATR inhibitor AZD6738. As it was already described in chapter 4, this drug is an ATP-competitive inhibitor of ATR that is orally bioactive and can pass the blood brain barrier. Until now, it has been tested in the oncological field, since absence of ATR activity in cancer cells is responsible for replication stress, mitotic catastrophe and indeed cell death [96]. Firstly, we evaluated effectiveness and AZD6738 duration of action in primary hippocampal cultures obtained from E18 rat embryos. We treated neurons with AZD6738 1  $\mu$ M for 2 hours, 24 hours, 48 hours and 96 hours, and 2 hours before scraping cultures we delivered H<sub>2</sub>O<sub>2</sub> 2mM, which is able to induce a DNA single strand break and specifically promote the activation of the ATR kinase [154, 155] (see the schematic representation at figure 8A).

Therefore, by Western Blotting experiments we quantified the extent of ATR phosphorylation, as ratio between the phospho-ATR (pATR) Thr1989 and ATR total form. As indicated in figure 7, while H<sub>2</sub>O<sub>2</sub> clearly activates ATR kinase activity, levels of pATR are significantly reduced starting from 2 hours after AZD6738 treatment. Also, in neurons treated with the ATR inhibitor 24 and 48 hours before H<sub>2</sub>O<sub>2</sub> delivery, the pATR/ATR ratio is persistently deregulated; instead, levels of pATR/ATR return high in cultures treated with AZD6738 96 hours prior H<sub>2</sub>O<sub>2</sub> administration. Thus, Western Blotting analysis revealed that ATR kinase inhibition is detectable starting from 2 hours the delivery and lasts for at least 2 days.

Accordingly, we decided to treat hippocampal cultures with AZD6738 and assess functional consequences in two protocols, i.e., upon a single and chronic administration characterized respectively by i) a single AZD treatment and evaluation of effects one day later; ii) AZD delivery every three days in the neuronal medium and analysis of activity the day after the latter administration.



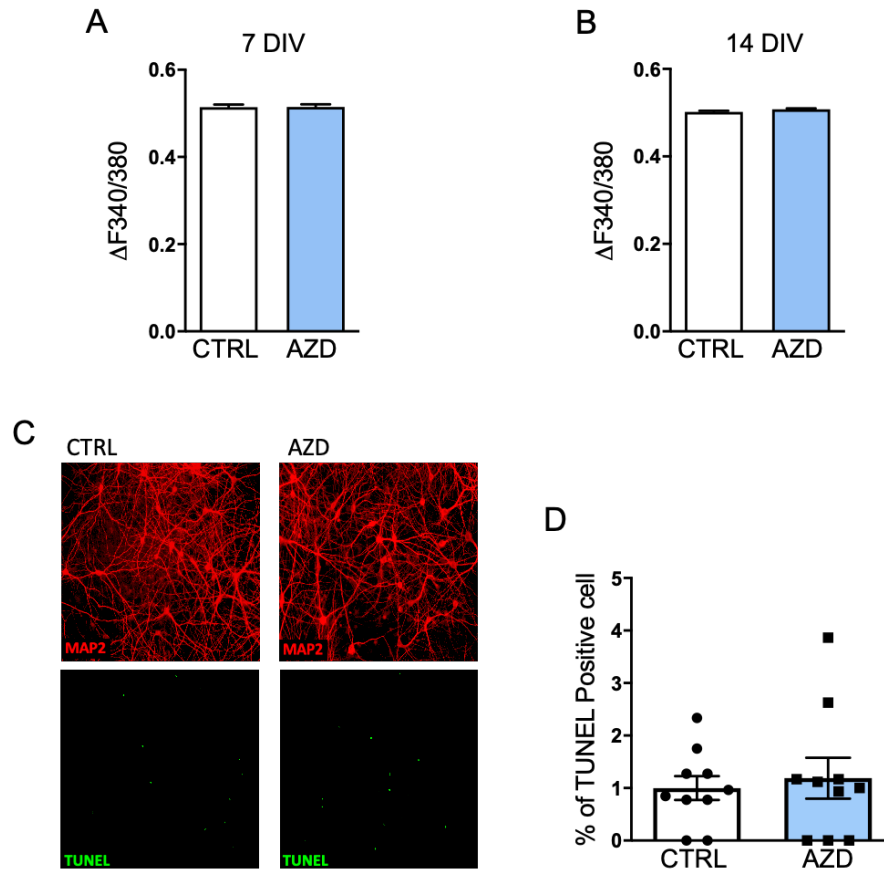
**Figure 7:** a) Schematic representation of the experimental procedure and Western Blotting analysis of AZD6738 duration of action in 7 DIV rat hippocampal neurons treated with H<sub>2</sub>O<sub>2</sub> 2 mM or H<sub>2</sub>O<sub>2</sub> 2 mM plus AZD6738 1 μM. The graph shows that the ATR inhibitor is already active since 2 hours from its application and its effect persists for at least 48 hours. b) Representative image of Western Blotting experiments carried out on 7 DIV hippocampal neurons.

### AZD6738 safety profile

After establishing AZD6738 effectiveness and duration of action, we monitored possible toxic effects induced by the inhibitor in our experimental protocols. In particular, we performed calcium imaging analysis one day after the neuronal treatment and we assessed neuronal damage by confocal analysis and cell death by TUNEL assay.

Calcium imaging performed in cultures loaded with the calcium indicator FURA-2AM revealed unmodified intracellular calcium levels in acutely-treated cells in both immature (7 DIV) and mature (14 DIV) cultures (Figure 8A and 8B), indicating normal calcium homeostasis. Secondly, confocal experiments carried out in chronically-treated cultures displays unmodified morphology of neuronal processes, as indicated by MAP2-staining (Figure 8C); also, evaluation of TUNEL positivity was almost undetectable in AZD and DMSO treated cultures (Figure 8D).

Thus, considering all that above, we can conclude that AZD6738 displays a good safety profile as it leaves neuronal cultures healthy and safe upon both the acute and chronic treatments.



**Figure 8:** a) Evaluation of resting calcium level in 7 DIV hippocampal neurons upon AZD treatment (Unpaired T Test,  $p > 0,05$  ns. CTRL n=80; AZD n=95). b) Evaluation of resting calcium level in 14 DIV hippocampal neurons upon AZD6738 acute treatment (Unpaired T Test,  $p > 0,05$  ns. CTRL n=304; AZD n=354). c) Above, representative images of neuronal branches labelled with MAP2 (red) of control and chronically AZD-treated neurons; below, representative images of TUNEL (green) staining to detect cell death in control and chronically AZD-treated neurons. d) Percentage of TUNEL positive cells upon chronic AZD administration in mature neurons (Unpaired T Test,  $p > 0,05$  ns. N=1 experiments, n=1 coverslips for each experiment).

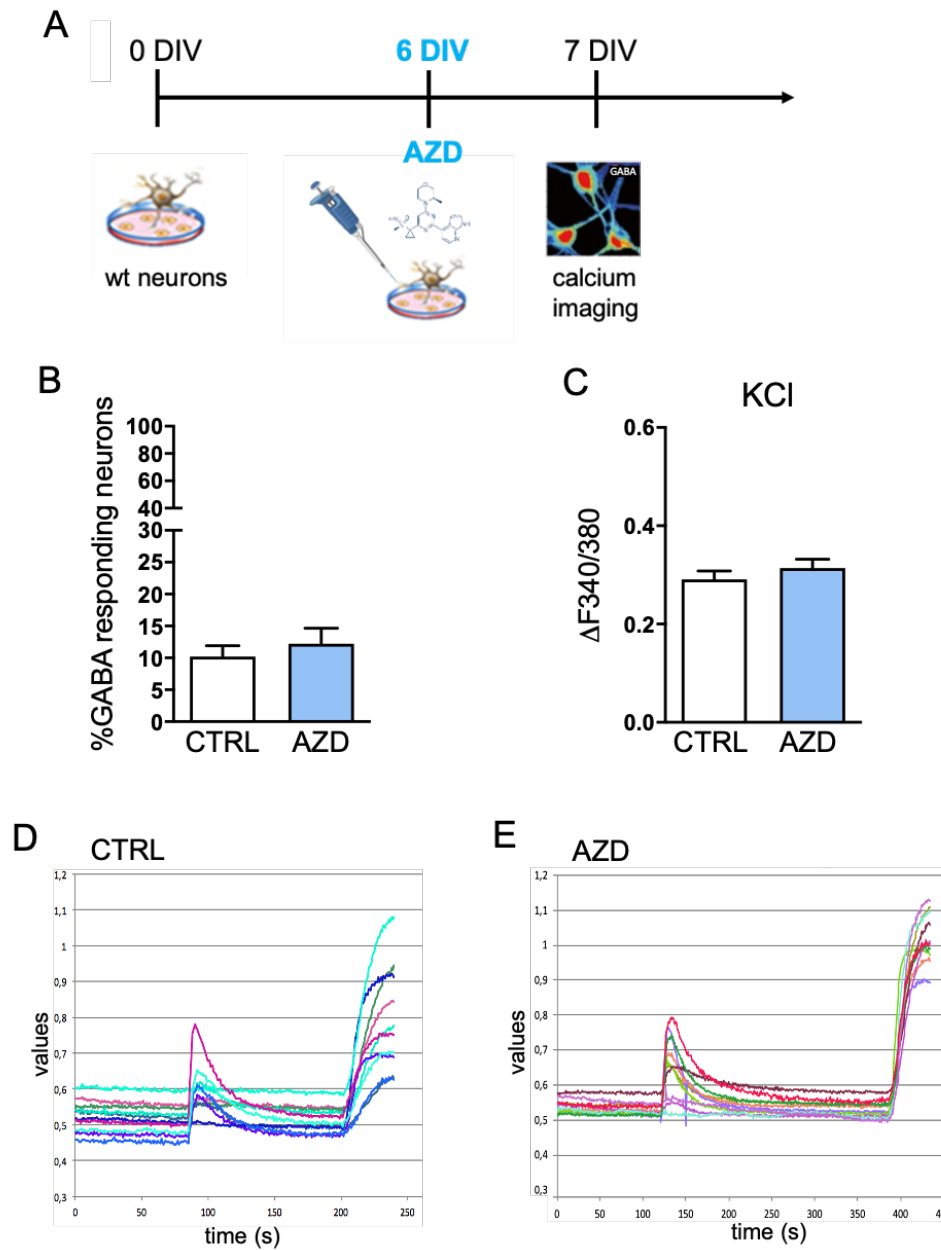
## **Evaluation of acute effects induced by AZD6738 on neuronal development**

Since recent results indicate that the DNA repair protein ATM controls development of the GABAergic system [149], we wanted to investigate if also ATR activity could generate a similar impact on neuronal development. To address this issue, we referred to a specific pathway that gives clear information regarding the GABAergic development: the excitatory-to-inhibitory switch of GABA (GABA switch). Indeed, at early stages of neuronal development, GABA acts as an excitatory neurotransmitter directly evoking action potentials and raising intracellular calcium levels in immature neurons. In fact in immature neurons, the activation of the GABA<sub>A</sub> receptor leads to the extrusion of chloride ions since the high intracellular chloride concentration generated by the strong expression levels of NKCC1, the chloride importer, and a low expression of the chloride exporter, KCC2 [150]. Then, during neuronal maturation, NKCC1 levels decrease, KCC2 expression increases and the normal low intracellular chloride concentrations is established, thus generating the typical intracellular chloride influx upon the GABA<sub>A</sub> receptor opening [158, 159]. From an experimental point of view, we can follow this transition by calcium imaging experiments; in fact, loading neurons with the calcium dye Fura-2AM, it is possible to detect calcium transients increments underlining neuronal depolarization.

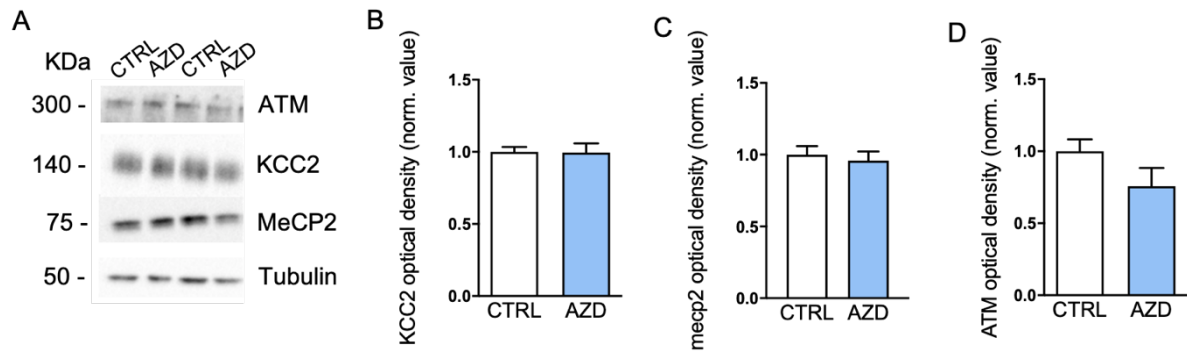
Ca<sup>2+</sup> imaging experiments were firstly performed on 7 DIV hippocampal neurons treated 24 hours earlier with AZD6738 1 μM. No significant differences were found among AZD-treated neurons and control cells as indicated by the similar percentage of neurons responding to GABA with neuronal depolarization (GABA 100 μM) and by comparable values of calcium increments (figure 9B). Since the aforementioned results directly depend on the voltage operated calcium channels (VOCC), we monitored possible VOCC changes in AZD-cells by measuring Ca<sup>2+</sup> transients evoked by a different depolarizing stimulation, KCl 50 mM. Once again no differences were found among the two groups (figure 9C). Altogether, these results demonstrate that inhibition of ATR activity in immature neurons has no impact on the excitatory-to-inhibitory GABAergic switch; interestingly they are coherent with recent evidence that exclude the involvement of ATR in different developmental processes in vivo.

Accordingly, biochemical analysis of the chloride cotransporter responsible for the GABA switch process, KCC2, as well as of transcription factors able to directly modulate KCC2 levels, namely MeCP2 [153] and ATM [154], revealed no changes in their expressions in our conditions (figure 10B, 10C and 10D).

Taken together, these data further confirm that loss of ATR activity does not impact GABAergic development; thus we looked at a possible involvement of ATR in mature hippocampal cells.



**Figure 9:** a) Scheme of the experimental time line of AZD treatment and related calcium imaging experiments. b) Percentage of 7 DIV hippocampal neurons, treated or not with AZD, responding to GABA application with depolarization (Mann-Whitney Test,  $p > 0,05$  ns. CTRL  $n=38$ ; AZD  $n=42$ ). c) Evaluation of KCl response in hippocampal neurons upon AZD or vehicle treatment (Mann-Whitney Test,  $p > 0,05$  ns. CTRL  $n=80$ ; AZD  $n=95$ ). d) and e) Representative traces of  $Ca^{2+}$  transients recorded from control neurons (d) and AZD-treated neurons (e); the first peak indicate the GABA response, whereas the second show the KCl-mediated depolarization.



**Figure 10:** a) Representative images of ATM, KCC2, MeCP2 expression in 7 DIV hippocampal neurons treated or not with AZD. b) Quantitative analysis of KCC2 expression (Unpaired T Test,  $p > 0,05$  ns. CTRL n=21; AZD n=21). c) Quantitative analysis of MeCP2 expression (Mann-Whitney Test,  $p > 0,05$  ns. CTRL n=21; AZD n=23). d) Quantitative analysis of ATM expression (Unpaired T Test,  $p > 0,05$  ns. CTRL n=9; AZD n=11).

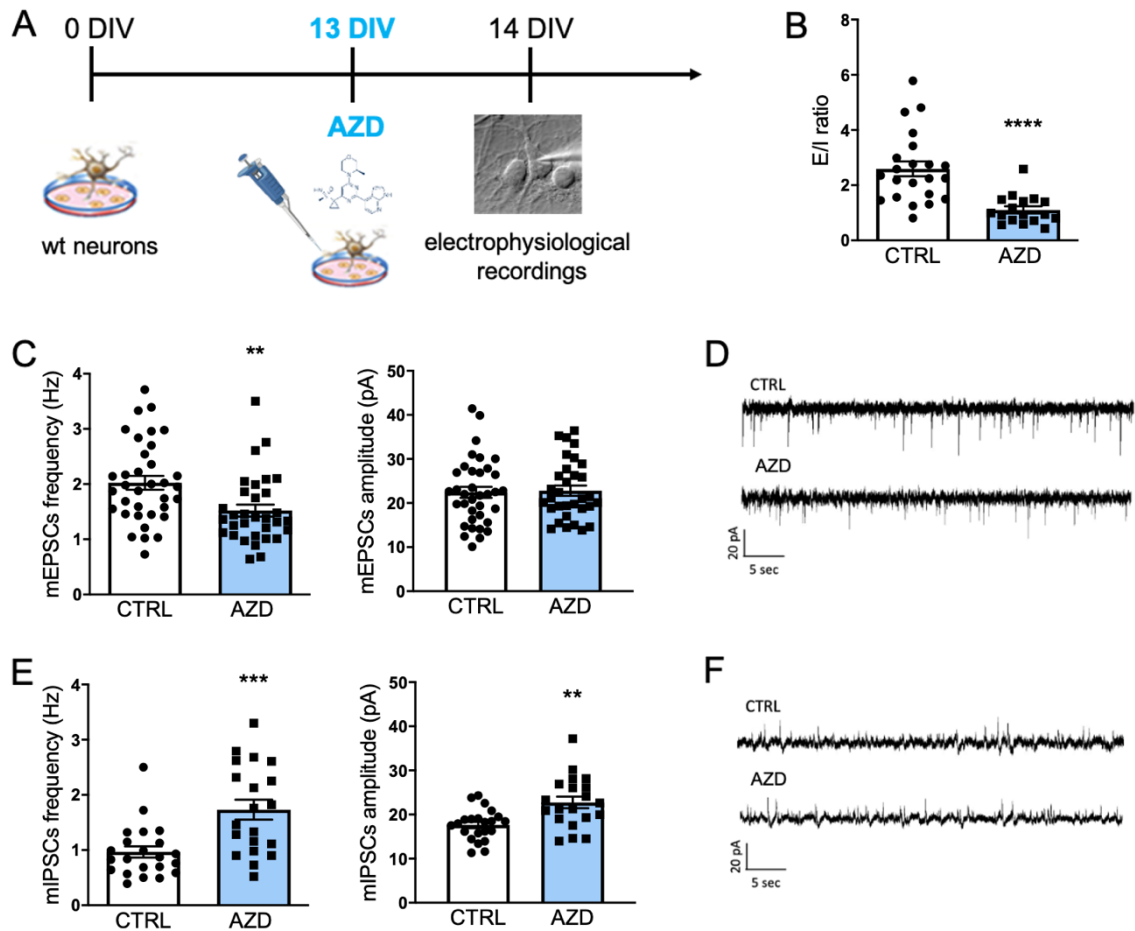
## **Evaluation of functional changes induced by ATR inhibition in mature neurons**

### **Acute treatment in mature neurons**

Supported by evidence that cytoplasmic ATR associates to synaptic vesicles [83], we decided to perform electrophysiological experiments monitoring possible changes in currents evoked by the spontaneous calcium-independent release of docked glutamatergic and GABAergic vesicle: the excitatory and inhibitory postsynaptic currents in miniature (mEPSCs and mIPSCs). We treated neurons with AZD6738 1  $\mu$ M (or vehicle, DMSO) and, the day after, we measured frequency and amplitude of mEPSCs and mIPSCs by blocking spontaneous spiking activity with the reversible sodium channels blocker tetrodotoxin (TTX, 1  $\mu$ M) by the means of whole-cell patch clamp recordings (see figure 11A). Indeed, frequency of miniature events, measured in Hertz (Hz), is the parameter influenced by the number of synaptic vesicles at the presynapse and by the number of presynaptic compartments overlooking the patched neurons. Differently, the amplitude is related to the number of receptors at the postsynaptic membrane, thus is a parameter strictly postsynaptic [162, 163].

Results showed in figure 11 revealed that a single application of AZD6738 impacts on the frequency of both mEPSCs and mIPSCs but in an opposite manner: AZD-neurons displayed a reduced frequency of mEPSCs and an increased frequency of mIPSCs (figure 11C and 11E). Accordingly, the excitatory/inhibitory (E/I) ratio analysed in individual cells was significantly reduced in hippocampal neurons treated 24 hours with the drug, meaning that inhibition of ATR activity directly modifies release of synaptic vesicles (figure 11B). Also, AZD-treated neurons displayed increased amplitude of mIPSCs, whereas mEPSCs amplitude showed no differences respect to control neurons (figure 11C and 11E). Taken together, these data suggest that loss of ATR activity controls also levels of GABA<sub>A</sub> receptors at the synapse, as suggested by the increased mIPSCs amplitude; thus, specific modifications occur both at the presynaptic and postsynaptic compartments.

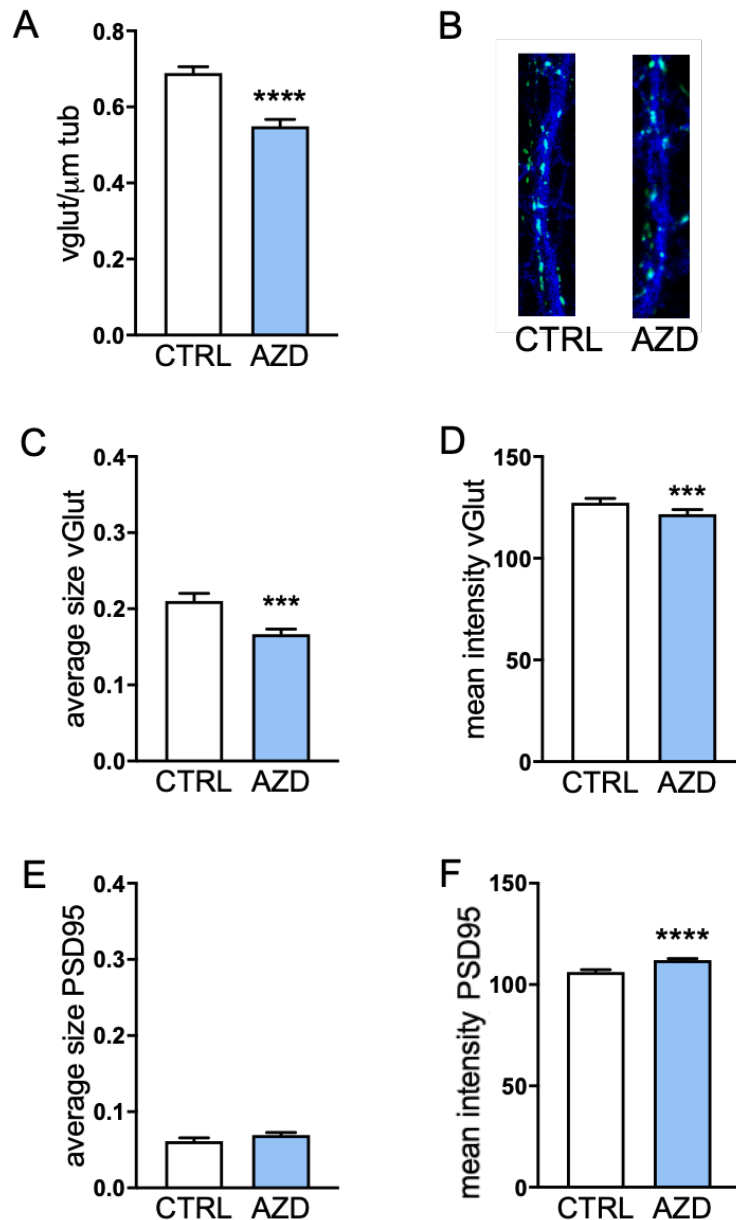




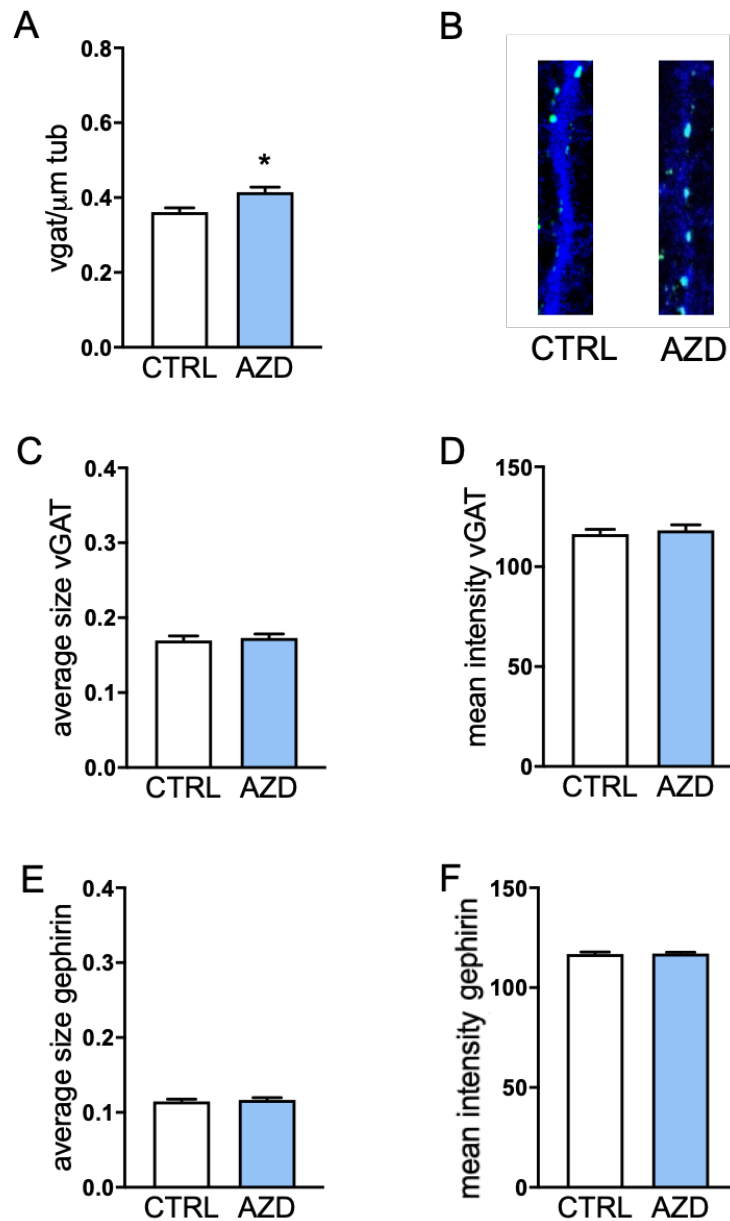
**Figure 11:** a) Scheme of the experimental timeline of AZD treatment and related electrophysiological experiments. b) Quantification of E/I ratio in 14 DIV hippocampal neurons upon AZD6738 acute treatment (Mann-Whitney Test, \*\*\*\*  $p < 0,0001$ . CTRL  $n = 22$ ; AZD  $n = 17$ ). c) Electrophysiological analysis of mEPSCs frequency and amplitude in 14 DIV hippocampal neurons, treated or not with AZD6738 (mEPSCs frequency: Mann-Whitney Test, \*\*  $p = 0,0014$ . CTRL  $n = 35$ ; AZD  $n = 32$ ; mEPSCs amplitude: Unpaired T Test,  $p > 0,05$  ns. CTRL  $n = 36$ ; AZD  $n = 32$ ). d) Representative electrophysiological traces of excitatory miniature post-synaptic currents measured in 14 DIV neurons. e) Electrophysiological analysis of mIPSCs frequency and amplitude in 14 DIV hippocampal neurons, treated or not with AZD6738 (mIPSCs frequency: Mann-Whitney Test, \*\*\*  $p = 0,0007$ . CTRL  $n = 22$ ; AZD  $n = 20$ ; mIPSCs amplitude: Unpaired T Test, \*\*  $p = 0,0012$ . CTRL  $n = 22$ ; AZD  $n = 20$ ). f) Representative electrophysiological traces of excitatory miniature post-synaptic currents measured in 14 DIV neurons.

We also performed immunocytochemical experiments in 14 DIV hippocampal neurons similarly treated with AZD6738 and significant changes were highlighted. In particular, analysis of the density of excitatory synapses, identified by positive immune-reactivity against the vesicular glutamate transporter vGlut1 per unit length of dendrite, confirmed a reduced presynaptic puncta number in AZD6738 cultures (figure 12A); coherently, vGlut1 positive puncta also showed a lower “mean fluorescence intensity” and “average size” (figure 12C and 12D), two additional quantitative parameters here evaluated. Immunoreactivity against PSD95, a postsynaptic protein of the excitatory compartment, revealed comparable “average size” signals and a slight even if significant increased “mean fluorescence intensity” (figure 12F). In regards of the inhibitory synapses, it was found an increased number of vGAT positive puncta per unit length of dendrites in AZD-treated neurons (figure 13A), confirming the higher number of GABAergic presynapses highlighted by electrophysiology. Normal “mean fluorescence intensity” and “average size” were detected for vGAT puncta. Also, similar results were collected regarding gephyrin positive puncta, the scaffolding protein of the postsynaptic inhibitory compartment (figure 13C-F).

Taken together, all these data indicate that 24 hours inhibition of the ATR kinase activity in mature hippocampal neurons produces an imbalanced neuronal network favoring the inhibitory transmission, as observed by electrophysiological and immunocytochemical experiments.



**Figure 12:** a) Quantitative analysis of vGlut1 puncta density in 14 DIV hippocampal neurons upon AZD6738 acute treatment (Mann-Whitney Test, \*\*\*\*  $p < 0,0001$ .  $N = 3$  experiments,  $n = 1$  coverslips for each experiment). b) Representative immunofluorescence images of neuronal branches labelled with the specific excitatory presynaptic marker vGlut1 (green) and B $_{III}$ -tubulin (blue) to highlight neuronal processes. c-d) Quantitative analysis of average size (c) and mean intensity (d) of vGlut1 positive puncta in AZD-treated neurons with respect to controls (Average size: Mann-Whitney Test, \*\*\*  $p = 0,0002$ . Mean intensity: Mann-Whitney Test, \*\*\*  $p = 0,0005$ .  $N = 3$  experiments,  $n = 1$  coverslips for each experiment). e-f) Quantitative analysis of average size (e) and mean intensity (f) of PSD95 positive puncta in AZD-treated neurons with respect to controls (Average size: Mann-Whitney Test,  $p > 0,5$  ns. Mean intensity: Unpaired T Test, \*\*\*\*  $p < 0,0001$ .  $N = 3$  experiments,  $n = 1$  coverslips for each experiment).



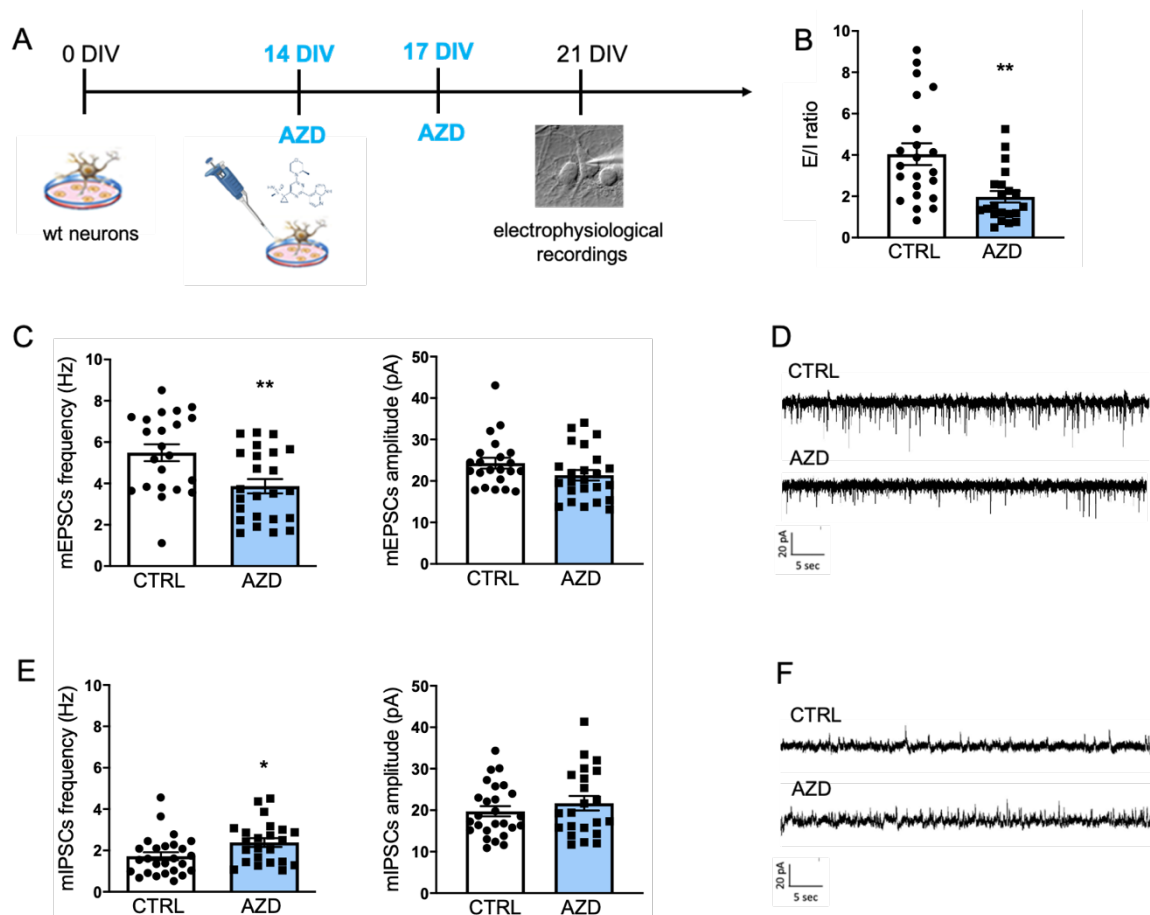
**Figure 13:** a) Quantitative analysis of vGAT puncta density in 14 DIV hippocampal neurons upon AZD6738 acute treatment (Mann-Whitney Test, \*  $p=0,0162$ .  $N=3$  experiments,  $n=1$  coverslips for each experiment). b) Representative immunofluorescence images of neuronal branches labelled with the specific inhibitory presynaptic marker vGAT (green) and BIII-tubulin (blue) to highlight neuronal processes. c-d) Quantitative analysis of average size (c) and mean intensity (d) of vGAT positive puncta in AZD-treated neurons with respect to controls (Average size: Mann-Whitney Test,  $p>0,05$  ns. Mean intensity: Mann-Whitney Test,  $p>0,05$  ns.  $N=3$  experiments,  $n=1$  coverslips for each experiment). e-f) Quantitative analysis of average size (e) and mean intensity (f) of gephyrin positive puncta in AZD-treated neurons with respect to controls (Average size: Unpaired T Test,  $p>0,5$  ns. Mean intensity: Unpaired T Test,  $p>0,5$  ns.  $N=3$  experiments,  $n=1$  coverslips for each experiment).

### **Chronic treatment in mature neurons**

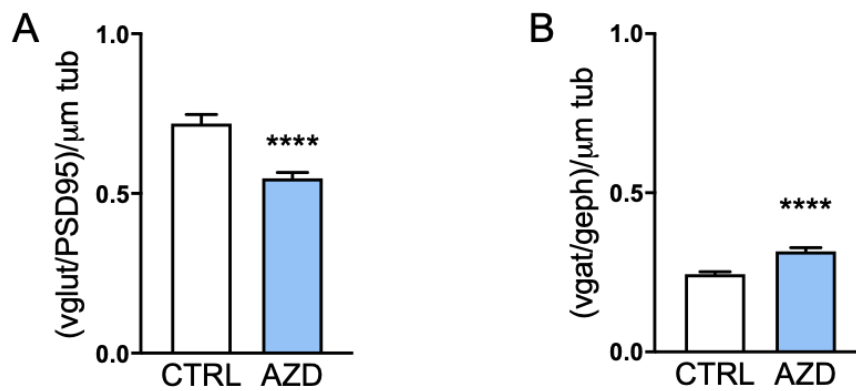
We evaluated the effects induced by a long-lasting ATR inhibition, that is for an entire week. Similar to what was previously found, in 21 DIV neurons treated with AZD6738 according to the chronic protocol (every three days in a week) electrophysiological experiments indicate that postsynaptic currents in miniature (mEPSCs and mIPSCs) were profoundly affected by the treatment: indeed, it was recorded a significant change in both frequency and amplitude of mEPSCs and mIPSCs. As indicated in figure 14, AZD-neurons showed a decreased mEPSCs frequency and an increased frequency of mIPSCs; consequently, a strong modification of the E/I ratio was obtained, favoring the establishment of a more inhibited tone (figure 14B). No differences in terms of amplitude have been found (figure 14C and 14E). Taken together, these data confirmed the results already obtained in the case of an acute AZD6738 treatment and suggest that a chronic ATR inhibition preferentially impacts the presynaptic compartments of both excitatory and inhibitory synapses.

Immunocytochemical experiments in 21 DIV hippocampal neurons chronically treated with the drug confirmed substantial changes in the neuronal network. Density of the complete excitatory synapses was reduced, whereas density of the complete inhibitory synapses was found increased (figure 15). In particular, no changes of both the excitatory and inhibitory postsynaptic markers (namely PSD95 and gephyrin) have been detected in AZD-neurons (figure 16C, 16D, 17C and 17D); whereas, in treated cultures, analysis of vGlut1 positive puncta displayed a lower distribution per unit length of dendrite (figure 16A) and an increase in the vesicular GABA transporter vGAT (figure 17A). In terms of “mean fluorescence intensity” and “average size” for the vGlut1 and vGAT immunoreactivity no differences were found in our experimental groups (figure 16B and 17B).

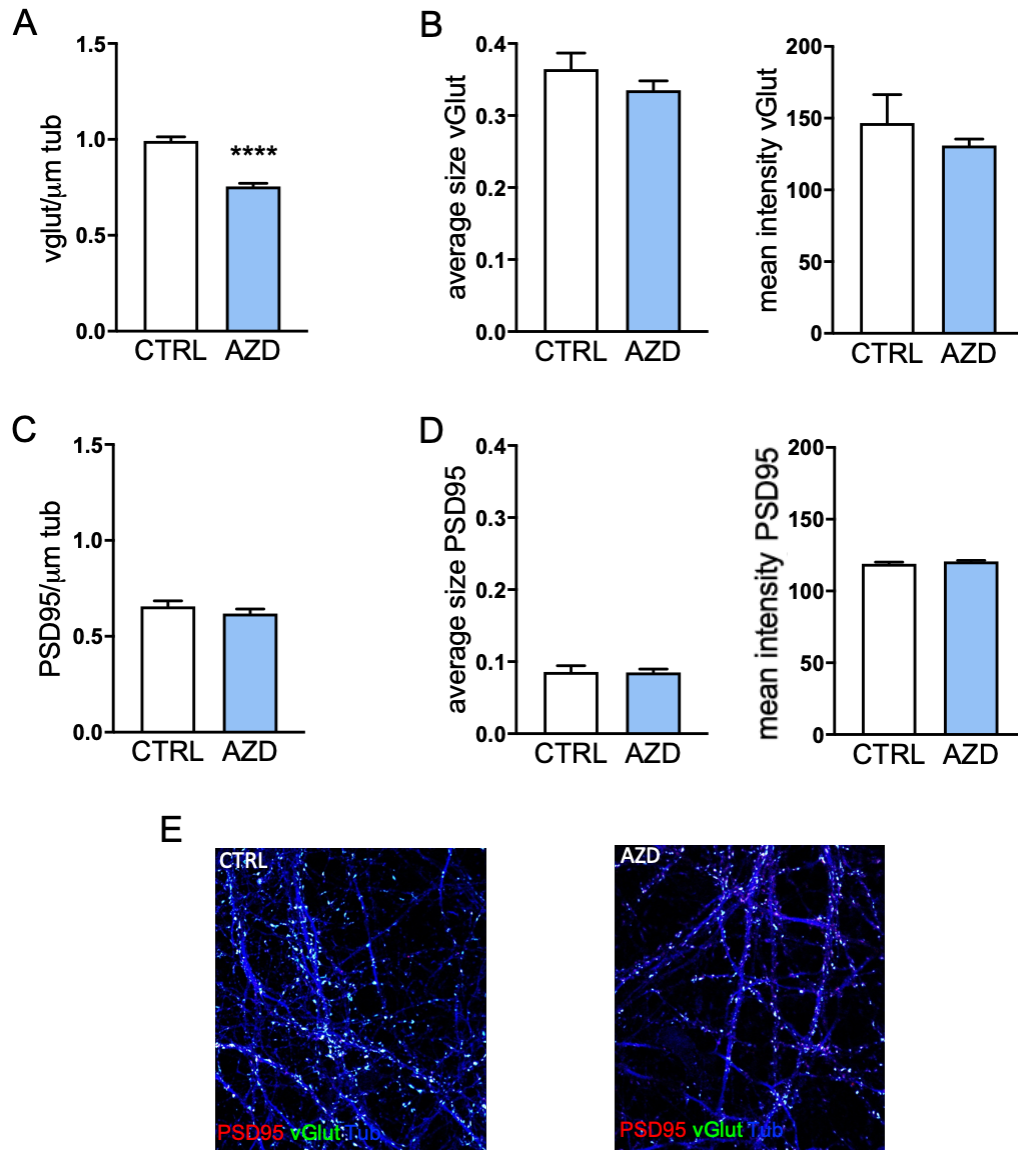
Altogether these data confirm that chronic ATR inhibition in mature hippocampal neurons induces a marked imbalance between excitation and inhibition, affecting preferentially the presynaptic compartment and leaving unaffected the abundance of both AMPA and GABA<sub>A</sub> receptors.



**Figure 14:** a) Scheme of the experimental time line of AZD treatment and related electrophysiological experiments. b) Quantification of E/I ratio in 21 DIV hippocampal neurons upon AZD6738 chronic treatment (Mann-Whitney Test, \*\*  $p=0,0010$ . CTRL  $n=22$ ; AZD  $n=21$ ). c) Electrophysiological analysis of mEPSCs frequency and amplitude in 21 DIV hippocampal neurons, treated or not with AZD6738 (mEPSCs frequency: Unpaired T Test, \*\*  $p=0,0039$ . CTRL  $n=22$ ; AZD  $n=24$ ; mEPSCs amplitude: Mann-Whitney Test,  $p>0,05$  ns. CTRL  $n=22$ ; AZD  $n=24$ ). d) Representative electrophysiological traces of excitatory miniature post-synaptic currents measured in 21 DIV neurons. e) Electrophysiological analysis of mIPSCs frequency and amplitude in 21 DIV hippocampal neurons, treated or not with AZD6738 (mIPSCs frequency: Unpaired T Test, \*  $p=0,0225$ . CTRL  $n=26$ ; AZD  $n=23$ ; mIPSCs amplitude: Mann-Whitney Test,  $p>0,05$  ns. CTRL  $n=26$ ; AZD  $n=23$ ). f) Representative electrophysiological traces of excitatory miniature post-synaptic currents measured in 21 DIV neurons.

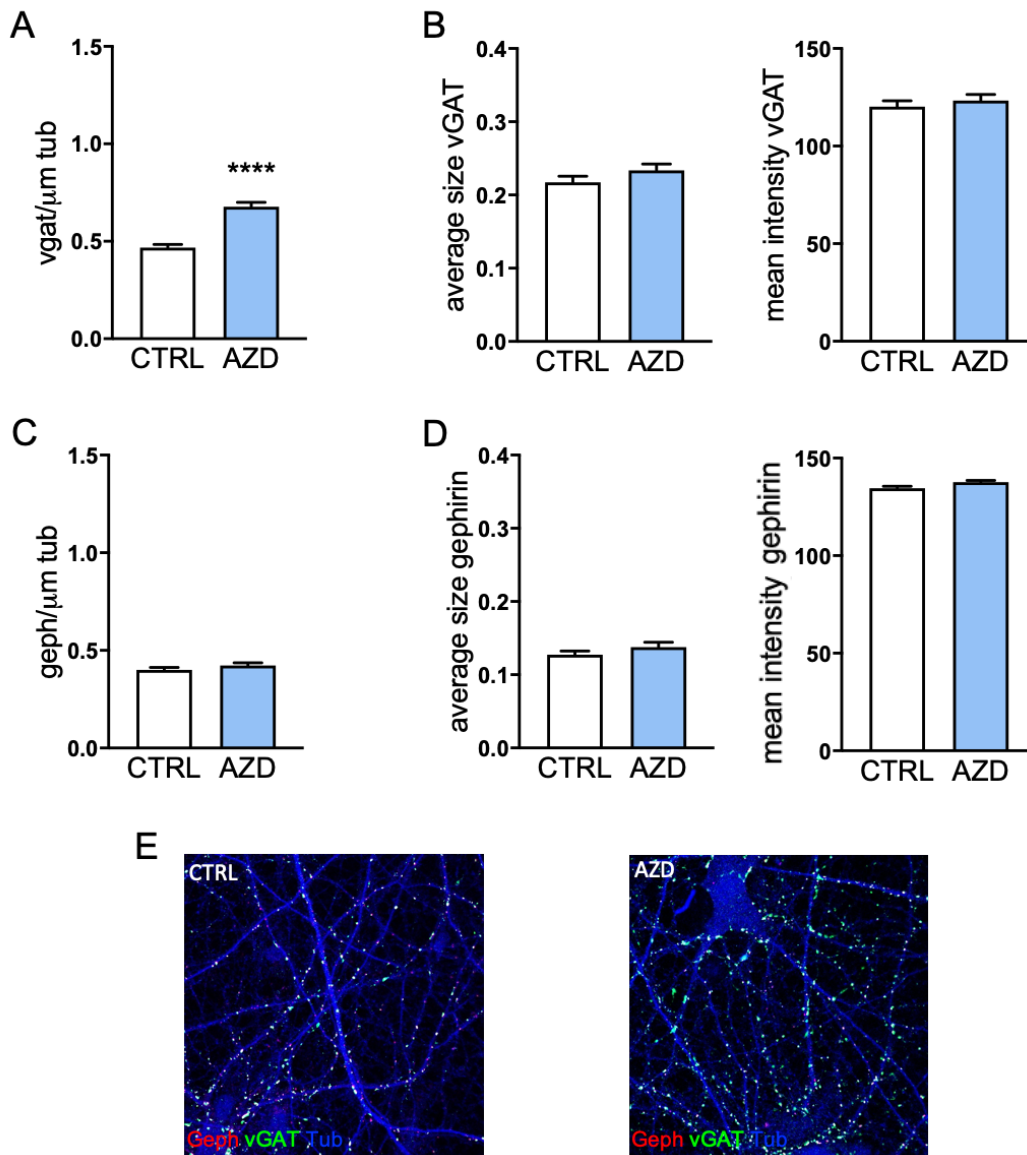


**Figure 15:** a) Quantitative analysis of vGlut1+PSD95 colocalizing puncta (complete excitatory synapse) density in 21 DIV hippocampal neurons upon AZD6738 chronic treatment (Mann-Whitney Test, \*\*\*\*  $p < 0,0001$ . N=3 experiments, n=1 coverslips for each experiment). b) Quantitative analysis of vGAT+gephyrin colocalizing puncta (complete inhibitory synapse) density in 21 DIV hippocampal neurons upon AZD6738 chronic treatment (Mann-Whitney Test, \*\*\*\*  $p < 0,0001$ . N=3 experiments, n=1 coverslips for each experiment).



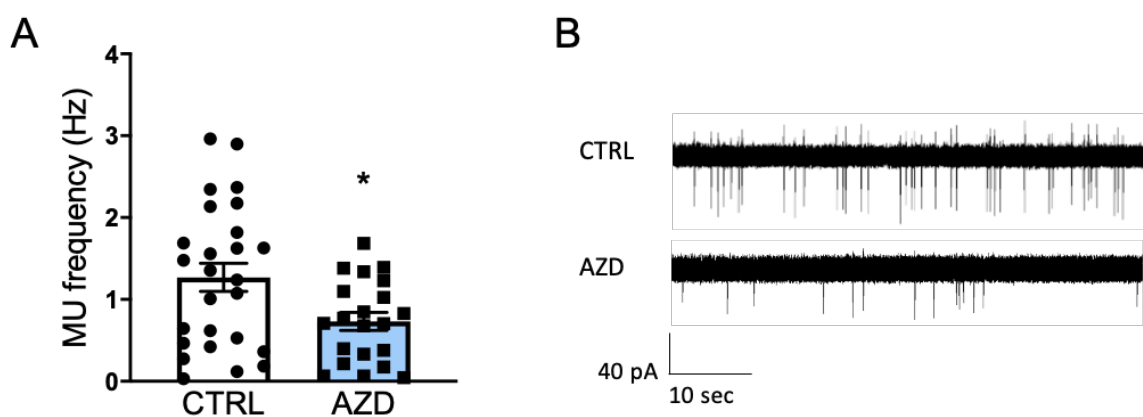
**Figure 16:** a) Quantitative analysis of vGlut1 puncta density in 21 DIV hippocampal neurons upon AZD6738 chronic treatment (Mann-Whitney Test, \*\*\*\*  $p < 0,0001$ . N=3 experiments, n=1 coverslips for each experiment). b) Quantitative analysis of average size and mean intensity of vGlut1 positive puncta in AZD-treated neurons with respect to controls (Average size: Mann-Whitney Test,  $p > 0,05$  ns. Mean intensity: Mann-Whitney Test,  $p > 0,05$  ns. N=3 experiments, n=1 coverslips for each experiment). c) Quantitative analysis of PSD95 puncta density in 21 DIV hippocampal neurons upon AZD6738 chronic treatment (Mann-Whitney Test,  $p > 0,05$  ns. N=3 experiments, n=1 coverslips for each experiment). d) Quantitative analysis of average size and mean intensity of PSD95 positive puncta in AZD-treated neurons with respect to controls (Average size: Mann-Whitney Test,  $p > 0,05$  ns. Mean intensity: Mann-Whitney Test,  $p > 0,05$  ns. N=3 experiments, n=1 coverslips for each experiment). e) Representative immunofluorescence images of neuronal branches labelled with the specific excitatory marker vGlut1 (green - presynaptic), PSD95 (red – postsynaptic) and B<sub>III</sub>-tubulin (blue) to highlight neuronal processes.





**Figure 17:** a) Quantitative analysis of vGAT puncta density in 21 DIV hippocampal neurons upon AZD6738 chronic treatment (Mann-Whitney Test, \*\*\*\*  $p < 0,0001$ .  $N = 3$  experiments,  $n = 1$  coverslips for each experiment). b) Quantitative analysis of average size and mean intensity of vGAT positive puncta in AZD-treated neurons with respect to controls (Average size: Unpaired T Test,  $p > 0,05$  ns. Mean intensity: Mann-Whitney Test,  $p > 0,05$  ns.  $N = 3$  experiments,  $n = 1$  coverslips for each experiment). c) Quantitative analysis of gephyrin puncta density in 21 DIV hippocampal neurons upon AZD6738 chronic treatment (Mann-Whitney Test,  $p > 0,05$  ns.  $N = 3$  experiments,  $n = 1$  coverslips for each experiment). d) Quantitative analysis of average size and mean intensity of gephyrin positive puncta in AZD-treated neurons with respect to controls (Average size: Unpaired Test,  $p > 0,05$  ns. Mean intensity: Mann-Whitney Test,  $p > 0,05$  ns.  $N = 3$  experiments,  $n = 1$  coverslips for each experiment). e) Representative immunofluorescence images of neuronal branches labelled with the specific excitatory marker vGAT (green - presynaptic), gephyrin (red – postsynaptic) and B<sub>III</sub>-tubulin (blue) to highlight neuronal processes.

Since a similar modification of the neuronal network points to a reduced release of glutamatergic vesicles (or of glutamatergic synapses) and to an increased release of the GABAergic vesicles (or higher density of inhibitory synapses), we decided to better characterize the electrophysiological properties of AZD-neurons recording, in the cell attached modality, the multiunit activity, which reflects action potential firing of neurons [157]. Accordingly, neurons chronically treated with AZD6738 showed a reduced spike frequency in contrast to DMSO-treated control neurons (figure 18A).

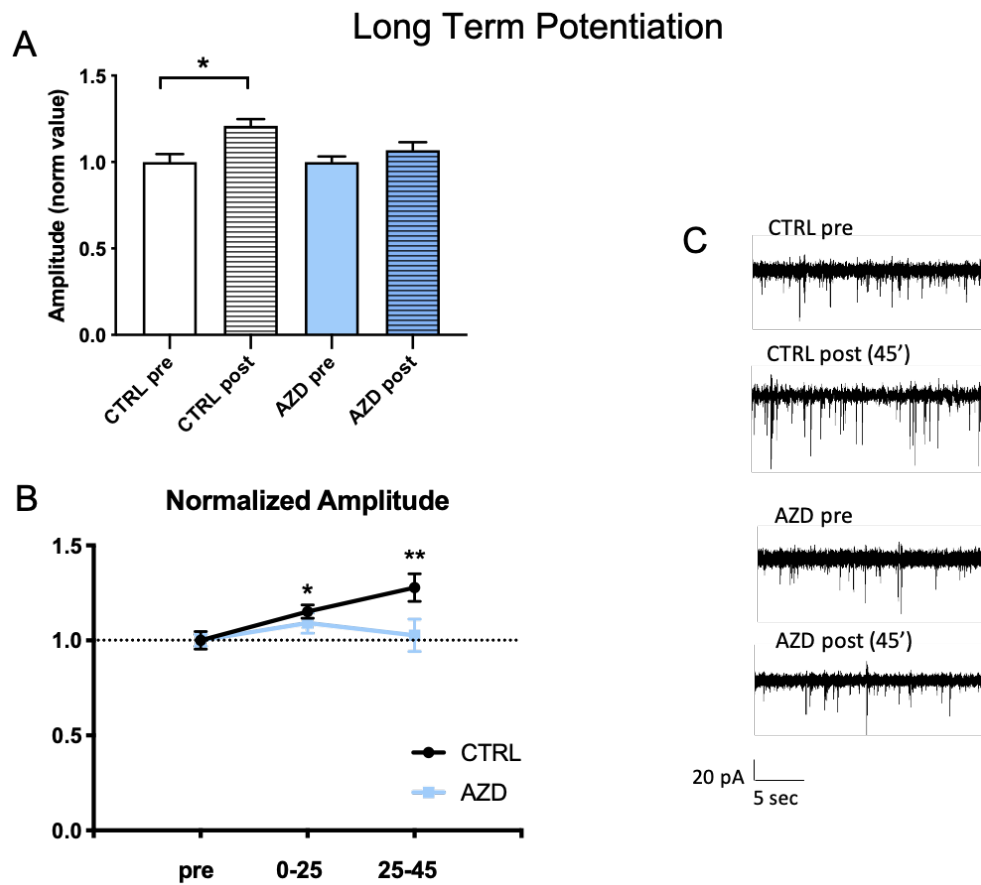


**Figure 18:** a) Quantification of Multi Unit activity upon AZD6738 chronic treatment (Unpaired T Test, \*  $p=0,0156$ . CTRL  $n=26$ ; AZD  $n=21$ ). b) Representative electrophysiological traces of spiking events recorded in control and AZD-treated hippocampal neurons.

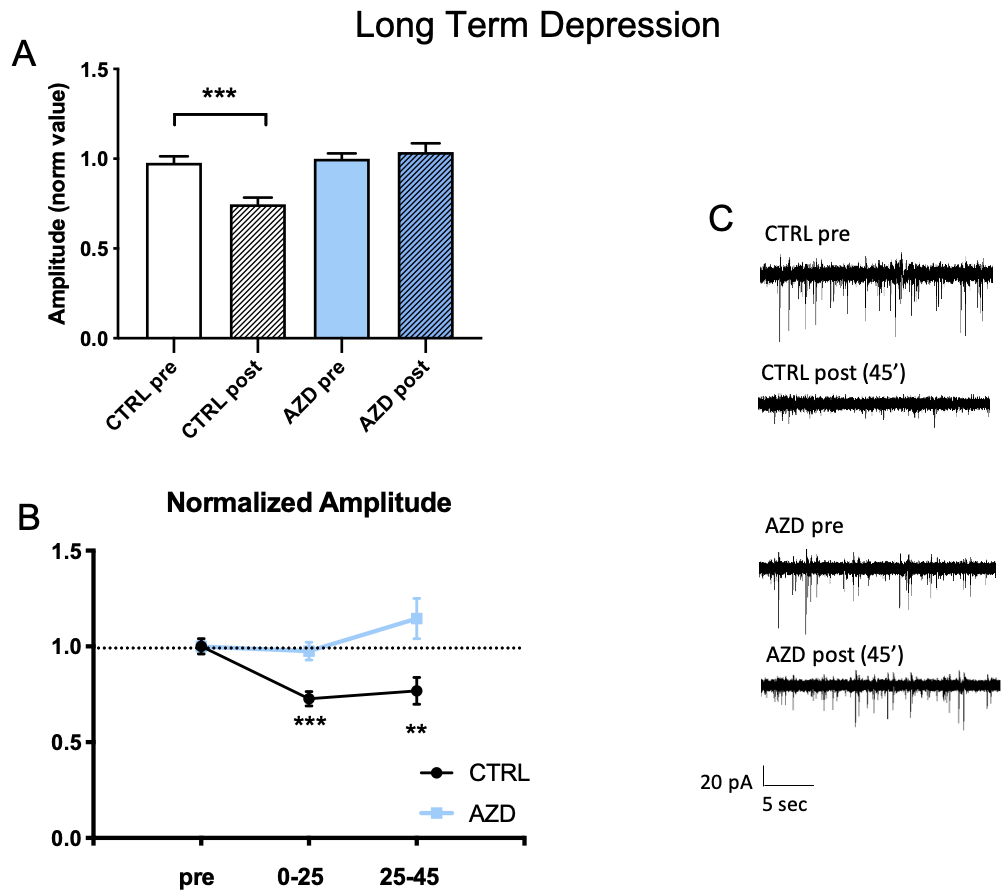
Finally, to assess a full characterization of neuronal properties upon a long lasting ATR inhibition, we investigated possible changes in the long term potentiation (LTP) and long term depression (LTD) processes. As already described in the methods section, mature hippocampal neurons were subjected to chemical induction of both LTP and LTD [158]. As shown in figure 19 and in figure 20, DMSO-control neurons adequately responded to chemical induction as evidenced by the constant increased excitatory events amplitude along the experimental time upon LTP induction (figure 19B); whereas, a diminished excitatory events amplitude was recorded upon LTD induction (figure 20B). On the contrary, in AZD-neurons plasticity defects were clearly detected: no changes, increase nor

decrease, in the amplitude parameters have been collected after, respectively, LTP or LTD induction (figure 19A and 20A). Also, LTP and LTD mechanisms have been evaluated in control and AZD-neurons by immunocytochemistry through the analysis of PSD95 density, which is a parameter usually exploited to characterized postsynaptic changes at the excitatory synapses upon plasticity protocol [165, 166]. Coherently to electrophysiology, control neurons showed an increased PSD95 density 45 minutes after LTP induction and reduced PSD95 density in case of LTD induction (figure 21A); no changes were instead obtained in the case of neurons chronically treated with the AZD6738, either after LTP or LTD chemical protocol (figure 21B). Thus, these results confirm that AZD-neurons are strongly affected by chronic ATR inhibition showing a disrupted E/I equilibrium and a significant inability to undergo plasticity processes, either strengthening or weakening the synapses.

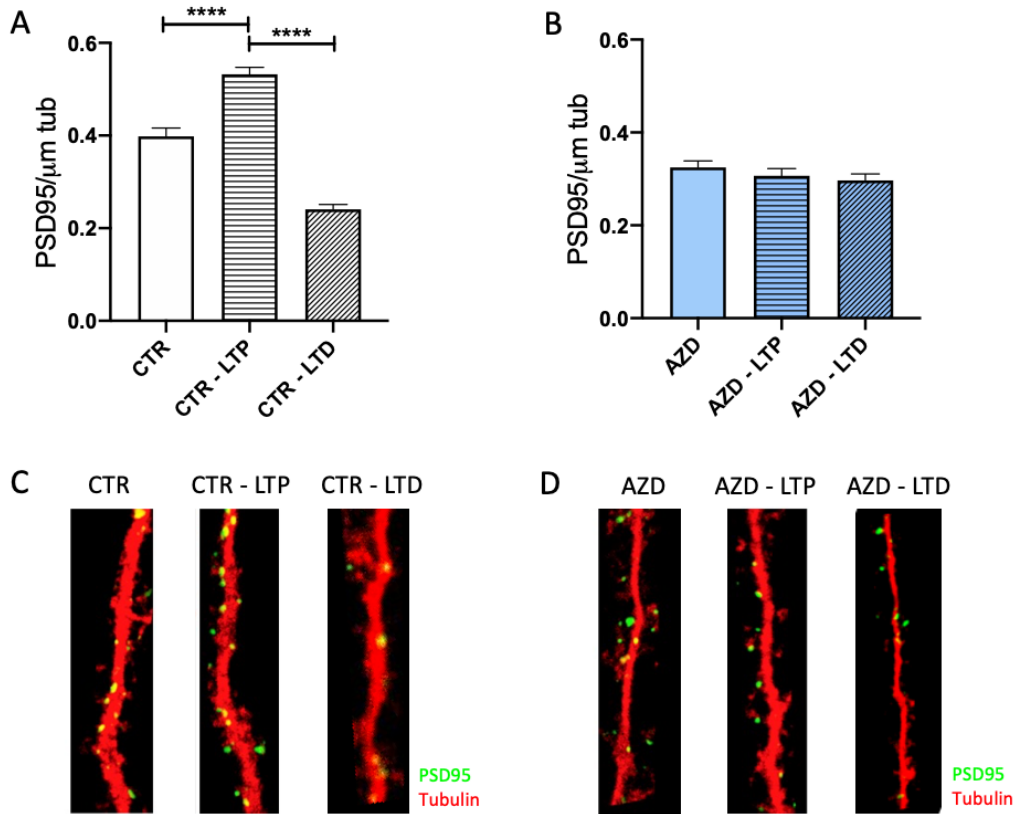
All together our electrophysiological and confocal data suggest that, in terms of neuronal transmission and function, the pharmacological inhibition of ATR (both the acute and chronic inhibition) in hippocampal neurons generates a network enriched of inhibitory synapses, lowered of glutamatergic puncta and overall less excitable, as evidenced by the multi-unit analysis. Considering all the above, we hypothesized that AZD6738 may represent a new strategy against epilepsy and ATR kinase a new biological target in neurological conditions associated to hyperexcitability.



**Figure 19:** a) Normalized analysis of excitatory events amplitude before and after LTP promotion in control and AZD-treated neurons (One-Way ANOVA followed by Tukey's Multiple Comparison Test, \*\*  $p=0,0035$ . CTRL pre  $n=23$ ; CTRL post  $n=33$ ; AZD pre  $n=28$ ; AZD post  $n=46$ ). b) Graphical representation of amplitude variation during the experimental procedures (CTRL: One-Way ANOVA followed by Holm-Sidak's Multiple Comparison Test, \*\*  $p=0,0041$ . CTRL  $n=23$ ; CTRL 0-25  $n=15$ ; CTRL 25-45  $n=18$ . AZD: One-Way ANOVA followed by Holm-Sidak's Multiple Comparison Test,  $p>0,05$  ns. AZD pre  $n=28$ ; AZD 0-25  $n=22$ ; AZD 25-45  $n=23$ ). c) Representative electrophysiological traces of excitatory events recorded in control and AZD-treated hippocampal neurons, before and after LTP chemical induction.



**Figure 20:** a) Normalized analysis of excitatory events amplitude before and after LTD promotion in control and AZD-treated neurons (Kruskal-Wallis followed by Dunn's Multiple Comparison Test, \*\*\*\*  $p < 0,0001$ . CTRL pre  $n = 26$ ; CTRL post  $n = 38$ ; AZD pre  $n = 32$ ; AZD post  $n = 36$ ). b) Graphical representation of amplitude variation during the experimental procedures (CTRL: Kruskal-Wallis followed by Dunn's Multiple Comparison Test, \*\*\*  $p = 0,0001$ . CTRL  $n = 27$ ; CTRL 0-25  $n = 17$ ; CTRL 25-45  $n = 21$ . AZD: Kruskal-Wallis followed by Dunn's Multiple Comparison Test,  $p > 0,05$  ns. AZD pre  $n = 32$ ; AZD 0-25  $n = 18$ ; AZD 25-45  $n = 18$ ). c) Representative electrophysiological traces of excitatory events recorded in control and AZD-treated hippocampal neurons, before and after LTP chemical induction.



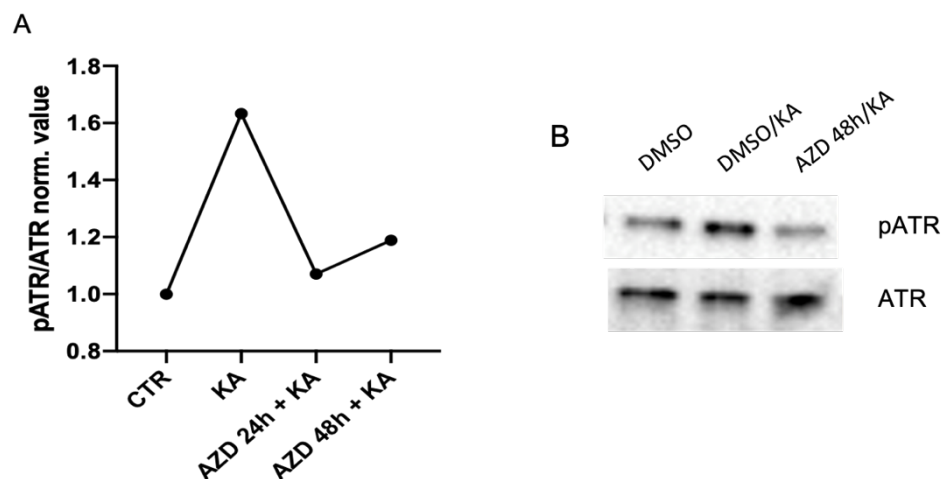
**Figure 21:** a) Quantitative analysis of PSD95 puncta density in control hippocampal neurons upon chemical induction of LTP and LTD (Kruskal-Wallis followed by Dunn's Multiple Comparison Test, \*\*\*\*  $p < 0,0001$ . N=1 experiments, n=2 coverslips for each experiment). b) Quantitative analysis of PSD95 puncta density in AZD-treated hippocampal neurons upon chemical induction of LTP and LTD (Kruskal-Wallis followed by Dunn's Multiple Comparison Test,  $p > 0,05$  ns. N=1 experiments, n=2 coverslips for each experiment). c) Representative immunofluorescence images of CTRL neuronal branches labelled with PSD95 (green) and B<sub>III</sub>-tubulin (red). d) Representative immunofluorescence images of AZD neuronal branches labelled with PSD95 (green) and B<sub>III</sub>-tubulin (red).

## Assessment of in vivo action of AZD6738

### **AZD6738 in vivo duration of action**

To further demonstrate and characterize the functioning of the ATR inhibitor and unveil the molecular mechanism responsible for the functional defects previously described, we investigated AZD6738 effectiveness in vivo. To this purpose, we performed intranasal administration of AZD6738 at the dose of 20 mg/kg in P90 (post-natal day) male wild type mice. We chose this administration paradigm since, by using a low dosage, the intranasal administration allows a good brain bioavailability and prevents the generation of unspecific effects at the periphery [167, 168]. We delivered the ATR inhibitor in adult mice and 24 or 48 hours later we administered kainic acid (KA, 25 mg/kg) intraperitoneally, since KA is known to promote a sustained neuronal hyperactivation as convulsant agent [162] and also to induce DNA damages, thus leading to the activation of ATR kinase activity [163]. Hippocampal tissues have been collected three hours later KA delivery and Western Blotting analysis was carried out to measure the pATR/ATR ratio.

As it is depicted from the graph (figure 22A), KA injection was able to increase the pATR/ATR ratio in DMSO-mice but not in animals treated with the drug one or two days earlier. Thus, Western Blotting analysis reveals that in vivo, upon intranasal delivery, the ATR inhibitor remains active for about 48 hours.



**Figure 22:** a) Western Blotting analysis of AZD6738 duration of action in hippocampal tissues collected from P90 wild type mice treated with kainic acid (25 mg/kg) or kainic acid (25 mg/kg) plus AZD6738 20 mg/kg. The graph shows that the ATR inhibitor action persists for at about 48 hours. b) Representative image of Western Blotting experiments carried out on P90 hippocampal tissues.

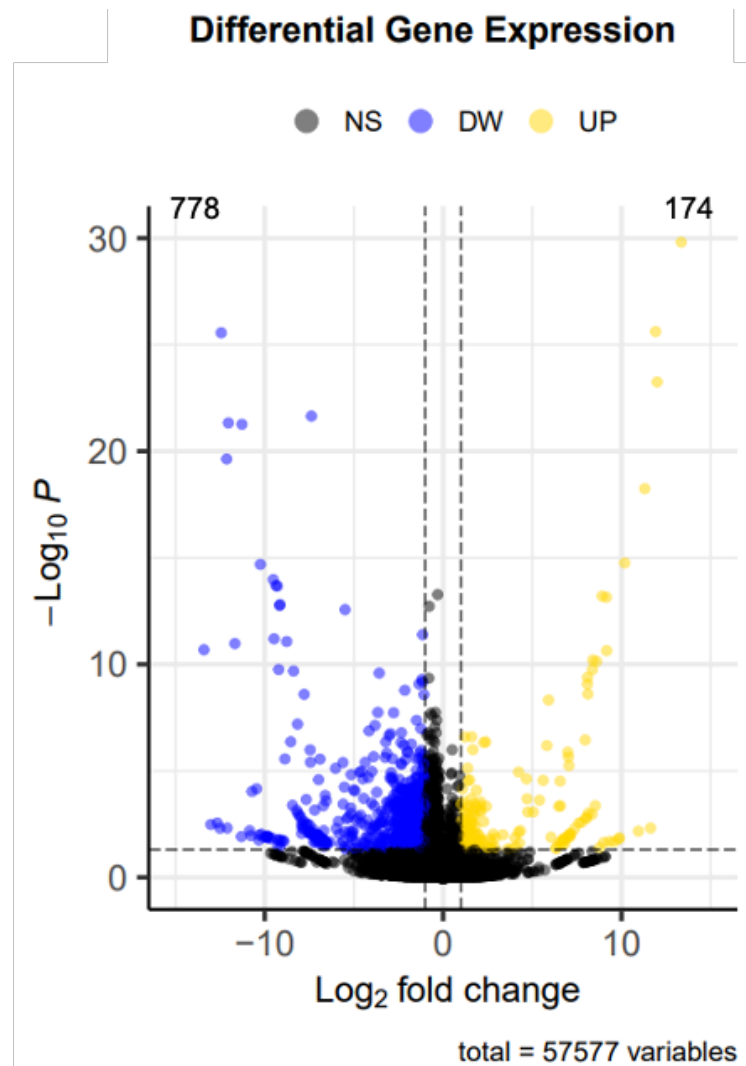
### **AZD6738 acts a master downregulator**

Having characterized the drug duration of action *in vivo*, we examined the transcriptional changes linked to the AZD6738 intranasal administration by RNA-sequencing experiments, by the fruitful collaboration with Giovanni Provenzano's group at the Trento University. P90 male wild type mice were subject to a single intranasal injection of AZD6738 or DMSO and then, 48 hours later, hippocampal tissues were collected for investigation of RNA profiling by Next Generation Sequencing (NGS). We identified n=952 deregulated genes, of which n=174 upregulated and n=778 downregulated (figure 23), thus suggesting for the ATR blocker a role of transcriptional downregulator. As highlighted by the bioinformatic analysis, in the repositories "Cellular Component" and "Molecular Function" from GEO, among the downregulated genes group we found a significant enrichment in terms such as "glutamatergic synapses, modulation of synaptic transmission, postsynaptic specialization and regulation of synaptic plasticity" (figure 24), thus strongly confirming our *in vitro* results by which both the acute and chronic ATR blockade results in a reduction of excitatory transmission. Also, looking at the list of transcriptional factors deregulated in hippocampi of AZD-treated mice, we found a long list of deregulated genes and one of the most significant was the *Egr1* transcription factor (figure 25). *Egr1* is known to be involved in the maintenance of neuronal plasticity as well as in spontaneous neurotransmission [171, 172]. Importantly, recent findings described *Egr1* as a key transcriptional regulator for genes involved in the development of hyperexcitability during epileptogenesis; indeed, recent results show that *Egr1* drives the expression of the voltage-gated calcium channel subunit  $\alpha_2\delta_4$ , which is augmented early and persistently after pilocarpine-induced SE [166]. Coherently, in hippocampal biopsies from epileptic individuals, increased expression levels of *Egr1* have been detected. Finally, to highlight potential similarity between AZD6738 and common antiepileptic drugs (AEDs), we queried several drug repositories among which "Drug perturbation from GEO" and "Drug Matrix". The bioinformatic analysis confirmed that AZD treatment shares DEGs with commonly used AEDs, corroborating our working hypothesis to exploit AZD6738 as anticonvulsant agent.

In conclusion, RNA seq data not only confirmed our hypothesis that the blockade of ATR activity may prevent hyperexcitability, as suggested by similarities with genes deregulated by AEDs and by the deregulation of genes responsible for



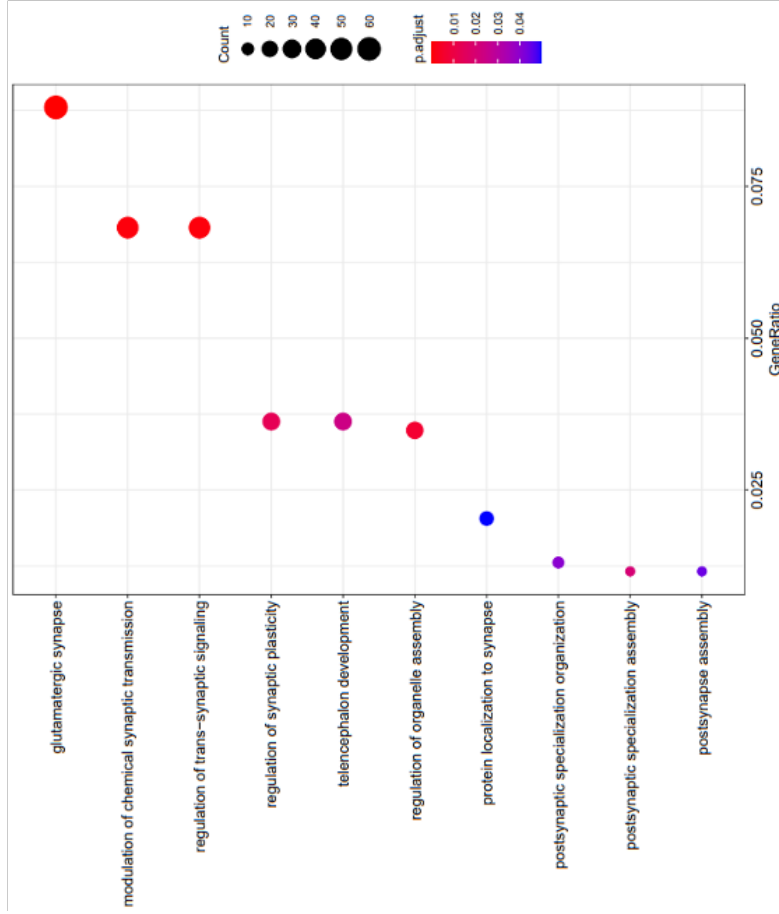
excitatory synapse composition, but also add important information regarding the specific molecular factor directly linked to the ATR inhibition, that is Egr1: importantly, Egr1 has been recently included among the master regulator transcription factor in epilepsy, whose activation drives epileptogenesis rearrangements. Thus, we decided to investigate the Egr1 mRNA levels upon hyperexcitability.



**Figure 23:** RNA profiling performed in hippocampi of DMSO- and AZD-treated mice revealed that the ATR blocker acts as a master downregulator. Volcano Plot representing the deregulated genes: 778 downregulated and 174 upregulated.

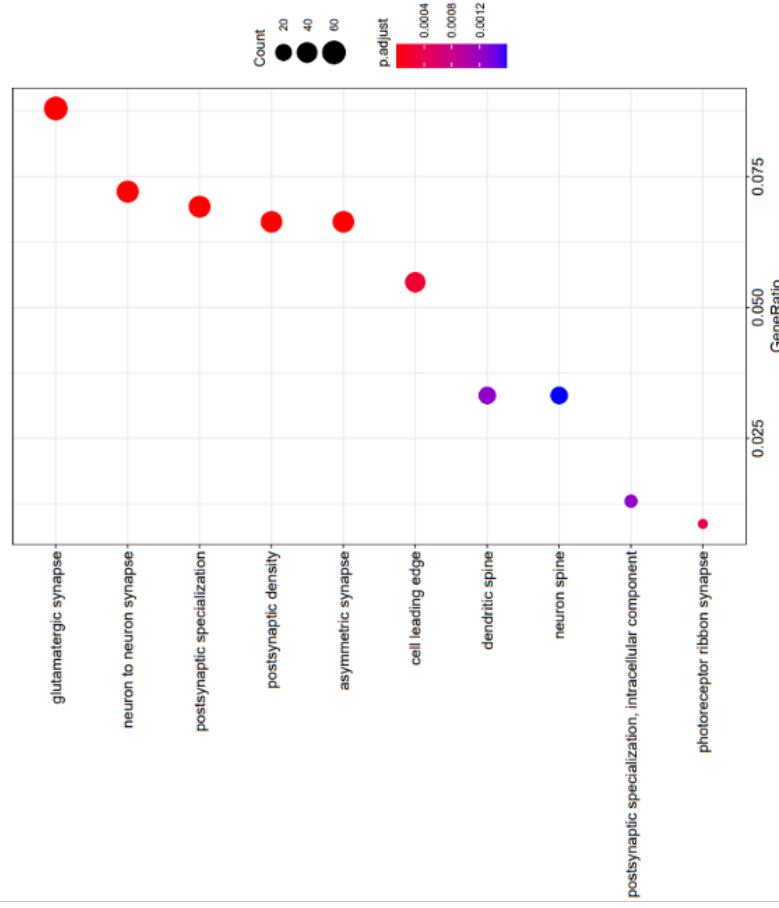
A

Cellular Component



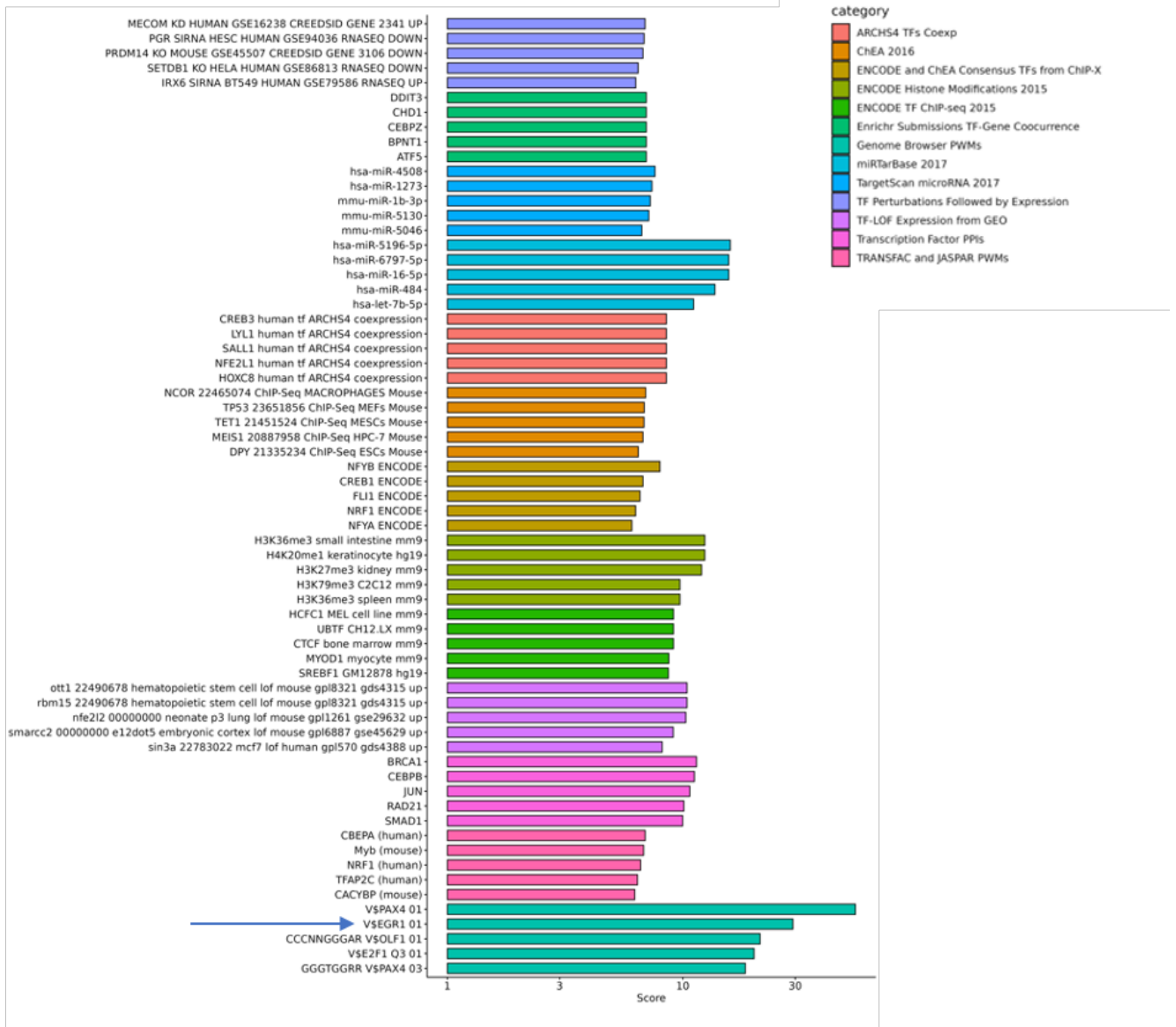
B

Molecular Functions



**Figure 24:** Bioinformatic analysis performed in both “Cellular Component” (a) and “Molecular Function” (b) repositories from GEO revealed that AZD treatment is responsible for a significant downregulation of terms belonging to the synaptic transmission, such as glutamatergic synapses, modulation of synaptic transmission, postsynaptic specialization and regulation of synaptic plasticity.

## Transcriptional Factors

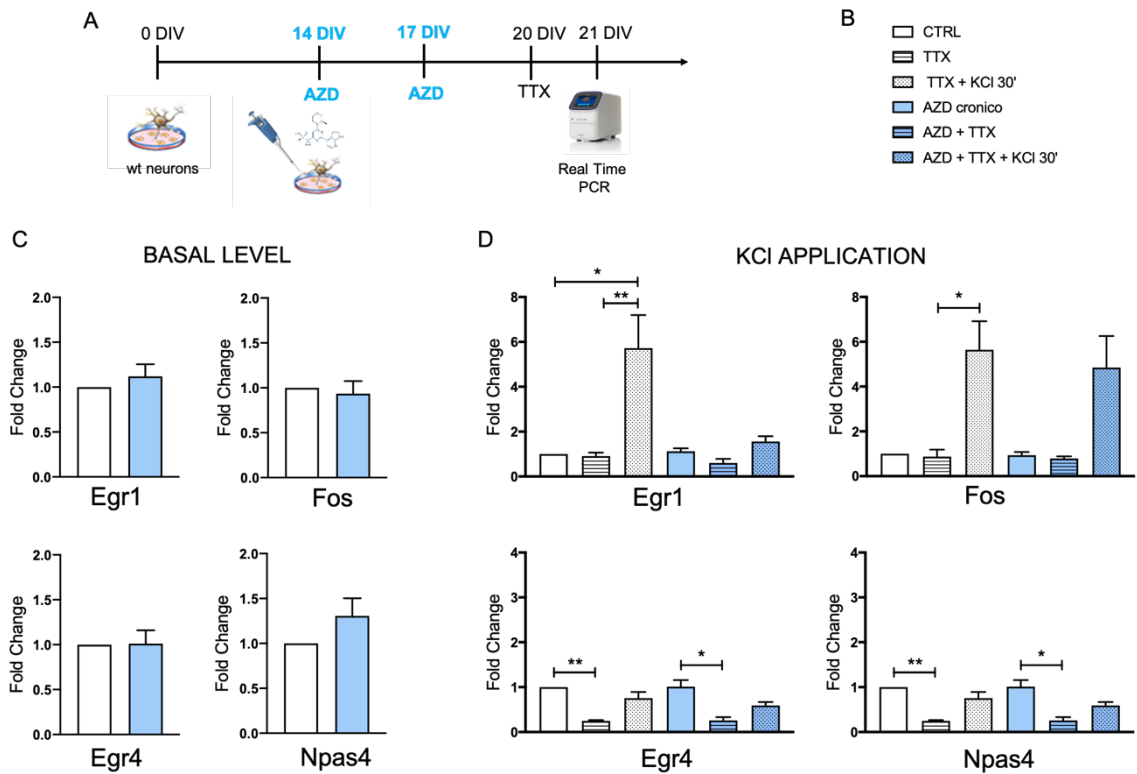


**Figure 25:** Bioinformatic analysis investigated several transcriptional factors (TF) repositories. Here are reported the five most significant deregulated factors for each repository of origin. The most deregulated TF belong to the category “Genome Browser PWMs” and among them it is highlighted Egr1.

### **ATR is involved in the control of transcriptional factors**

To further confirm the link between ATR inhibition and changes in Egr1 mRNA levels and in order to evaluate this link in an hyperexcitability condition, we moved into neuronal cultures, since among the advantages of the in vitro system there is the ability to rule out the possible contributions of other non-neuronal cell types by our analysis. Besides Egr1, we monitored changes of a selected panel of transcriptional factors fundamental for the development and maintenance of neuronal transmission and for the induction of neuronal plasticity, such as Npas4 and Fos [174, 175]. We included in our analysis also Egr4, since we recently demonstrated to be regulated by ATM kinase activity during neuronal development [154].

We investigated mRNA expression changes of all these transcriptional factors through real time PCR experiments in mature hippocampal neurons. While, at basal level, we couldn't reveal any differences between control neurons and neurons chronically treated with the ATR inhibitor in any of these factors (figure 26C), we found - as expected - an increased transcription of these regulators in the hyperactivity condition induced through a KCl 50 mM stimulus that neurons received for 30 minutes; in order to prevent neuronal death due to the strong synaptic activation, we added in the external solution TTX 1  $\mu$ M as described in Machado et al. (2008) [169]. In control DMSO-neurons, this protocol was able to effectively modulate the transcription factors expression, as indicated by the "fold change" analysis (figure 26D). Neurons chronically treated with AZD6738, upon KCl-induced depolarization, displayed similar results in terms of Npas4, Egr4 and Fos transcription but a significant reduction was observed for Egr1 mRNA levels (26D – Egr1). Thus, these data confirm the RNA seq results as well as the specific regulation of ATR kinase on Egr1 transcription upon neuronal depolarization.



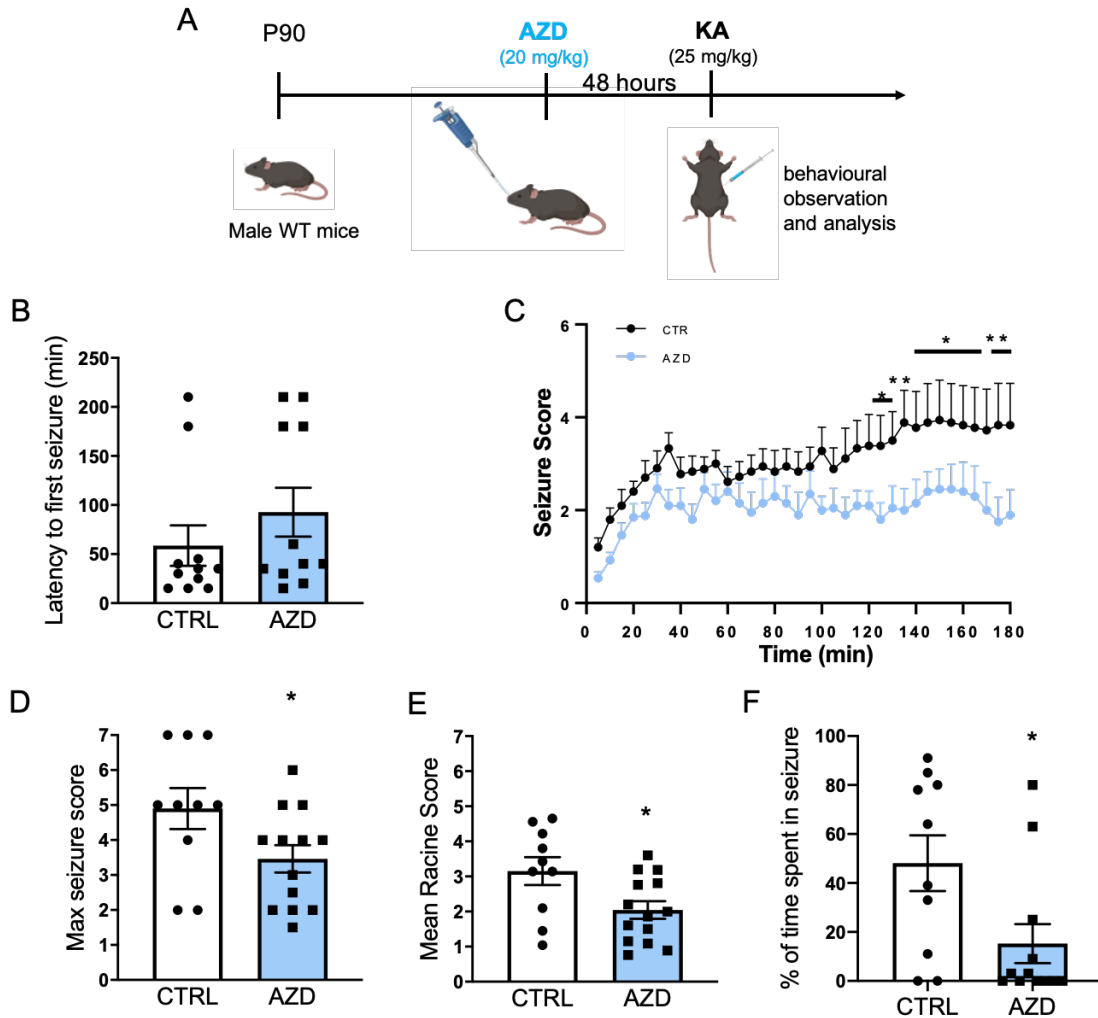
**Figure 26:** a) Scheme of the experimental time line of AZD treatment and related Real Time PCR experiments. b) Legend depicting all the experimental condition. c) Quantification of Egr1, Fos, Egr4 and Npas4 basal mRNA levels by Real Time PCR experiments in hippocampal cultured neurons treated chronically with AZD6738 (Egr1: Mann-Whitney Test,  $p > 0,05$  ns. CTRL n=8; AZD n=11. Fos: Mann-Whitney Test,  $p > 0,05$  ns. CTRL n=8; AZD n=11. Egr4: Mann-Whitney Test,  $p > 0,05$  ns. CTRL n=8; AZD n=11. Npas4: Mann-Whitney Test,  $p > 0,05$  ns. CTRL n=8; AZD n=11). d) Quantification of Egr1, Fos, Egr4 and Npas4 mRNA levels upon KCI 50mM application by Real Time PCR experiments in hippocampal cultured neurons treated chronically with AZD6738 (Egr1: Kruskal-Wallis followed by Dunn's Multiple Comparison Test, \*\*\*\*  $p < 0,0001$ . CTRL n=8; TTX n=5; TTX+KCI 30' n=11; AZD n=11; AZD+TTX n=4; AZD+TTX+KCI 30' n=12. Fos: Kruskal-Wallis followed by Dunn's Multiple Comparison Test, \*\*\*  $p = 0,0001$ . CTRL n=8; TTX n=5; TTX+KCI 30' n=10; AZD n=11; AZD+TTX n=5; AZD+TTX+KCI 30' n=12. Egr4: Kruskal-Wallis followed by Dunn's Multiple Comparison Test, \*\*\*  $p = 0,0002$ . CTRL n=8; TTX n=5; TTX+KCI 30' n=11; AZD n=11; AZD+TTX n=5; AZD+TTX+KCI 30' n=12. Npas4: Kruskal-Wallis followed by Dunn's Multiple Comparison Test, \*\*\*  $p = 0,0001$ . CTRL n=8; TTX n=5; TTX+KCI 30' n=11; AZD n=11; AZD+TTX n=5; AZD+TTX+KCI 30' n=12.).

## **Evaluation of AZD6738 applicability as anticonvulsant drug**

### **AZD6738 anticonvulsant effects in the kainate mouse model**

Supported by our in vivo and in vitro results, we assessed the behavioral response of AZD-treated mice to systemic administration of kainic acid (KA). Indeed, it is largely established that parenteral KA induces limbic motor seizures originating in the hippocampus [177, 178], making it a good model of induced seizures. P90 male wild type mice received intranasal administration of AZD6738 at the dose of 20 mg/kg or DMSO (as previously done for the evaluation of AZD6738 in vivo duration of action) and 48 hours later responses to intraperitoneal injection of a low, but still convulsant, dose of KA (25 mg/kg) was compared between the two groups. Following this protocol, seizures recur as discrete episodes for about 180 minutes from their onset and are constantly monitored by behavioral evaluation every 5 minutes, over a 3-hour period. According to the Racine scale, we ascribed a specific score to each epileptic stage [179, 180]. We found that 80% of DMSO-mice displayed, upon KA delivery, immobility and staring, followed by head bobbing and isolated limbic motor seizures (stage 4, Racine scale), characterized by forelimb clonus and rearing and falling, but in AZD-mice this percentage was lowered to 50%. Despite the onset time to seizures was comparable between the two groups (latency time, figure 27B), progression of clinical signs was significantly reduced in mice pretreated with the ATR inhibitor, as indicated by assigning the maximum seizure rating scale value to each animal during the 3 hours of observation. We analysed the behavioural outcome through the seizure rating of every one animal for each time point during the complete observation and, as indicated by the trajectory of the behavior score, we measured a drastically difference starting from 100 minutes after KA injection. Indeed, DMSO-control mice showed continuous generalized activity lasting for about 80 minutes, whereas AZD-animals rapidly progressed to sub-convulsive behaviors (figure 28C). Coherently, both the mean seizure score and the maximum seizure score, indicating the seizure severity, display lower values in AZD/KA mice in respect to the relative DMSO/KA animals (figure 27D and 27E). Finally, AZD/KA mice also showed a decreased total time spent in seizure activity (figure 27F), and the toxicity induced by kainic acid was also abolished by AZD6738 injection, whereas it

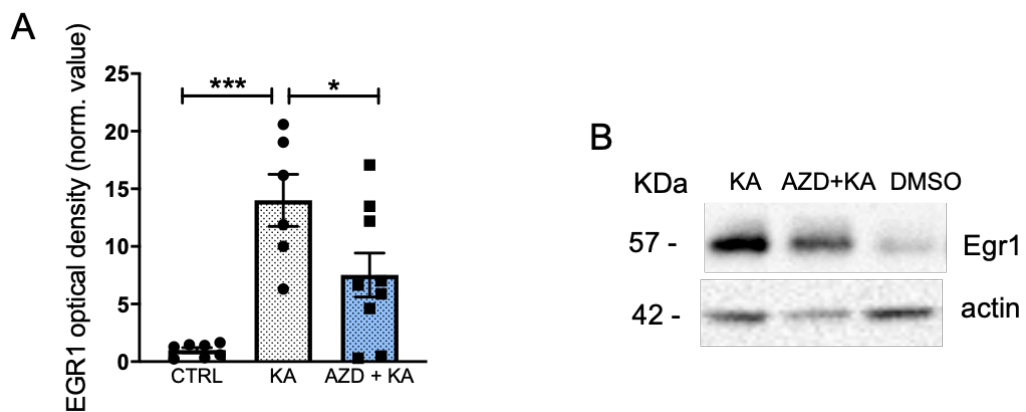
reaches about the 30% in DMSO-treated animals. Taken together, these results point to a novel utilization of the ATR inhibitor, revealing its effect as anticonvulsant drug.



**Figure 27:** a) Scheme of the experimental time line of in vivo AZD treatment and KA-induced seizures monitoring. b) Quantification of time latency to the first seizure event in control and AZD-pretreated animals (Mann-Whitney Test,  $p > 0,05$  ns. CTRL  $n=11$ ; AZD  $n=11$ ). c) Graphical representation of seizure severity during the behavioral monitoring (Two-Way ANOVA followed by Uncorrected Fisher's LSD: Row Factor \*\*\*\*  $p < 0,0001$ ,  $F=88,35$ ; Column Factor \*\*\*  $p=0,0005$ ,  $F=2,028$ . Number of columns =36; number of rows =2; number of values =708). d) Quantification of the maximum seizure score for each animal, pretreated or not with AZD6738 (Unpaired T Test, \*  $p=0,0461$ . CTRL  $n=10$ ; AZD  $n=13$ ). e) Quantification of the mean seizure score for each animal, pretreated or not with AZD6738 (Unpaired T Test, \*  $p=0,0215$ . CTRL  $n=10$ ; AZD  $n=14$ ). f) Percentage of time spent in active epileptic activity of each animal, pretreated or not with AZD6738 (Mann-Whitney Test, \*  $p=0,0275$ . CTRL  $n=10$ ; AZD  $n=12$ ).

### Controlled Egr1 levels in AZD6738 treated mice and related consequences

Since previous results, obtained both in vitro and in vivo, point to an involvement of the immediate early gene Egr1 in the effects mediated by ATR inhibition and knowing that it controls mechanisms of hyperexcitability in models of epilepsy, we performed Western Blotting analysis of hippocampal tissues collected 3 hours after KA injection. As indicated in the figure 28, animals that received intranasal DMSO and 2 days later intraperitoneal KA showed a significantly increases of Egr1 levels at 3 hours from KA delivery. This increment was significantly prevented in AZD6738 treated animals (figure 28A); thus, these preliminary data confirm the link between ATR inhibition and prevention of Egr1 enhancement.



**Figure 28:** a) Quantitative analysis of Egr1 protein expression in hippocampal tissues collected from P90 wild type mice upon seizure induction (One-Way ANOVA followed by Tukey's Multiple Comparison Test, \*\*\* p=0,0004. CTRL n=7; KA n=6; AZD+KA n=9). b) Representative image of Western Blotting experiments carried out on P90 hippocampal tissues.

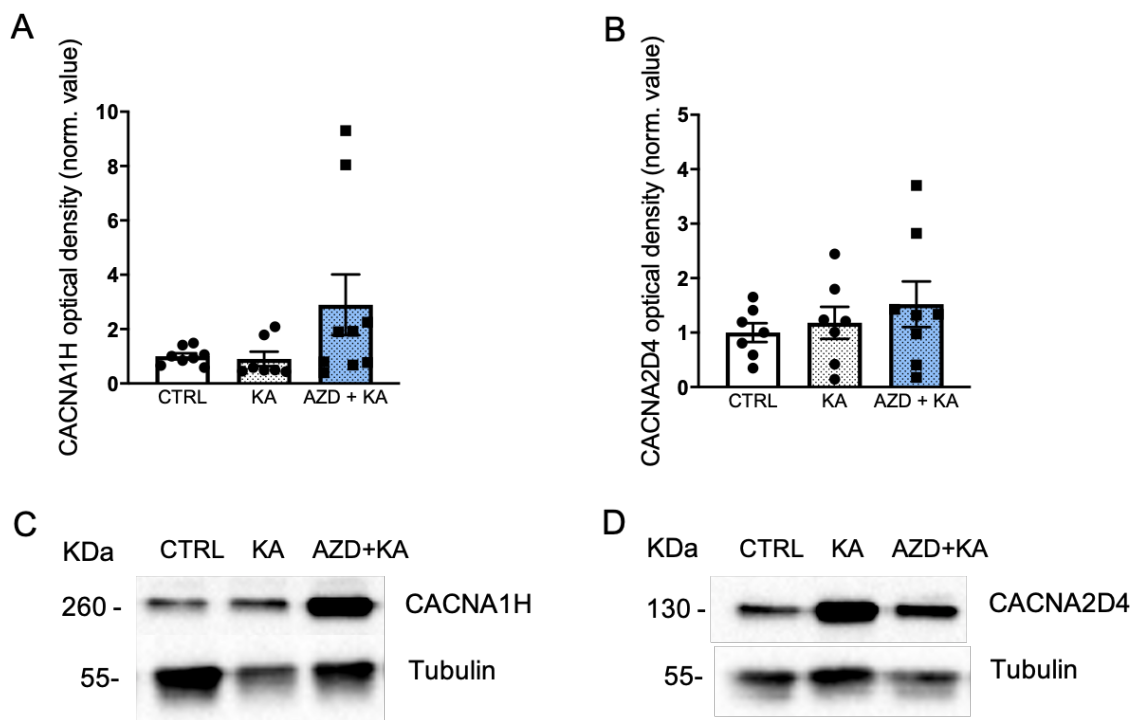


Starting from these data, we decided to evaluate if the AZD6738-induced positive effects in this model of acute seizures may be ascribed to a controlled transcription and expression of calcium channels by an Egr1-dependent mechanism as demonstrated in Van Loo et al. (2019).

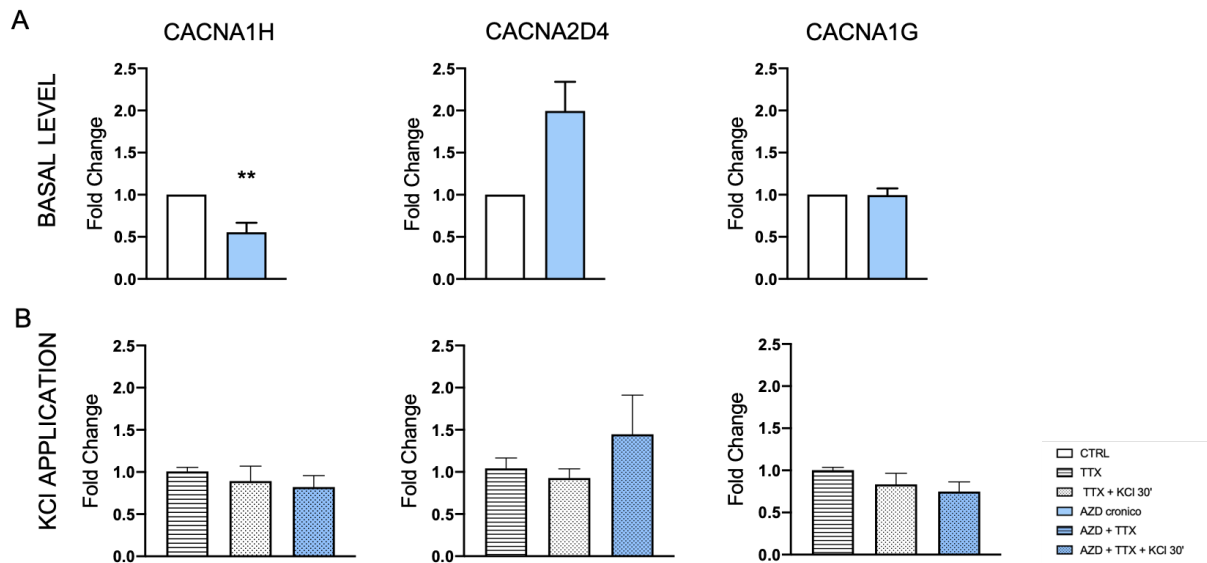
We focused our attention on the CACNA1H and CACNA2D4 subunits and firstly we studied their expression levels through Western Blotting analysis in the same hippocampal tissues collected 3 hours after the kainic acid injection. As shown in figure 29, no differences have been revealed between DMSO-control animals and AZD-treated mice. Actually, data reported in literature indicate that calcium channels undergo significant increases during epileptogenesis but later in time respect to our protocol, that is 3 hours later KA delivery.

Thus, to better evaluate changes in calcium channels expression we moved once again into the vitro system and decided to include in our analysis also the CACNA1G calcium channel. Interestingly, in AZD-neurons we measured a reduced expression of the channel CACNA1H at basal level, whereas no other significant differences were highlighted in the case of CACNA2D4 and CACNA1G (figure 30A). Neurons treated with AZD6738 and exposed to KCl 50 mM for 30 min did not display any differences in terms of calcium channel expressions respect to DMSO cultures as revealed by real time PCR data (figure 30B). Actually, also DMSO-neurons did not shown an increased expression of the calcium channels in these conditions, thus suggesting that we need to test again our hypothesis choosing a wider time window of investigation, in order to better define the regulation played by Egr1 on the transcription of these channels.

Hence, the preliminary data obtained so far highlight the anticonvulsant effect mediated by the selective ATR kinase activity inhibitor AZD6738. This effect could be mediated by the downregulation of the Egr1 transcription factor, which contributes to the establishment of epileptogenesis and seizures controlling the expression of calcium channels during hyperexcitability.



**Figure 29:** a) Quantitative analysis of CACNA1H protein expression in hippocampal tissues collected from P90 wild type mice upon seizure induction (Kruskal-Wallis followed by Dunn's Multiple Comparison Test,  $p > 0,05$  ns. CTRL  $n=8$ ; KA  $n=7$ ; AZD+KA  $n=9$ ). b) Quantitative analysis of CACNA2D4 protein expression in hippocampal tissues collected from P90 wild type mice upon seizure induction (One-Way ANOVA followed by Tukey's Multiple Comparison Test,  $p > 0,05$  ns. CTRL  $n=7$ ; KA  $n=7$ ; AZD+KA  $n=8$ ). c-d) Representative images of Western Blotting experiments carried out on P90 hippocampal tissues.



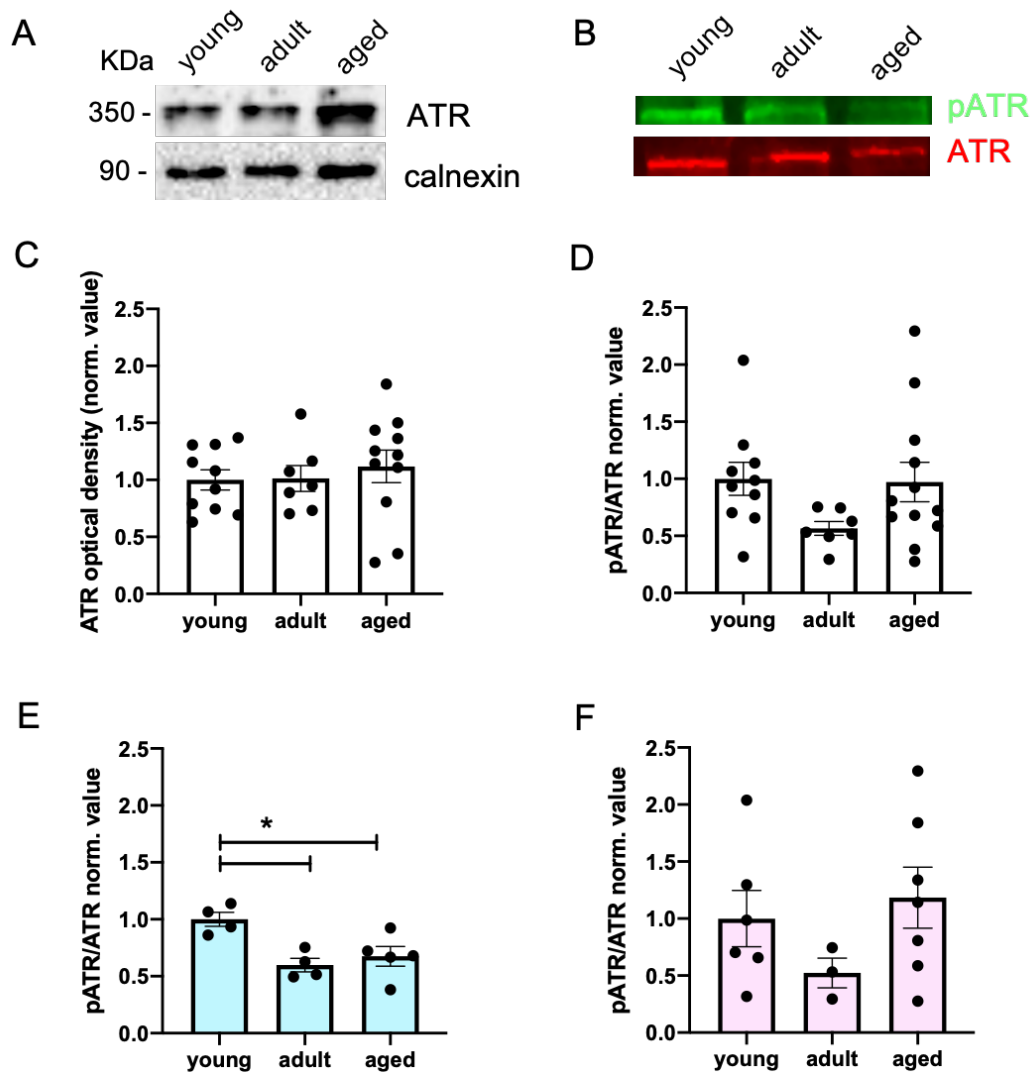
**Figure 30:** a) Quantification of calcium channels CACNA1H, CACNA2D4 and CACNA1G basal mRNA levels by Real Time PCR experiments in hippocampal cultured neurons treated chronically with AZD6738 (CACNA1H: Mann-Whitney Test, \*\*  $p=0,0021$ . CTRL  $n=7$ ; AZD  $n=11$ . CACNA2D4: Mann-Whitney Test,  $p>0,05$  ns. CTRL  $n=7$ ; AZD  $n=11$ . CACNA1G: Mann-Whitney Test,  $p>0,05$  ns. CTRL  $n=6$ ; AZD  $n=11$ ). b) Quantification of CACNA1H, CACNA2D4 and CACNA1G mRNA levels upon KCl 50mM application by Real Time PCR experiments in hippocampal cultured neurons treated chronically with AZD6738 (CACNA1H: One-Way ANOVA followed by Tukey's Multiple Comparison Test,  $p>0,05$  ns. TTX  $n=7$ ; TTX+KCl 30'  $n=11$ ; AZD+TTX+KCl 30'  $n=10$ . CACNA2D4: One-Way ANOVA followed by Tukey's Multiple Comparison Test,  $p>0,05$  ns. TTX  $n=7$ ; TTX+KCl 30'  $n=10$ ; AZD+TTX+KCl 30'  $n=8$ . CACNA1G: One-Way ANOVA followed by Tukey's Multiple Comparison Test,  $p>0,05$  ns. TTX  $n=5$ ; TTX+KCl 30'  $n=7$ ; AZD+TTX+KCl 30'  $n=8$ ).

## **Evaluation of possible ATR involvement during aging**

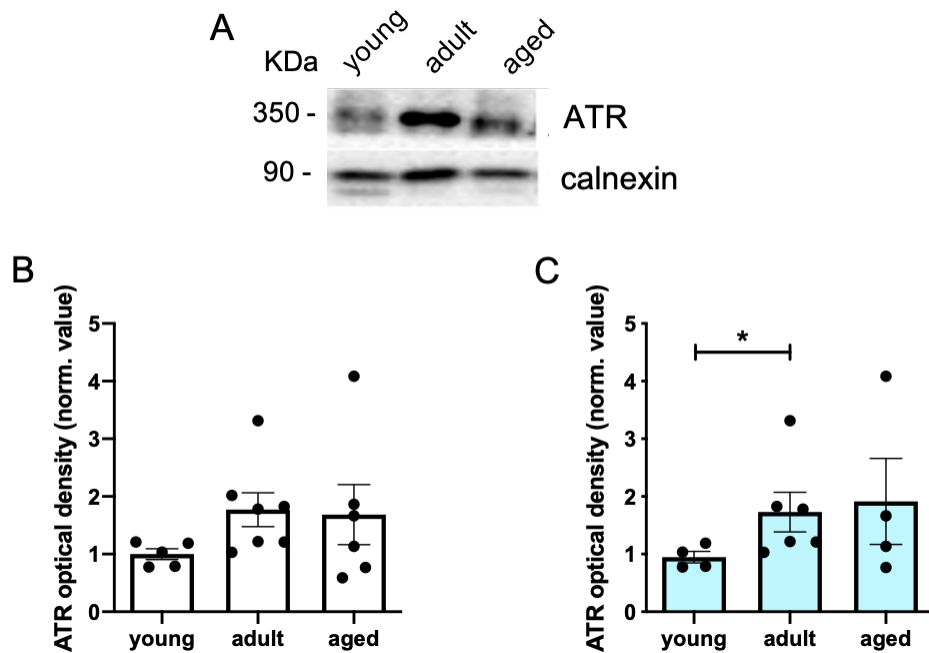
Since we described that chronic ATR inhibition is responsible for marked defects on neuronal transmission and synaptic plasticity and knowing that loss of neuronal plasticity physiologically correlates with aging and decline of cognitive performances [174], we evaluated the ATR protein expression along life. In particular, we collected hippocampal tissues from mice of different months of ages, namely at 4, 8 and 15 months, and performed Western Blotting experiments to analyze both the total ATR expression and the pATR/ATR ratio. Surprisingly, no statistical differences were obtained in both cases among the three groups (figure 31C and 31D), but we noticed two different tendencies among males and females. Interestingly, only adult and aged male animals present a significant reduction of the pATR/ATR ratio (figure 31E). No differences were obtained in the female group (figure 31F).

We had the opportunity to carry out a similar analysis in hippocampal tissues collected from young, adult and aged human individuals whose cause of death was not related to central nervous system alterations. Similar to the results obtain in mice, we couldn't find any statistical differences among the three groups in case of total ATR expression (figure 32B), only revealing a slight tendency in its increase. Unfortunately, in human tissues it was impossible to detect the phosphorylated form of ATR due to post-mortem degradation and so we only analyzed the total ATR expression, which resulted increased in the male adult group (figure 32C). Importantly, these data suggest changes in ATR along life and are not in contrast to what found in mice since ATR functions are mediated by its active form that we were not able to detect in humans due to experimental limitations.

Even though these results are only preliminary, they are coherent with our in vitro results in which the inhibition of ATR kinase activity leads to impaired neuronal plasticity. Starting from this point we speculate that, above all in male, the precocious inhibition of ATR activity may result in premature cognitive decline and aging.



**Figure 31:** a) Representative image of Western Blotting experiments carried out on hippocampal tissues collected from young, adult and aged wild type male and female mice. b) Representative image of Western Blotting experiments carried out on hippocampal tissues collected from young, adult and aged male mice. c) Quantitative analysis of ATR protein expression (One-Way ANOVA followed by Tukey's Multiple Comparison Test,  $p > 0,05$  ns. Young  $n=10$ ; Adult  $n=7$ ; Aged  $n=11$ ). d) Quantitative analysis of pATR/ATR ratio (One-Way ANOVA followed by Tukey's Multiple Comparison Test,  $p > 0,05$  ns. Young  $n=10$ ; Adult  $n=7$ ; Aged  $n=12$ ). e-f) Quantitative analysis of pATR/ATR ratio in male (e) or female (f) mice (Male: One-Way ANOVA followed by Tukey's Multiple Comparison Test,  $** p=0,009$ . Young  $n=4$ ; Adult  $n=4$ ; Aged  $n=5$ . Female: One-Way ANOVA followed by Tukey's Multiple Comparison Test,  $p > 0,05$  ns. Young  $n=6$ ; Adult  $n=3$ ; Aged  $n=7$ ).



**Figure 32:** a) Representative image of Western Blotting experiments carried out on hippocampal human tissues collected from young, adult and aged individuals. b) Quantitative analysis of ATR protein expression (One-Way ANOVA followed by Tukey's Multiple Comparison Test,  $p > 0,05$  ns. Young  $n=5$ ; Adult  $n=7$ ; Aged  $n=6$ ). c) Quantitative analysis of ATR expression in male individuals (One-Way ANOVA followed by Tukey's Multiple Comparison Test,  $p > 0,05$  ns. Young  $n=4$ ; Adult  $n=6$ ; Aged  $n=4$ . Young vs Adults: Mann-Whitney Test, \*  $p=0,0381$ ).

## **DISCUSSION**

In this thesis, we highlight the importance of the ATR kinase activity in the control of the excitatory/inhibitory balance in the neuronal network and discover that inhibition of its activity plays an important anticonvulsant effect. Notably, we demonstrate a completely novel application of the ATR inhibitor AZD6738, which is already used in oncological pre-clinical research, as an innovative pharmacological tool for the treatment of neurologic disorders characterized by hyperexcitability. Importantly, this new drug utilization has been patented.

Role of the ATR protein in dividing cells has been largely described, however increasing evidence suggest a different function of this kinase in post mitotic neurons, pointing to the lack of a complete understanding of the activities played by ATR. Recent studies showed a fundamental ATR role in the regulation of vesicles release [83] and in the maintenance of proper neuronal transmission [89] by exploiting the genetic animal model characterized by the complete ATR deletion; no data regarding the effects induced by the pharmacological inhibition of ATR kinase activity have been provided. Here, we filled this scientific gap abolishing the protein kinase activity and analyzing consequences in terms of neuronal network changes from both a functional and molecular point of view.

To this purpose, we exploited the selective ATR kinase activity inhibitor AZD6738, a potent inhibitor largely studied in the oncological field because of its ability to inhibit cancer proliferation by generating replication stress and cellular checkpoints inactivation [96]. We first identified the duration of action using the drug at the concentration of 1  $\mu$ M, which is a concentration that allows a good margin of selectivity against other kinases in broad in vitro assay screens and no significant inhibition of other PI3K-like kinases (such as DNA-PK, ATM and mTOR) [175]. Specificity of the inhibitor activity was also confirmed through this work, considering that no changes in the ATM protein expression have been revealed upon AZD6738 application.

We decided to set two different protocols to treat hippocampal cultures with AZD6738. In particular, we exploited inhibition of the ATR activity for 24 hours in case of a single day administration or a chronic inhibition, performing two drugs application along a week. Importantly, treatment did not affect the viability of cultured neurons as indicated by both normal intracellular calcium levels at resting



condition [176] and comparable signal in the TUNEL assay with vehicle-treated neurons, confirming its safety profile.

Since previous publications produced by our laboratory demonstrate a key role of the protein ATM in the regulation of the GABAergic maturation, in particular in the excitatory-to-inhibitory switch of GABA process [149], we wanted to verify if also ATR could be involved in the physiological development of hippocampal neurons. The results here presented clearly show that inhibition of ATR activity does not affect the development of the GABAergic system, unveiling the possibility for a completely different role of this protein in the context of the central nervous system. Indeed, further investigations revealed that ATR is essential for the maintenance of the proper balance between excitation and inhibition in mature neuronal network, which is fundamental for the correct brain function and plasticity [177]. Importantly, both an acute and a chronic pharmacological inhibition of ATR activity in mature neurons are responsible for an imbalance between excitation (E) and inhibition (I) in the neuronal network, resulting in a reduced E/I ratio. In respect to what is described in literature, our data appear in contrast: in Kirtay et al. (2021), authors show an increased neuronal activity generated by increased presynaptic firing in ATR deleted mice. Also, they reported an augmented excitatory response with the onset of sporadic non-lethal epileptic seizures in 12 months-old mice [89]. Of course, the genetic model completely differs from the pharmacological blockade of the ATR kinase activity in a restricted time window, thus our different conclusions may be ascribed to the very different model here exploited. In addition, Kirtay and collaborators do not correlate the functional alterations to molecular changes, thus we cannot explain in detail the origin of this discrepancy. They reported changes in the synaptic vesicle proteins synaptotagmin 2 (SYT2) and indicate that, in absence of ATR, SYT2 is highly upregulated and aberrantly translocated to excitatory neurons in the hippocampus; thus we looked at changes in SYT2 through our RNA seq experiments performed in hippocampi of mice treated with AZD6738 but no alterations have been detected. This result further suggests a strong discrepancy between mechanisms occurring upon the ATR genetic deletion and those induced by the ATR kinase activity inhibition.

The results collected in this work acquire particular relevance since ATR emerges as a novel potential target to reduce the excitatory/inhibitory transmission. Accordingly, we demonstrated that, in vivo in wild type animals, ATR inhibition is responsible for a potent anticonvulsant effect. In particular, we took advantage of a pharmacological model of acute seizures [178] revealing that pretreatment with the drug AZD6738 ameliorates the outcomes of seizure-like events, affecting positively the seizure severity and duration, and abolishes the lethal toxicity induced by injection of the convulsant agent, kainic acid. Our data have been also corroborated by the RNA profiling, which revealed how the transcriptional modifications found upon ATR inhibition are similar to those obtained with conventional antiepileptic drugs.

Hence, inhibition of ATR could be tested as an innovative treatment in those neurological disorders characterized by an excessive level of excitation.

Real Time PCR investigations and RNA sequencing profiling aimed at assessing the molecular mechanisms underlying the effects mediated by ATR inhibition. From the results here obtained, we propose the immediate early gene *Egr1* as one of the main targets controlled by ATR. Indeed, *Egr1* is a transcription factor largely known to be involved in proper maintenance of the neuronal activity. In particular, it is involved in the processes of neuronal plasticity, with particular importance in the late phase of LTP as demonstrated by defects in mice completely lacking of the gene [179]. Also, it plays a role in the development of inhibitory synapses controlling the expression of specific subunits ( $\alpha 2$ ,  $\alpha 4$  and  $\theta$ ) of the GABA<sub>A</sub> receptors [180]. Finally, deregulation of *Egr1* have been associated to hyperexcitability and epilepsy onset [188, 189]. Thus, our results that highlighted *Egr1* as one of the molecular players responsible for the anticonvulsant effect induced by the ATR inhibition appear coherent with these recent studies in literature. Anyway, further investigations are needed to better characterize the molecular changes induced by ATR inhibition.

Additionally, our work fits with several studies highlighting the role of proteins involved in the DNA repair signaling as regulators of neuronal function [190, 191]. In particular, it has been shown that different kind of neuronal stimulation can generate DNA damages and double strand breaks. Activity-dependent damages

are particularly enriched in loci of the early response genes Fos, Npas4, Egr1 and Nr4a, whose activation is responsible for modifications in the synapse structure including neurite outgrowth, synaptic strength and maturation and synaptogenesis [185]. Accordingly, alterations in this process are known to result in cognitive disabilities, thus underlying their crucial relevance [186].

Recent studies describe how Egr1 directly regulates the expression of several calcium channels during epileptogenesis. Accordingly, consensus binding sites for the Egr-family are highly overrepresented in the promoter regions of Voltage Dependent Calcium Channels and their subunits. In particular, CACNA1H and CACNA2D4 have been found increased during epileptogenesis, upon Egr1 transcriptional activation [173, 194]. Thus, we hypothesized reduced levels of both these two channels upon AZD6738 treatment. Unfortunately, neither the protein or the mRNA expression levels were found changed in our experimental settings. Indeed, we would have expected high expression levels in case of hyperexcitability induction, either in vivo upon KA injection and in vitro with KCl stimulation. Actually, experiments performed in this work could not reveal such modifications: data found in literature reports longer activation time for the calcium subunits transcription [166]. Thus, we are planning to repeat the molecular investigation modifying the time window of the experimental setting.

In addition, considering that the equilibrium between excitation and inhibition is the key for a functioning network and that it is necessary to perform plasticity, the defects affecting the processes of long term potentiation and depression were indeed expected. More recent investigations have demonstrated that the inhibitory transmission can effectively modulate the efficacy and the threshold of excitatory synaptic plasticity [188], thus this is a further demonstrations that changes in GABAergic synaptic transmission can have important functional and pathological consequences. Processes of synaptic plasticity are fundamental in learning, memory and in the normal brain maturation and involve primarily AMPA and NMDA receptors [189]. Indeed, synaptic plasticity is characterized by insertion or removal of AMPAR, a process necessary for the synaptic strengthening or weakening [190]. Integrity of the synaptic structure are thus critical for generating long-plasticity modifications [191]. Synaptic dysfunctions which are at the basis of many

neurological conditions, such as neurodegenerative disease or neuropsychiatric conditions, can occur precociously, during the early asymptomatic phase of the disease [192]. In this context, our data suggest ATR as a new player involved in the cognitive dysfunctions, since its kinase function is essential for the correct induction of neuronal plasticity processes. Starting by these premises, we hypothesized a possible relation between ATR activity and cognitive decline ascribed to aging, since it is associated with progressive deterioration of physiological integrity and decline in neuronal excitability and synaptic function, contributing to memory loss [193]. In order to assess this point we monitored changes in total ATR and pATR/ATR levels along life.

Both in mouse and human tissues, no changes in ATR total expression were revealed. However, the reduced ratio analyzed in this study between the phosphorylated ATR and its total form during aging support our idea that changes in pATR/ATR may contribute to a precocious decline of cognitive functions in vivo. Indeed, all the pathways controlled by ATR are mediated by the active phosphorylated protein. As a matter of fact, ATR phosphorylation has been defined as a good biomarker for the detection of the active protein [194] and thus allowed us to verify the presence of subtle changes in its activity. Interestingly, pATR/ATR levels do not change in aged females, but only male individuals were characterized by a reduced ratio already at early phase of aging, pointing at a completely unexpected finding. This underlines the well-documented gender gap in health and longevity of individuals' life world-wide. Indeed, it has been demonstrated that the rate of aging in men is 1,4-fold higher than the rate of adult women, suggesting the man disadvantage for longevity [195]. Although the loss of neuronal functions may occur during aging as consequence of physiological events, it may be responsible for an increased vulnerability to different neurological diseases. Indeed, prevention of premature aging is needed to increase the general well-being and to reduce vulnerability. In this context, our data showing that inhibition of ATR leads to impaired plasticity and that it physiologically occurs in males support the importance of identifying sex-specific aging biomarkers for a better identification of neuronal health, synaptic ability and the possible onset of a disease state. Also, it would ameliorate the stratification of individuals with the same chronological age but characterized by different aging rate and potentially predict health span [196]. Even though further analysis will be necessary to confirm these preliminary results,

our study paves the way for the recognition of the active ATR as precocious aging marker in male individuals.

In conclusion, the results collected in this thesis propose the involvement of the protein ATR in two very different contexts. We suggest that delivery of the ATR kinase activity inhibitor, AZD6738, is responsible for a decreased E/I ratio in vitro, a reduced neuronal firing and prevents Egr1 transcription, thus acting as an anticonvulsant drug in vivo. On the other hand, our results indicate that during the physiological aging males are characterized by reduced active ATR, coherent with the neuronal transmission defects affecting the synaptic plasticity. Finally, all these results highlight a novel role of ATR in the maintenance of the proper neuronal function in mature hippocampal neurons and suggest i) the ATR inhibition as an important therapeutic tool for the treatment of neurological disorders characterized by hyperexcitability and ii) the promotion of ATR kinase activity to counteract neuronal plasticity impairments during physiological aging.

## **ACKNOWLEDGMENTS**

At the end of my PhD training, I want to thank Prof. Flavia Antonucci for the opportunity I was given to work and study in her laboratory during my PhD period. A sincere acknowledgment to Prof. Giovanni Provenzano and his group and to Dr. Silvano Piazza (University of Trento) that contributed to this project performing the RNA sequencing profiling and the bioinformatic analysis.

Finally, an important thanks to Prof. Elena Battaglioli and Dr. Francesco Rusconi (University of Milan) that allowed us to carry out the biochemical analysis on human hippocampal samples.

The attendance to the PhD course was supported by the fellowship provided by the University of Milan.

## REFERENCES

- [1] R. D. Paulsen and K. A. Cimprich, "The ATR pathway: Fine-tuning the fork," *DNA Repair (Amst.)*, vol. 6, no. 7, pp. 953–966, 2007, doi: 10.1016/j.dnarep.2007.02.015.
- [2] I. Corcoles-Saez, K. Dong, and R. S. Cha, "Versatility of the Mec1 ATM/ATR signaling network in mediating resistance to replication, genotoxic, and proteotoxic stresses," *Curr. Genet.*, vol. 65, no. 3, pp. 657–661, 2019, doi: 10.1007/s00294-018-0920-y.
- [3] N. J. Bentley *et al.*, "The schizosaccharomyces pombe rad3 checkpoint gene," *EMBO J.*, vol. 15, no. 23, pp. 6641–6651, 1996, doi: 10.1002/j.1460-2075.1996.tb01054.x.
- [4] K. A. Cimprich, T. B. Shin, C. T. Keith, and S. L. Schreiber, "cDNA cloning and gene mapping of a candidate human cell cycle checkpoint protein," *Proc. Natl. Acad. Sci. U. S. A.*, vol. 93, no. 7, pp. 2850–2855, 1996, doi: 10.1073/pnas.93.7.2850.
- [5] A. N. Blackford and S. P. Jackson, "ATM, ATR, and DNA-PK: The Trinity at the Heart of the DNA Damage Response," *Mol. Cell*, vol. 66, no. 6, pp. 801–817, 2017, doi: 10.1016/j.molcel.2017.05.015.
- [6] A. Maréchal and L. Zou, "DNA damage sensing by the ATM and ATR kinases," *Cold Spring Harb. Perspect. Biol.*, vol. 5, no. 9, pp. 1–17, 2013, doi: 10.1101/cshperspect.a012716.
- [7] R. T. Abraham, "Cell cycle checkpoint signaling through the ATR and ATM kinases," *Gene Dev.*, pp. 2177–2196, 2018, doi: 10.1109/ICISE.2010.5689338.
- [8] E. J. Brown and D. Baltimore, "Essential and dispensable roles of ATR in cell cycle arrest and genome maintenance," *Genes Dev.*, vol. 17, no. 5, pp. 615–628, 2003, doi: 10.1101/gad.1067403.
- [9] R. S. Tibbetts *et al.*, "A role for ATR in the DNA damage-induced phosphorylation of p53," *Genes Dev.*, vol. 13, no. 2, pp. 152–157, 1999, doi: 10.1101/gad.13.2.152.
- [10] R. S. Tibbetts *et al.*, "Functional interactions between BRCA1 and the checkpoint kinase ATR during genotoxic stress," *Genes Dev.*, vol. 14, no. 23, pp. 2989–3002, 2000, doi: 10.1101/gad.851000.
- [11] E. J. Brown and D. Baltimore, "ATR disruption leads to chromosomal fragmentation and early embryonic lethality," *Genes Dev.*, vol. 14, no. 4,



- pp. 397–402, 2000, doi: 10.1101/gad.14.4.397.
- [12] A. De Klein *et al.*, “Targeted disruption of the cell-cycle checkpoint gene ATR leads to early embryonic lethality in mice,” *Curr. Biol.*, vol. 10, no. 8, pp. 479–482, 2000, doi: 10.1016/S0960-9822(00)00447-4.
- [13] G. K. Alderton, H. Joenje, R. Varon, A. D. Børglum, P. A. Jeggo, and M. O’Driscoll, “Seckel syndrome exhibits cellular features demonstrating defects in the ATR-signalling pathway,” *Hum. Mol. Genet.*, vol. 13, no. 24, pp. 3127–3138, 2004, doi: 10.1093/hmg/ddh335.
- [14] Y. Ruzankina *et al.*, “Deletion of the developmentally essential gene ATR in adult mice leads to age-related phenotypes and stem cell loss,” vol. 1, no. 1, pp. 113–126, 2007, doi: 10.1016/j.stem.2007.03.002.Deletion.
- [15] M. O’Driscoll and P. A. Jeggo, “The role of double-strand break repair - Insights from human genetics,” *Nat. Rev. Genet.*, vol. 7, no. 1, pp. 45–54, 2006, doi: 10.1038/nrg1746.
- [16] G. E. Matos-Rodrigues *et al.*, “Progenitor death drives retinal dysplasia and neuronal degeneration in a mouse model of ATRIP-Seckel syndrome,” *DMM Dis. Model. Mech.*, vol. 13, no. 10, 2020, doi: 10.1242/dmm.045807.
- [17] A. Verloes, S. Drunat, P. Gressens, and S. Passemard, “Primary Autosomal Recessive Microcephalies and Seckel Syndrome Spectrum Disorders,” *GeneReviews*®, pp. 1–42, 1993, [Online]. Available: <http://www.ncbi.nlm.nih.gov/pubmed/20301772>.
- [18] L. Faivre *et al.*, “Clinical and genetic heterogeneity of Seckel syndrome,” *Am. J. Med. Genet.*, vol. 112, no. 4, pp. 379–383, 2002, doi: 10.1002/ajmg.10677.
- [19] L. Faivre and V. Cormier-Daire, “Seckel syndrome,” Accessed: Nov. 23, 2021. [Online]. Available: <http://www.orpha.net/data/patho/GB/uk-Seckel>.
- [20] A. Shanske, D. G. Caride, L. Menasse-Palmer, A. Bogdanow, and R. W. Marion, “Central nervous system anomalies in Seckel syndrome: Report of a new family and review of the literature,” *Am. J. Med. Genet.*, vol. 70, no. 2, pp. 155–158, 1997, doi: 10.1002/(SICI)1096-8628(19970516)70:2<155::AID-AJMG10>3.0.CO;2-I.
- [21] M. Murga *et al.*, “A mouse model of ATR-Seckel Syndrome reveals that replicative stress during embryogenesis limits mammalian lifespan,” vol. 41, no. 8, pp. 891–898, 2010, doi: 10.1038/ng.420.A.

- [22] M. O. Akkurt, K. Pakay, I. Akkurt, M. Temur, and E. Korkmazer, "Prenatal diagnosis of Seckel syndrome at 21 weeks' gestation and review of the literature," *J. Matern. Neonatal Med.*, vol. 32, no. 11, pp. 1905–1908, 2019, doi: 10.1080/14767058.2017.1419467.
- [23] A. Gupta, T. S. Fazal, and R. Arora, "Antenatal Diagnosis of Seckel Syndrome," *J. Obstet. Gynecol. India*, vol. 64, no. 1, pp. 6–8, 2014, doi: 10.1007/s13224-012-0339-1.
- [24] K. M. Takikawa *et al.*, "Perinatal findings of Seckel syndrome: A case report of a fetus showing primordial dwarfism and severe microcephaly," *Fetal Diagn. Ther.*, vol. 24, no. 4, pp. 405–408, 2009, doi: 10.1159/000167269.
- [25] D. F. Majoor-Krakauer, J. W. Wladimiroff, P. A. Stewart, and J. J. Van De Harten, "Bird-Headed Dwarfism : Prenatal Diagnosis of a Seckel-Like Syndrome," *Am. J. Med. Genet.*, vol. 188, pp. 183–188, 1987.
- [26] E. Thompson and M. Pembrey, "Seckel syndrome: An overdiagnosed syndrome," *J. Med. Genet.*, vol. 22, no. 3, pp. 192–201, 1985, doi: 10.1136/jmg.22.3.192.
- [27] T. Ogi *et al.*, "Identification of the First ATRIP-Deficient Patient and Novel Mutations in ATR Define a Clinical Spectrum for ATR-ATRIP Seckel Syndrome," *PLoS Genet.*, vol. 8, no. 11, 2012, doi: 10.1371/journal.pgen.1002945.
- [28] M. O'Driscoll, V. L. Ruiz-Perez, C. G. Woods, P. A. Jeggo, and J. A. Goodship, "A splicing mutation affecting expression of ataxia-telangiectasia and Rad3-related protein (ATR) results in Seckel syndrome," *Nat. Genet.*, vol. 33, no. 4, pp. 497–501, 2003, doi: 10.1038/ng1129.
- [29] J. Ichisima *et al.*, "Verification and rectification of cell type-specific splicing of a Seckel syndrome-associated ATR mutation using iPS cell model," *J. Hum. Genet.*, vol. 64, no. 5, pp. 445–458, 2019, doi: 10.1038/s10038-019-0574-8.
- [30] M. Murga *et al.*, "A mouse model of ATR-Seckel shows embryonic replicative stress and accelerated aging," *Nat. Genet.*, vol. 41, no. 8, pp. 891–898, 2009, doi: 10.1038/ng.420.
- [31] H. S. E. Tivey *et al.*, "Small molecule inhibition of p38 MAP kinase extends the replicative life span of human ATR-seckel syndrome fibroblasts," *Journals Gerontol. - Ser. A Biol. Sci. Med. Sci.*, vol. 68, no. 9, pp. 1001–

- 1009, 2013, doi: 10.1093/gerona/gls336.
- [32] S. Lautrup *et al.*, “Studying Werner syndrome to elucidate mechanisms and therapeutics of human aging and age-related diseases,” *Biogerontology*, vol. 20, no. 3, pp. 255–269, 2019, doi: 10.1007/s10522-019-09798-2.
- [33] J. Oshima, J. M. Sidorova, and R. J. Monnat Jr, “Werner Syndrome: clinical features, pathogenesis and potential therapeutic interventions,” *Physiol. Behav.*, vol. 176, no. 12, pp. 139–148, 2017, doi: 10.1016/j.arr.2016.03.002.Werner.
- [34] J. C. Saldivar, D. Cortez, and K. A. Cimprich, “The essential kinase ATR: ensuring faithful duplication of challenging genome,” *Nat Rev Mol Cell Biol*, 2017.
- [35] A. Jazayeri *et al.*, “ATM- and cell cycle-dependent regulation of ATR in response to DNA double-strand breaks,” *Nat. Cell Biol.*, vol. 8, no. 1, pp. 37–45, 2006, doi: 10.1038/ncb1337.
- [36] M. Cuadrado *et al.*, “ATM regulates ATR chromatin loading in response to DNA double-strand breaks,” *J. Exp. Med.*, vol. 203, no. 2, pp. 297–303, 2006, doi: 10.1084/jem.20051923.
- [37] H. Royo *et al.*, “ATR acts stage specifically to regulate multiple aspects of mammalian meiotic silencing,” *Genes Dev.*, vol. 27, no. 13, pp. 1484–1494, Jul. 2013, doi: 10.1101/GAD.219477.113.
- [38] J. Maciejowski and T. De Lange, “Telomeres in cancer: tumour suppression and genome instability,” *Nat. Rev. Mol. Cell Biol.*, vol. 18, no. 3, pp. 175–186, Mar. 2017, doi: 10.1038/NRM.2016.171.
- [39] A. Kumar *et al.*, “ATR Mediates a Checkpoint at the Nuclear Envelope in Response to Mechanical Stress,” *Cell*, vol. 158, no. 3, p. 633, Jul. 2014, doi: 10.1016/J.CELL.2014.05.046.
- [40] S. M. Barr, C. G. Leung, E. E. Chang, and K. A. Cimprich, “ATR kinase activity regulates the intranuclear translocation of ATR and RPA following ionizing radiation,” *Curr. Biol.*, vol. 13, no. 12, pp. 1047–1051, Jun. 2003, doi: 10.1016/S0960-9822(03)00376-2.
- [41] D. Cortez, S. Guntuku, J. Qin, and S. J. Elledge, “ATR and ATRIP: Partners in checkpoint signaling,” *Science (80-. )*, vol. 294, no. 5547, pp. 1713–1716, 2001, doi: 10.1126/science.1065521.
- [42] L. Zou, D. Cortez, and S. J. Elledge, “Regulation of ATR substrate selection

- by Rad17-dependent loading of Rad9 complexes onto chromatin,” *Genes Dev.*, vol. 16, no. 2, pp. 198–208, 2002, doi: 10.1101/gad.950302.
- [43] M. Sokka, D. Koalick, P. Hemmerich, J. E. Syväoja, and H. Pospiech, “The ATR-Activation Domain of TopBP1 Is Required for the Suppression of Origin Firing during the S Phase,” *Int. J. Mol. Sci.*, vol. 19, no. 8, Aug. 2018, doi: 10.3390/IJMS19082376.
- [44] D. Achuthankutty *et al.*, “Regulation of ETAA1-mediated ATR activation couples DNA replication fidelity and genome stability,” *J. Cell Biol.*, vol. 218, no. 12, pp. 3943–3953, Dec. 2019, doi: 10.1083/JCB.201905064.
- [45] V. Thada and D. Cortez, “Common motifs in ETAA1 and TOPBP1 required for ATR kinase activation,” *J. Biol. Chem.*, vol. 294, no. 21, pp. 8395–8402, May 2019, doi: 10.1074/JBC.RA119.008154.
- [46] K. A. Cimprich and D. Cortez, “ATR: an essential regulator of genome integrity,” *Nat. Rev. Mol. Cell Biol.*, vol. 9, no. 8, pp. 616–627, Aug. 2008, doi: 10.1038/NRM2450.
- [47] V. A. J. Smits, D. O. Warmerdam, Y. Martin, and R. Freire, “Mechanisms of ATR-mediated checkpoint signalling,” *Front. Biosci.*, vol. 15, no. 3, pp. 840–853, 2010, doi: 10.2741/3649.
- [48] A. M. Casper, P. Nghiem, M. F. Arlt, and T. W. Glover, “ATR regulates fragile site stability,” *Cell*, vol. 111, no. 6, pp. 779–789, Dec. 2002, doi: 10.1016/S0092-8674(02)01113-3.
- [49] Q. Liu *et al.*, “Chk1 is an essential kinase that is regulated by Atr and required for the G2/M DNA damage checkpoint,” *Genes Dev.*, vol. 14, no. 12, pp. 1448–1459, 2000, doi: 10.1101/gad.14.12.1448.
- [50] C. S. Sørensen, R. G. Syljuåsen, J. Lukas, and J. Bartek, “ATR, claspin and the Rad9-Rad1-Hus1 complex Chk1 and Cdc25A in the absence of DNA damage,” *Cell Cycle*, vol. 3, no. 7, pp. 941–945, 2004, doi: 10.4161/cc.3.7.972.
- [51] H. Zhao and H. Piwnicka-Worms, “ATR-Mediated Checkpoint Pathways Regulate Phosphorylation and Activation of Human Chk1,” *Mol. Cell. Biol.*, vol. 21, no. 13, pp. 4129–4139, 2001, doi: 10.1128/mcb.21.13.4129-4139.2001.
- [52] J. M. Bradbury and S. P. Jackson, “ATM and ATR,” *Curr. Biol.*, vol. 13, no. 12, p. 468, 2003, doi: 10.1016/s0960-9822(03)00403-2.

- [53] T. Stiff *et al.*, “ATR-dependent phosphorylation and activation of ATM in response to UV treatment or replication fork stalling,” *EMBO J.*, vol. 25, no. 24, pp. 5775–5782, 2006, doi: 10.1038/sj.emboj.7601446.
- [54] A. Guleria and S. Chandna, “ATM kinase: Much more than a DNA damage responsive protein,” *DNA Repair (Amst.)*, vol. 39, pp. 1–20, Mar. 2016, doi: 10.1016/J.DNAREP.2015.12.009.
- [55] P. J. McKinnon, “ATM and ataxia telangiectasia,” *EMBO Rep.*, vol. 5, no. 8, pp. 772–776, Aug. 2004, doi: 10.1038/SJ.EMBOR.7400210.
- [56] D. Shechter, V. Costanzo, and J. Gautier, “Regulation of DNA replication by ATR: Signaling in response to DNA intermediates,” *DNA Repair (Amst.)*, vol. 3, no. 8–9, pp. 901–908, 2004, doi: 10.1016/j.dnarep.2004.03.020.
- [57] K. Liu *et al.*, “The role of CDC25C in cell cycle regulation and clinical cancer therapy: a systematic review,” *Cancer Cell Int.*, vol. 20, no. 1, Jun. 2020, doi: 10.1186/S12935-020-01304-W.
- [58] J. Chen, “The Cell-Cycle Arrest and Apoptotic Functions of p53 in Tumor Initiation and Progression,” *Cold Spring Harb. Perspect. Med.*, vol. 6, no. 3, Mar. 2016, doi: 10.1101/CSHPERSPECT.A026104.
- [59] J. M. A. Turner *et al.*, “Silencing of unsynapsed meiotic chromosomes in the mouse,” *Nat. Genet.*, vol. 37, no. 1, pp. 41–47, Jan. 2005, doi: 10.1038/NG1484.
- [60] J. M. A. Turner, “Meiotic Silencing in Mammals,” *Annu. Rev. Genet.*, vol. 49, pp. 395–412, Nov. 2015, doi: 10.1146/ANNUREV-GENET-112414-055145.
- [61] A. J. Yeo, O. J. Becherel, J. E. Luff, M. E. Graham, D. Richard, and M. F. Lavin, “Senataxin controls meiotic silencing through ATR activation and chromatin remodeling,” *Cell Discov.*, vol. 1, Sep. 2015, doi: 10.1038/CELLDISC.2015.25.
- [62] K. Daniel *et al.*, “Meiotic homologue alignment and its quality surveillance are controlled by mouse *HORMAD1*,” *Nat. Cell Biol.* 2011 135, vol. 13, no. 5, pp. 599–610, Apr. 2011, doi: 10.1038/ncb2213.
- [63] C. Pereira, M. B. Smolka, R. S. Weiss, and M. A. Briño-Enríquez, “ATR signaling in mammalian meiosis: From upstream scaffolds to downstream signaling,” *Environ. Mol. Mutagen.*, vol. 61, no. 7, pp. 752–766, Aug. 2020, doi: 10.1002/EM.22401.

- [64] J. M. Cloutier, S. K. Mahadevaiah, E. Ellnati, A. Tóth, and J. Turner, “Mammalian meiotic silencing exhibits sexually dimorphic features,” *Chromosoma*, vol. 125, no. 2, pp. 215–226, Jun. 2016, doi: 10.1007/S00412-015-0568-Z.
- [65] S. M. Mir *et al.*, “Shelterin Complex at Telomeres: Implications in Ageing,” *Clin. Interv. Aging*, vol. 15, pp. 827–839, 2020, doi: 10.2147/CIA.S256425.
- [66] T. De Lange, “Shelterin-Mediated Telomere Protection,” *Annu. Rev. Genet.*, vol. 52, pp. 223–247, Nov. 2018, doi: 10.1146/ANNUREV-GENET-032918-021921.
- [67] G. Pennarun *et al.*, “ATR contributes to telomere maintenance in human cells,” *Nucleic Acids Res.*, vol. 38, no. 9, pp. 2955–2963, Feb. 2010, doi: 10.1093/NAR/GKP1248.
- [68] K. Baumann, “Nuclear envelope: ATR senses mechanical stress,” *Nat. Rev. Mol. Cell Biol.*, vol. 15, no. 9, p. 559, 2014, doi: 10.1038/NRM3864.
- [69] R. Bermejo, A. Kumar, and M. Foiani, “Preserving the genome by regulating chromatin association with the nuclear envelope,” *Trends Cell Biol.*, vol. 22, no. 9, pp. 465–473, Sep. 2012, doi: 10.1016/J.TCB.2012.05.007.
- [70] G. Rao Kidiyoor *et al.*, “ATR is essential for preservation of cell mechanics and nuclear integrity during interstitial migration,” doi: 10.1038/s41467-020-18580-9.
- [71] G. R. Kidiyoor, A. Kumar, and M. Foiani, “ATR-mediated regulation of nuclear and cellular plasticity,” *DNA Repair (Amst)*., vol. 44, pp. 143–150, Aug. 2016, doi: 10.1016/J.DNAREP.2016.05.020.
- [72] S. Biton, A. Barzilai, and Y. Shiloh, “The neurological phenotype of ataxia-telangiectasia: solving a persistent puzzle,” *DNA Repair (Amst)*., vol. 7, no. 7, pp. 1028–1038, Jul. 2008, doi: 10.1016/J.DNAREP.2008.03.006.
- [73] A. Traven and J. Heierhorst, “SQ/TQ cluster domains: concentrated ATM/ATR kinase phosphorylation site regions in DNA-damage-response proteins,” *Bioessays*, vol. 27, no. 4, pp. 397–407, Apr. 2005, doi: 10.1002/BIES.20204.
- [74] L. Cara, M. Baitemirova, F. Duong, M. Larios-Sanz, and A. Ribes-Zamora, “SCDFinder, a web-based tool for the identification of putative novel ATM and ATR targets,” *Bioinformatics*, vol. 30, no. 23, pp. 3394–3395, Dec.

- 2014, doi: 10.1093/BIOINFORMATICS/BTU551.
- [75] L. Cara, M. Baitemirova, J. Follis, M. Larios-Sanz, and A. Ribes-Zamora, "The ATM- and ATR-related SCD domain is over-represented in proteins involved in nervous system development," *Sci. Reports* 2016 61, vol. 6, no. 1, pp. 1–8, Jan. 2016, doi: 10.1038/srep19050.
- [76] D.-S. Lim *et al.*, "ATM binds to-adaptin in cytoplasmic vesicles," *Med. Sci.*, vol. 95, pp. 10146–10151, 1998, Accessed: Nov. 23, 2021. [Online]. Available: [www.pnas.org](http://www.pnas.org).
- [77] S. Lindtner *et al.*, "Genomic Resolution of DLX-Orchestrated Transcriptional Circuits Driving Development of Forebrain GABAergic Neurons," *Cell Rep.*, vol. 28, no. 8, pp. 2048-2063.e8, Aug. 2019, doi: 10.1016/J.CELREP.2019.07.022.
- [78] C. Englund *et al.*, "Pax6, Tbr2, and Tbr1 are expressed sequentially by radial glia, intermediate progenitor cells, and postmitotic neurons in developing neocortex," *J. Neurosci.*, vol. 25, no. 1, pp. 247–251, Jan. 2005, doi: 10.1523/JNEUROSCI.2899-04.2005.
- [79] M. L. Brinkmeier *et al.*, "Discovery of transcriptional regulators and signaling pathways in the developing pituitary gland by bioinformatic and genomic approaches," *Genomics*, vol. 93, no. 5, pp. 449–460, 2009, doi: 10.1016/j.ygeno.2008.11.010.
- [80] S. Y. Park, J. B. Kim, and Y.-M. Han, "REST is a key regulator in brain-specific homeobox gene expression during neuronal differentiation," *J. Neurochem.*, vol. 103, no. 6, pp. 071018045431010-???, Oct. 2007, doi: 10.1111/J.1471-4159.2007.04947.X.
- [81] H. Fujisawa, "Discovery of semaphorin receptors, neuropilin and plexin, and their functions in neural development," *J. Neurobiol.*, vol. 59, no. 1, pp. 24–33, Apr. 2004, doi: 10.1002/NEU.10337.
- [82] S. Yamagishi, Y. Bando, and K. Sato, "Involvement of Netrins and Their Receptors in Neuronal Migration in the Cerebral Cortex," *Front. cell Dev. Biol.*, vol. 8, Jan. 2021, doi: 10.3389/FCELL.2020.590009.
- [83] A. Cheng *et al.*, "ATM and ATR play complementary roles in the behavior of excitatory and inhibitory vesicle populations," *Proc. Natl. Acad. Sci. U. S. A.*, vol. 115, no. 2, pp. E292–E301, 2017, doi: 10.1073/pnas.1716892115.
- [84] D. S. Lim *et al.*, "ATM binds to beta-adaptin in cytoplasmic vesicles," *Proc.*

- Natl. Acad. Sci. U. S. A.*, vol. 95, no. 17, pp. 10146–10151, Aug. 1998, doi: 10.1073/PNAS.95.17.10146.
- [85] T. Kim, J. H. Tao-Cheng, L. E. Eiden, and Y. P. Loh, “Large dense-core secretory granule biogenesis is under the control of chromogranin A in neuroendocrine cells,” *Ann. N. Y. Acad. Sci.*, vol. 971, pp. 323–331, Jun. 2002, doi: 10.1111/J.1749-6632.2002.TB04487.X.
- [86] C. Wang *et al.*, “Different regions of synaptic vesicle membrane regulate VAMP2 conformation for the SNARE assembly,” *Nat. Commun.* 2020 111, vol. 11, no. 1, pp. 1–12, Mar. 2020, doi: 10.1038/s41467-020-15270-4.
- [87] J. Rizo, “Mechanism of neurotransmitter release coming into focus,” *Protein Sci.*, vol. 27, no. 8, pp. 1364–1391, Aug. 2018, doi: 10.1002/PRO.3445.
- [88] A. Denker *et al.*, “A small pool of vesicles maintains synaptic activity in vivo,” *Proc. Natl. Acad. Sci. U. S. A.*, vol. 108, no. 41, pp. 17177–17182, Oct. 2011, doi: 10.1073/PNAS.1112688108/-/DCSUPPLEMENTAL/PNAS.201112688SI.PDF.
- [89] M. Kirtay *et al.*, “ATR regulates neuronal activity by modulating presynaptic firing,” *Nat. Commun.*, vol. 12, no. 1, pp. 1–18, 2021, doi: 10.1038/s41467-021-24217-2.
- [90] Z. P. Pang *et al.*, “Synaptotagmin-2 is essential for survival and contributes to Ca<sup>2+</sup> triggering of neurotransmitter release in central and neuromuscular synapses,” *J. Neurosci.*, vol. 26, no. 52, pp. 13493–13504, Dec. 2006, doi: 10.1523/JNEUROSCI.3519-06.2006.
- [91] J. Xu, T. Mashimo, and T. C. Südhof, “Synaptotagmin-1, -2, and -9: Ca(2+) sensors for fast release that specify distinct presynaptic properties in subsets of neurons,” *Neuron*, vol. 54, no. 4, pp. 567–581, May 2007, doi: 10.1016/J.NEURON.2007.05.004.
- [92] S. E. Renick *et al.*, “The Mammalian Brain High-Affinity L-Proline Transporter Is Enriched Preferentially in Synaptic Vesicles in a Subpopulation of Excitatory Nerve Terminals in Rat Forebrain,” *J. Neurosci.*, vol. 19, no. 1, p. 21, Jan. 1999, doi: 10.1523/JNEUROSCI.19-01-00021.1999.
- [93] A. Monasor *et al.*, “INK4a/ARF limits the expansion of cells suffering from replication stress,” *Cell Cycle*, vol. 12, no. 12, p. 1948, Jun. 2013, doi: 10.4161/CC.25017.



- [94] M. Murga *et al.*, “Exploiting oncogene-induced replicative stress for the selective killing of Myc-driven tumors,” *Nat. Struct. Mol. Biol.*, vol. 18, no. 12, pp. 1331–1335, Dec. 2011, doi: 10.1038/NSMB.2189.
- [95] D. W. Schoppy *et al.*, “Oncogenic stress sensitizes murine cancers to hypomorphic suppression of ATR,” *J. Clin. Invest.*, vol. 122, no. 1, pp. 241–252, Jan. 2012, doi: 10.1172/JCI58928.
- [96] E. Fokas, R. Prevo, E. M. Hammond, T. B. Brunner, W. G. McKenna, and R. J. Muschel, “Targeting ATR in DNA damage response and cancer therapeutics,” *Cancer Treat. Rev.*, vol. 40, no. 1, pp. 109–117, 2014, doi: 10.1016/j.ctrv.2013.03.002.
- [97] A. Blasina, B. D. Price, G. A. Turenne, and C. H. McGowan, “Caffeine inhibits the checkpoint kinase ATM,” *Curr. Biol.*, vol. 9, no. 19, pp. 1135–1138, Oct. 1999, doi: 10.1016/S0960-9822(99)80486-2.
- [98] J. N. Sarkaria *et al.*, “Inhibition of ATM and ATR kinase activities by the radiosensitizing agent, caffeine,” *Cancer Res.*, vol. 59, no. 17, pp. 4375–4382, 1999.
- [99] H. Nishida *et al.*, “Inhibition of ATR protein kinase activity by schisandrin B in DNA damage response,” *Nucleic Acids Res.*, vol. 37, no. 17, pp. 5678–5689, Jul. 2009, doi: 10.1093/NAR/GKP593.
- [100] L. I. Toledo *et al.*, “A cell-based screen identifies ATR inhibitors with synthetic lethal properties for cancer-associated mutations,” *Nat. Struct. Mol. Biol.*, vol. 18, no. 6, pp. 721–727, Jun. 2011, doi: 10.1038/NSMB.2076.
- [101] A. Peasland *et al.*, “Identification and evaluation of a potent novel ATR inhibitor, NU6027, in breast and ovarian cancer cell lines,” *Br. J. Cancer* 2011 1053, vol. 105, no. 3, pp. 372–381, Jul. 2011, doi: 10.1038/bjc.2011.243.
- [102] A. M. Weber and A. J. Ryan, “ATM and ATR as therapeutic targets in cancer,” *Pharmacol. Ther.*, vol. 149, pp. 124–138, 2015, doi: 10.1016/j.pharmthera.2014.12.001.
- [103] J. D. Charrier *et al.*, “Discovery of Potent and Selective Inhibitors of Ataxia Telangiectasia Mutated and Rad3 Related (ATR) Protein Kinase as Potential Anticancer Agents,” *J. Med. Chem.*, vol. 54, no. 7, pp. 2320–2330, 2011, doi: 10.1021/jm101488z.

- [104] C. J. Huntoon *et al.*, “ATR inhibition broadly sensitizes ovarian cancer cells to chemotherapy independent of BRCA status,” *Cancer Res.*, vol. 73, no. 12, pp. 3683–3691, Jun. 2013, doi: 10.1158/0008-5472.CAN-13-0110.
- [105] A. B. Hall *et al.*, “Potentiation of tumor responses to DNA damaging therapy by the selective ATR inhibitor VX-970,” *Oncotarget*, vol. 5, no. 14, pp. 5674–5685, 2014, doi: 10.18632/ONCOTARGET.2158.
- [106] M. R. Middleton *et al.*, “Phase 1 study of the ATR inhibitor berzosertib (formerly M6620, VX-970) combined with gemcitabine ± cisplatin in patients with advanced solid tumours,” *British Journal of Cancer*, Aug. 17, 2021. .
- [107] L. M. and L. Z. Karnitz, “Molecular Pathways: targeting ATR in cancer therapy,” *Clin. Cancer Res.*, 2015, doi: 10.1158/1078-0432.CCR-15-0479.Molecular.
- [108] X. Jacq *et al.*, “AZ20, a novel potent and selective inhibitor of ATR kinase with in vivo antitumour activity,” *Cancer Res.*, vol. 72, no. 8 Supplement, pp. 1823–1823, Apr. 2012, doi: 10.1158/1538-7445.AM2012-1823.
- [109] K. M. Foote *et al.*, “Discovery of 4-{4-[(3R)-3-Methylmorpholin-4-yl]-6-[1-(methylsulfonyl)cyclopropyl]pyrimidin-2-yl}-1H-indole (AZ20): a potent and selective inhibitor of ATR protein kinase with monotherapy in vivo antitumor activity,” *J. Med. Chem.*, vol. 56, no. 5, pp. 2125–2138, Mar. 2013, doi: 10.1021/JM301859S.
- [110] S. M. Guichard *et al.*, “The pre-clinical in vitro and in vivo activity of AZD6738: A potent and selective inhibitor of ATR kinase.,” *Cancer Res.*, vol. 73, no. 8 Supplement, pp. 3343–3343, Apr. 2013, doi: 10.1158/1538-7445.AM2013-3343.
- [111] C. D. Jones *et al.*, “Discovery of AZD6738, a potent and selective inhibitor with the potential to test the clinical efficacy of ATR kinase inhibition in cancer patients.,” *Cancer Res.*, vol. 73, no. 8 Supplement, pp. 2348–2348, Apr. 2013, doi: 10.1158/1538-7445.AM2013-2348.
- [112] M. T. Dillon *et al.*, “PATRIOT: A phase I study to assess the tolerability, safety and biological effects of a specific ataxia telangiectasia and Rad3-related (ATR) inhibitor (AZD6738) as a single agent and in combination with palliative radiation therapy in patients with solid,” *Clin. Transl. Radiat. Oncol.*, vol. 12, pp. 16–20, 2018, doi: 10.1016/j.ctro.2018.06.001.
- [113] C. Gov, “Phase I Study to Assess Safety of AZD6738 Alone and in

Combination With Radiotherapy in Patients With Solid Tumours - ClinicalTrials.gov." <https://clinicaltrials.gov/ct2/show/NCT02223923> (accessed Nov. 23, 2021).

- [114] L. M. Karnitz and L. Zou, "Molecular pathways: Targeting ATR in cancer therapy," *Clin. Cancer Res.*, vol. 21, no. 21, pp. 4780–4785, 2015, doi: 10.1158/1078-0432.CCR-15-0479.
- [115] G. Fròsina, A. Profumo, D. Marubbi, D. Marcello, J. L. Ravetti, and A. Daga, "ATR kinase inhibitors NVP-BEZ235 and AZD6738 effectively penetrate the brain after systemic administration," *Radiat. Oncol.*, vol. 13, no. 1, pp. 1–7, 2018, doi: 10.1186/s13014-018-1020-3.
- [116] F. P. Vendetti, A. Lau, S. Schamus, T. P. Conrads, M. J. O'Connor, and C. J. Bakkenist, "The orally active and bioavailable ATR kinase inhibitor AZD6738 potentiates the anti-tumor effects of cisplatin to resolve ATM-deficient non-small cell lung cancer in vivo," *Oncotarget*, vol. 6, no. 42, pp. 44289–44305, 2015, doi: 10.18632/oncotarget.6247.
- [117] A. B. Bukhari, C. W. Lewis, J. J. Pearce, D. Luong, G. K. Chan, and A. M. Gamper, "Inhibiting Wee1 and ATR kinases produces tumor-selective synthetic lethality and suppresses metastasis," *J. Clin. Invest.*, vol. 129, no. 3, pp. 1329–1344, 2019, doi: 10.1172/JCI122622.
- [118] E. Lecona and O. Fernandez-Capetillo, "Targeting ATR in cancer," *Nat. Rev. Cancer*, vol. 18, no. 9, pp. 586–595, 2018, doi: 10.1038/s41568-018-0034-3.
- [119] Z. Qiu, N. L. Oleinick, and J. Zhang, "ATR/CHK1 inhibitors and cancer therapy," *Radiother Oncol*, 2018, doi: 10.1016/j.radonc.2017.09.043.ATR/CHK1.
- [120] R. M. Meredith, "Sensitive and critical periods during neurotypical and aberrant neurodevelopment: a framework for neurodevelopmental disorders," *Neurosci. Biobehav. Rev.*, vol. 50, pp. 180–188, Mar. 2015, doi: 10.1016/J.NEUBIOREV.2014.12.001.
- [121] F. Antonucci *et al.*, "Cracking down on inhibition: selective removal of GABAergic interneurons from hippocampal networks," *J. Neurosci.*, vol. 32, no. 6, pp. 1989–2001, Feb. 2012, doi: 10.1523/JNEUROSCI.2720-11.2012.
- [122] G. Di Cristo, "Development of cortical GABAergic circuits and its implications for neurodevelopmental disorders," *Clin. Genet.*, vol. 72, no. 1,

- pp. 1–8, 2007, doi: 10.1111/J.1399-0004.2007.00822.X.
- [123] J. K. Chilton, “Molecular mechanisms of axon guidance,” *Dev. Biol.*, vol. 292, no. 1, pp. 13–24, Apr. 2006, doi: 10.1016/J.YDBIO.2005.12.048.
- [124] J. C. Silbereis, S. Pochareddy, Y. Zhu, M. Li, and N. Sestan, “The Cellular and Molecular Landscapes of the Developing Human Central Nervous System,” *Neuron*, vol. 89, no. 2, p. 248, 2016, doi: 10.1016/J.NEURON.2015.12.008.
- [125] O. Marín, M. Valiente, X. Ge, and L. H. Tsai, “Guiding neuronal cell migrations,” *Cold Spring Harb. Perspect. Biol.*, vol. 2, no. 2, 2010, doi: 10.1101/CSHPERSPECT.A001834.
- [126] M. Valiente and O. Marín, “Neuronal migration mechanisms in development and disease,” *Curr. Opin. Neurobiol.*, vol. 20, no. 1, pp. 68–78, Feb. 2010, doi: 10.1016/J.CONB.2009.12.003.
- [127] A. Sale, N. Berardi, M. Spolidoro, L. Baroncelli, and L. Maffei, “GABAergic inhibition in visual cortical plasticity,” *Front. Cell. Neurosci.*, vol. 4, no. MAR, Mar. 2010, doi: 10.3389/FNCEL.2010.00010.
- [128] K. F. Barald, Y. chi Shen, and L. M. Bianchi, “Chemokines and cytokines on the neuroimmunoaxis: Inner ear neurotrophic cytokines in development and disease. Prospects for repair?,” *Exp. Neurol.*, vol. 301, no. Pt B, pp. 92–99, Mar. 2018, doi: 10.1016/J.EXPNEUROL.2017.10.009.
- [129] A. Cheffer, A. Tárnok, and H. Ulrich, “Cell cycle regulation during neurogenesis in the embryonic and adult brain,” *Stem cell Rev. reports*, vol. 9, no. 6, pp. 794–805, Dec. 2013, doi: 10.1007/S12015-013-9460-5.
- [130] T. K. Hensch and M. Fagiolini, “Excitatory-inhibitory balance and critical period plasticity in developing visual cortex,” *Prog. Brain Res.*, vol. 147, no. SPEC. ISS., pp. 115–124, 2005, doi: 10.1016/S0079-6123(04)47009-5.
- [131] F. Filipello *et al.*, “The Microglial Innate Immune Receptor TREM2 Is Required for Synapse Elimination and Normal Brain Connectivity,” *Immunity*, vol. 48, no. 5, pp. 979-991.e8, May 2018, doi: 10.1016/J.IMMUNI.2018.04.016.
- [132] R. C. Froemke, “Plasticity of cortical excitatory-inhibitory balance,” *Annu. Rev. Neurosci.*, vol. 38, pp. 195–219, Jul. 2015, doi: 10.1146/ANNUREV-NEURO-071714-034002.
- [133] S. B. Nelson and V. Valakh, “Excitatory/Inhibitory Balance and Circuit

- Homeostasis in Autism Spectrum Disorders,” *Neuron*, vol. 87, no. 4, pp. 684–698, Aug. 2015, doi: 10.1016/J.NEURON.2015.07.033.
- [134] R. Tuchman and I. Rapin, “Epilepsy in autism,” *Lancet. Neurol.*, vol. 1, no. 6, pp. 352–358, Jun. 2002, doi: 10.1016/S1474-4422(02)00160-6.
- [135] R. Gao and P. Penzes, “Common mechanisms of excitatory and inhibitory imbalance in schizophrenia and autism spectrum disorders,” *Curr. Mol. Med.*, vol. 15, no. 2, pp. 146–167, Mar. 2015, doi: 10.2174/1566524015666150303003028.
- [136] D. J. Thurman *et al.*, “Standards for epidemiologic studies and surveillance of epilepsy,” *Epilepsia*, vol. 52, no. SUPPL. 7, pp. 2–26, Sep. 2011, doi: 10.1111/J.1528-1167.2011.03121.X.
- [137] V. Novak, “Epilepsy Treatment introduction,” *Clin Ther.*, 2019, doi: 10.1016/S0140-6736(14)62339-4.
- [138] R. S. Fisher *et al.*, “ILAE official report: a practical clinical definition of epilepsy,” *Epilepsia*, vol. 55, no. 4, pp. 475–482, 2014, doi: 10.1111/EPI.12550.
- [139] C. Bernard, “Understanding and Predicting Epilepsy [Life Sciences],” *undefined*, vol. 33, no. 4, pp. 90–95, 2016, doi: 10.1109/MSP.2016.2554632.
- [140] Y. Liu, V. Grigorovsky, and B. Bardakjian, “Excitation and Inhibition Balance Underlying Epileptiform Activity,” *IEEE Trans. Biomed. Eng.*, vol. 67, no. 9, pp. 2473–2481, 2020, doi: 10.1109/TBME.2019.2963430.
- [141] N. Dehghani *et al.*, “Dynamic balance of excitation and inhibition in human and monkey neocortex,” *Sci. Rep.*, vol. 6, pp. 1–12, 2016, doi: 10.1038/srep23176.
- [142] J. Žiburkus, J. R. Cressman, and S. J. Schiff, “Seizures as imbalanced up states: Excitatory and inhibitory conductances during seizure-like events,” *J. Neurophysiol.*, vol. 109, no. 5, pp. 1296–1306, 2013, doi: 10.1152/jn.00232.2012.
- [143] J. M. Fritschy, “Epilepsy, E/I balance and GABAA receptor plasticity,” *Front. Mol. Neurosci.*, vol. 1, no. MAR, 2008, doi: 10.3389/neuro.02.005.2008.
- [144] L.-R. Shao, C. W. Habela, and C. E. Stafstrom, “Pediatric Epilepsy Mechanisms: Expanding the Paradigm of Excitation/Inhibition Imbalance,” *Children*, vol. 6, no. 2, p. 23, 2019, doi: 10.3390/children6020023.

- [145] J. R. Cressman, G. Ullah, J. Ziburkus, S. J. Schiff, and E. Barreto, "The influence of sodium and potassium dynamics on excitability, seizures, and the stability of persistent states: I. Single neuron dynamics," *J. Comput. Neurosci.*, vol. 26, no. 2, pp. 159–170, 2009, doi: 10.1007/S10827-008-0132-4.
- [146] G. Ullah, J. R. Cressman, E. Barreto, and S. J. Schiff, "The influence of sodium and potassium dynamics on excitability, seizures, and the stability of persistent states: II. Network and glial dynamics," *J. Comput. Neurosci.*, vol. 26, no. 2, p. 171, 2009, doi: 10.1007/S10827-008-0130-6.
- [147] N. Driessens *et al.*, "Hydrogen peroxide induces DNA single- and double-strand breaks in thyroid cells and is therefore a potential mutagen for this organ," *Endocr. Relat. Cancer*, vol. 16, no. 3, pp. 845–856, Sep. 2009, doi: 10.1677/ERC-09-0020.
- [148] J. Willis, Y. Patel, B. L. Lentz, and S. Yan, "APE2 is required for ATR-Chk1 checkpoint activation in response to oxidative stress," *Proc. Natl. Acad. Sci. U. S. A.*, vol. 110, no. 26, pp. 10592–10597, 2013, doi: 10.1073/pnas.1301445110.
- [149] L. Pizzamiglio *et al.*, "New Role of ATM in Controlling GABAergic Tone during Development," *Cereb. Cortex*, vol. 26, no. 10, pp. 3879–3888, 2016, doi: 10.1093/cercor/bhw125.
- [150] N. C. Spitzer, "Neurotransmitter Switching? No Surprise," *Neuron*, vol. 86, no. 5, pp. 1131–1144, Jun. 2015, doi: 10.1016/J.NEURON.2015.05.028.
- [151] C. Rivera *et al.*, "The K<sup>+</sup>/Cl<sup>-</sup> co-transporter KCC2 renders GABA hyperpolarizing during neuronal maturation," *Nat.* 1999 3976716, vol. 397, no. 6716, pp. 251–255, Jan. 1999, doi: 10.1038/16697.
- [152] M. Leonzino, M. Busnelli, F. Antonucci, C. Verderio, M. Mazzanti, and B. Chini, "The Timing of the Excitatory-to-Inhibitory GABA Switch Is Regulated by the Oxytocin Receptor via KCC2," *Cell Rep.*, vol. 15, no. 1, pp. 96–103, Apr. 2016, doi: 10.1016/J.CELREP.2016.03.013.
- [153] X. Tang *et al.*, "KCC2 rescues functional deficits in human neurons derived from patients with Rett syndrome," *Proc. Natl. Acad. Sci. U. S. A.*, vol. 113, no. 3, pp. 751–756, Jan. 2016, doi: 10.1073/PNAS.1524013113/-/DCSUPPLEMENTAL.
- [154] L. Pizzamiglio *et al.*, "The DNA repair protein ATM as a target in autism

- spectrum disorder,” *JCI insight*, vol. 6, no. 3, Feb. 2021, doi: 10.1172/JCI.INSIGHT.133654.
- [155] N. Ropert, R. Miles, and H. Korn, “Characteristics of miniature inhibitory postsynaptic currents in CA1 pyramidal neurones of rat hippocampus.,” *J. Physiol.*, vol. 428, no. 1, p. 707, Sep. 1990, doi: 10.1113/JPHYSIOL.1990.SP018236.
- [156] J. M. Bekkers and C. F. Stevens, “Quantal analysis of EPSCs recorded from small numbers of synapses in hippocampal cultures,” *J. Neurophysiol.*, vol. 73, no. 3, pp. 1145–1156, 1995, doi: 10.1152/JN.1995.73.3.1145.
- [157] M. Zeitler, P. Fries, and S. Gielen, “Assessing neuronal coherence with single-unit, multi-unit, and local field potentials,” *Neural Comput.*, vol. 18, no. 9, pp. 2256–2281, 2006, doi: 10.1162/neco.2006.18.9.2256.
- [158] G. Fossati *et al.*, “Reduced SNAP-25 increases PSD-95 mobility and impairs spine morphogenesis,” *Cell Death Differ.* 2015 229, vol. 22, no. 9, pp. 1425–1436, Feb. 2015, doi: 10.1038/cdd.2014.227.
- [159] I. Ehrlich and R. Malinow, “Postsynaptic density 95 controls AMPA receptor incorporation during long-term potentiation and experience-driven synaptic plasticity,” *J. Neurosci.*, vol. 24, no. 4, pp. 916–927, Jan. 2004, doi: 10.1523/JNEUROSCI.4733-03.2004.
- [160] F. Erdő, L. A. Bors, D. Farkas, Á. Bajza, and S. Gizurarson, “Evaluation of intranasal delivery route of drug administration for brain targeting,” *Brain Res. Bull.*, vol. 143, pp. 155–170, Oct. 2018, doi: 10.1016/J.BRAINRESBULL.2018.10.009.
- [161] M. C. Veronesi, M. Alhamami, S. B. Miedema, Y. Yun, M. Ruiz-Cardozo, and M. W. Vannier, “Imaging of intranasal drug delivery to the brain,” *Am. J. Nucl. Med. Mol. Imaging*, vol. 10, no. 1, p. 1, 2020, Accessed: Dec. 17, 2021. [Online]. Available: /pmc/articles/PMC7076302/.
- [162] A. B. Chatt and J. S. Ebersole, “The convulsant effects of kainic acid microinjections into cerebral cortex are concentration but not laminar dependent,” *Exp. Neurol.*, vol. 103, no. 1, pp. 105–109, 1989, doi: 10.1016/0014-4886(89)90192-1.
- [163] Y. Kinoshita, H. Jürgen Wenzel, C. Kinoshita, P. A. Schwartzkroin, and R. S. Morrison, “Acute, but reversible, kainic acid-induced DNA damage in

- hippocampal CA1 pyramidal cells of p53-deficient mice,” *Epilepsia*, vol. 53 Suppl 1, no. SUPPL. 1, pp. 125–133, Jun. 2012, doi: 10.1111/J.1528-1167.2012.03483.X.
- [164] N. Mataga, S. Fujishima, B. G. Condie, and T. K. Hensch, “Experience-Dependent Plasticity of Mouse Visual Cortex in the Absence of the Neuronal Activity-Dependent Marker *egr1/zif268*,” 2001.
- [165] F. Duclot and M. Kabbaj, “The role of early growth response 1 (EGR1) in brain plasticity and neuropsychiatric disorders,” *Front. Behav. Neurosci.*, vol. 11, Mar. 2017, doi: 10.3389/FNBEH.2017.00035.
- [166] K. M. J. Van Loo *et al.*, “Calcium Channel Subunit  $\alpha 2\delta 4$  Is Regulated by Early Growth Response 1 and Facilitates Epileptogenesis,” *J. Neurosci.*, vol. 39, no. 17, pp. 3175–3187, Apr. 2019, doi: 10.1523/JNEUROSCI.1731-18.2019.
- [167] J. Fu, O. Guo, Z. Zhen, and J. Zhen, “Essential Functions of the Transcription Factor *Npas4* in Neural Circuit Development, Plasticity, and Diseases,” *Front. Neurosci.*, vol. 14, p. 1262, Dec. 2020, doi: 10.3389/FNINS.2020.603373/BIBTEX.
- [168] L. Chung, “A Brief Introduction to the Transduction of Neural Activity into Fos Signal,” *Dev. Reprod.*, vol. 19, no. 2, p. 61, Jun. 2015, doi: 10.12717/DR.2015.19.2.061.
- [169] H. B. Machado, L. J. Vician, and H. R. Herschman, “The MAPK Pathway Is Required for Depolarization-induced ‘Promiscuous’ Immediate-Early Gene Expression but Not for Depolarization-Restricted Immediate-Early Gene Expression in Neurons,” *J. Neurosci. Res.*, 2008.
- [170] F. Kienzler-Norwood *et al.*, “A novel animal model of acquired human temporal lobe epilepsy based on the simultaneous administration of kainic acid and lorazepam,” *Epilepsia*, vol. 58, no. 2, pp. 222–230, Feb. 2017, doi: 10.1111/EPI.13579.
- [171] D. Bertoglio *et al.*, “Kainic acid-induced post-status epilepticus models of temporal lobe epilepsy with diverging seizure phenotype and neuropathology,” *Front. Neurol.*, vol. 8, no. NOV, p. 588, Nov. 2017, doi: 10.3389/FNEUR.2017.00588/FULL.
- [172] R. J. Racine, “Modification of seizure activity by electrical stimulation: II. Motor seizure,” *Electroencephalogr. Clin. Neurophysiol.*, vol. 32, no. 3, pp.



- 281–294, Mar. 1972, doi: 10.1016/0013-4694(72)90177-0.
- [173] J. Van Erum, D. Van Dam, and P. P. De Deyn, “PTZ-induced seizures in mice require a revised Racine scale,” *Epilepsy Behav.*, vol. 95, pp. 51–55, Jun. 2019, doi: 10.1016/J.YEBEH.2019.02.029.
- [174] H. W. Mahncke, A. Bronstone, and M. M. Merzenich, “Brain plasticity and functional losses in the aged: scientific bases for a novel intervention,” *Prog. Brain Res.*, vol. 157, pp. 81–109, 2006, doi: 10.1016/S0079-6123(06)57006-2.
- [175] Openinnovation AstraZeneca, “AZD6738.”  
<https://openinnovation.astrazeneca.com/preclinical-research/preclinical-molecules/azd6738.html> (accessed Dec. 07, 2021).
- [176] I. Gasterstädt, A. Jack, T. Stahlhut, L. M. Rennau, S. Gonda, and P. Wahle, “Genetically Encoded Calcium Indicators Can Impair Dendrite Growth of Cortical Neurons,” *Front. Cell. Neurosci.*, vol. 14, p. 307, Oct. 2020, doi: 10.3389/FNCEL.2020.570596/BIBTEX.
- [177] Hai-yun He and Hollis T Cline, “What is Excitation/Inhibition and How Is It Regulated? A case of the elephant and the wiseman,” *J. Exp. Neurosci.*, vol. 13, 2019, doi: 10.1038/nn.4243.
- [178] E. Rusina, C. Bernard, and A. Williamson, “The Kainic Acid Models of Temporal Lobe Epilepsy,” *eNeuro*, vol. 8, no. 2, Mar. 2021, doi: 10.1523/ENEURO.0337-20.2021.
- [179] M. W. Jones *et al.*, “A requirement for the immediate early gene Zif268 in the expression of late LTP and long-term memories,” *Nat. Neurosci.*, vol. 4, no. 3, pp. 289–296, 2001, doi: 10.1038/85138.
- [180] J. Mo, C. H. Kim, D. Lee, W. Sun, H. W. Lee, and H. Kim, “Early growth response 1 (Egr-1) directly regulates GABAA receptor  $\alpha 2$ ,  $\alpha 4$ , and  $\theta$  subunits in the hippocampus,” *J. Neurochem.*, vol. 133, no. 4, pp. 489–500, 2015, doi: 10.1111/jnc.13077.
- [181] Janusz Szyndler, Piotr Maciejak, Aleksandra Witsowska-Stanek, Matgorzata Lehner, and Adam Ptañnik, “Changes in the Egr1 and Arc expression in brain structures of pentylenetetrazole-kindled rats,” *Pharmacol. Reports*, 2013.
- [182] S. N. Rakhade, A. K. Shah, R. Agarwal, B. Yao, E. Asano, and J. A. Loeb, “Activity-dependent Gene Expression Correlates with Interictal Spiking in

- Human Neocortical Epilepsy,” *Epilepsia*, vol. 48, no. SUPPL. 5, pp. 86–95, Sep. 2007, doi: 10.1111/J.1528-1167.2007.01294.X.
- [183] C. Cholewa-Waclaw, ; Justyna, and A. Bird, “The Role of Epigenetic Mechanisms in the Regulation of Gene Expression in the Nervous System,” *J. Neurosci.*, vol. 36, no. 45, pp. 11427–11434, 2016, doi: 10.1523/JNEUROSCI.2492-16.2016.
- [184] E. Suberbielle *et al.*, “Physiologic brain activity causes DNA double-strand breaks in neurons, with exacerbation by amyloid- $\beta$ ,” *Nat. Neurosci.*, vol. 16, no. 5, pp. 613–621, May 2013, doi: 10.1038/NN.3356.
- [185] R. Madabhushi *et al.*, “Activity-Induced DNA Breaks Govern the Expression of Neuronal Early-Response Genes,” *Cell*, vol. 161, no. 7, pp. 1592–1605, Jun. 2015, doi: 10.1016/J.CELL.2015.05.032.
- [186] F. Gómez-Herreros *et al.*, “TDP2 protects transcription from abortive topoisomerase activity and is required for normal neural function,” *Nat. Genet.*, vol. 46, no. 5, pp. 516–521, 2014, doi: 10.1038/NG.2929.
- [187] K. M. J. Van Loo *et al.*, “Transcriptional Regulation of T-type Calcium Channel CaV3.2: BI-DIRECTIONALITY BY EARLY GROWTH RESPONSE 1 (Egr1) AND REPRESSOR ELEMENT 1 (RE-1) PROTEIN -SILENCING TRANSCRIPTION FACTOR (REST)\*,” *J. Biol. Chem.*, vol. 287, no. 19, p. 15489, May 2012, doi: 10.1074/JBC.M111.310763.
- [188] C. Bonansco and M. Fuenzalida, “Plasticity of hippocampal excitatory-inhibitory balance: Missing the synaptic control in the epileptic brain,” *Neural Plast.*, vol. 2016, 2016, doi: 10.1155/2016/8607038.
- [189] D. L. Hunt, P. E. Castillo, and D. P. Purpura, “Synaptic plasticity of NMDA receptors: mechanisms and functional implications,” 2012, doi: 10.1016/j.conb.2012.01.007.
- [190] T. Sumi and K. Harada, “Mechanism underlying hippocampal long-term potentiation and depression based on competition between endocytosis and exocytosis of AMPA receptors,” *Sci. Reports 2020 101*, vol. 10, no. 1, pp. 1–14, Sep. 2020, doi: 10.1038/s41598-020-71528-3.
- [191] J. K. Forsyth and D. A. Lewis, “Mapping the Consequences of Impaired Synaptic Plasticity in Schizophrenia through Development: An Integrative Model for Diverse Clinical Features,” *Trends Cogn. Sci.*, vol. 21, no. 10, p. 760, Oct. 2017, doi: 10.1016/J.TICS.2017.06.006.

- [192] G. Martella, P. Bonsi, S. W. Johnson, and A. Quartarone, "Synaptic plasticity changes: Hallmark for neurological and psychiatric disorders," *Neural Plast.*, vol. 2018, 2018, doi: 10.1155/2018/9230704.
- [193] A. Orock, S. Logan, F. Deak, and R. Anderson, "Age-Related Cognitive Impairment: Role of Reduced Synaptobrevin-2 Levels in Deficits of Memory and Synaptic Plasticity," *J. Gerontol. A. Biol. Sci. Med. Sci.*, vol. 75, no. 9, pp. 1624–1632, Jun. 2020, doi: 10.1093/GERONA/GLZ013.
- [194] E. A. Nam, R. Zhao, G. G. Glick, C. E. Bansbach, D. B. Friedman, and D. Cortez, "Thr-1989 Phosphorylation Is a Marker of Active Ataxia Telangiectasia-mutated and Rad3-related (ATR) Kinase," *J. Biol. Chem.*, vol. 286, no. 33, p. 28707, Aug. 2011, doi: 10.1074/JBC.M1111.248914.
- [195] E. Nakamura and K. Miyao, "Sex Differences in Human Biological Aging," *Journals Gerontol. Ser. A*, vol. 63, no. 9, pp. 936–944, Sep. 2008, doi: 10.1093/GERONA/63.9.936.
- [196] J. D. J. Han, X. Xia, W. Chen, and J. McDermott, "Molecular and phenotypic biomarkers of aging," *F1000Research 2017 6860*, vol. 6, p. 860, Jun. 2017, doi: 10.12688/f1000research.10692.1.

## **LIST OF FIGURES**

- **Figure 1: introduction, chapter 1 – pag. 13;** “a) ATR, ATM and DNA-PKcs are large proteins belonging to the PI3K superfamily. They are characterized by the presence of similar domains: FAT, the catalytic domain and FATC, all located near the carboxyl termini. Here are also shown the ATR regions recognized by the proteins ATRIP and TOPBP1, fundamental during modulation of ATR activation. Image from Marechal and Zou, 2013. b) Three-dimensional structure of ATR; the kinase domain is green colored and circled. Image from Williams et al., 2020.”
- **Figure 2: introduction, chapter 1 – pag. 16;** “Representative pictures of  $Atr^{S/S}$  and  $Atr^{+/+}$  mice at three months of age. The SS mouse model well recapitulate all the classic features characteristic of the human syndrome: severe dwarfism and disproportionate decrease in the dimension of the head are evident in  $Atr^{S/S}$  mouse in contrast to control mouse. Image from Murga et al., 2009.”
- **Figure 3: introduction, chapter 2 – pag. 19;** “Model of replication checkpoint activation and function. In case of DNA lesion, the polymerase and the helicase on the opposing DNA strand will continue to unwind and synthesize new DNA, leading to ssDNA accumulation. The ssDNA recruits the ATR-ATRIP complex and immediately after several other replication checkpoint proteins for the activation of ATR and CHK1 (the ATR effector protein), promoting genomic stability by blocking the cell cycle progression and new origin firing, stabilizing and facilitating the replication fork restart. Image from Paulsen and Cimprich, 2007.”
- **Figure 4: introduction, chapter 2 – pag. 22;** “a) ATR responds to RPA-bound ssDNA and regulates the cell cycle progression. Image from Gautier et al., 2004. b) The signaling pathway involving ATR, ATM and DNA-PK following DNA damage. Once activated, these kinases phosphorylates several downstream effectors leading to cell cycle arrest and in some cases also apoptosis. Image from Yang et al., 2003.”
- **Figure 5: introduction, chapter 3 – pag. 27;** “ATR is present at the neuronal synapse, in association to synaptic vesicles. In particular, ATR is found colocalizing with vGAT<sup>+</sup> inhibitory vesicles. Image modified from Cheng et al., 2017.”
- **Figure 6: introduction, chapter 4 - pag. 31;** “a) List of ATR inhibitors: for each compound are shown the chemical formula and the list of targets selectively inhibited. Image modified from Weber and Ryan, 2014. b) List of

ATR inhibitors currently in clinical trials: for each drug are reported the cancer type in which the molecule is tested, the agents the molecule is tested with and the year and the phase of the trial. Image from Lecona et al., 2018.”

- **Figure 7: results – pag. 50;** “a) Schematic representation of the experimental procedure and Western Blotting analysis of AZD6738 duration of action in 7 DIV rat hippocampal neurons treated with H<sub>2</sub>O<sub>2</sub> 2 mM or H<sub>2</sub>O<sub>2</sub> 2 mM plus AZD6738 1 μM. The graph shows that the ATR inhibitor is already active since 2 hours from its application and its effect persists for at least 48 hours. b) Representative image of Western Blotting experiments carried out on 7 DIV hippocampal neurons.”
- **Figure 8: results – pag. 51;** “a) Evaluation of resting calcium level in 7 DIV hippocampal neurons upon AZD treatment. b) Evaluation of resting calcium level in 14 DIV hippocampal neurons upon AZD6738 acute treatment. c) Above, representative images of neuronal branches labelled with MAP2 (red) of control and chronically AZD-treated neurons; below, representative images of TUNEL (green) staining to detect cell death in control and chronically AZD-treated neurons. d) Percentage of TUNEL positive cells upon chronic AZD administration in mature neurons.”
- **Figure 9: results – pag. 54;** “a) Scheme of the experimental time line of AZD treatment and related calcium imaging experiments. b) Percentage of 7 DIV hippocampal neurons, treated or not with AZD, responding to GABA application with depolarization. c) Evaluation of KCl response in hippocampal neurons upon AZD or vehicle treatment. d) and e) Representative traces of Ca<sup>2+</sup> transients recorded from control neurons (d) and AZD-treated neurons (e); the first peak indicate the GABA response, whereas the second show the KCl-mediated depolarization.”
- **Figure 10: results – pag. 55;** “a) Representative images of ATM, KCC2, MeCP2 expression in 7 DIV hippocampal neurons treated or not with AZD. b) Quantitative analysis of KCC2 expression. c) Quantitative analysis of MeCP2 expression. d) Quantitative analysis of ATM expression.”
- **Figure 11: results – pag. 57;** “a) Scheme of the experimental timeline of AZD treatment and related electrophysiological experiments. b) Quantification of E/I ratio in 14 DIV hippocampal neurons upon AZD6738 acute treatment. c) Electrophysiological analysis of mEPSCs frequency and amplitude in 14 DIV hippocampal neurons, treated or not with AZD6738. d)

Representative electrophysiological traces of excitatory miniature post-synaptic currents measured in 14 DIV neurons. e) Electrophysiological analysis of mIPSCs frequency and amplitude in 14 DIV hippocampal neurons, treated or not with AZD6738. f) Representative electrophysiological traces of excitatory miniature post-synaptic currents measured in 14 DIV neurons.”

- **Figure 12: results – pag. 59;** “a) Quantitative analysis of vGlut1 puncta density in 14 DIV hippocampal neurons upon AZD6738 acute treatment. b) Representative immunofluorescence images of neuronal branches labelled with the specific excitatory presynaptic marker vGlut1 (green) and BIII-tubulin (blue) to highlight neuronal processes. c-d) Quantitative analysis of average size (c) and mean intensity (d) of vGlut1 positive puncta in AZD-treated neurons with respect to controls. e-f) Quantitative analysis of average size (e) and mean intensity (f) of PSD95 positive puncta in AZD-treated neurons with respect to controls.”
- **Figure 13: results – pag. 60;** “a) Quantitative analysis of vGAT puncta density in 14 DIV hippocampal neurons upon AZD6738 acute treatment. b) Representative immunofluorescence images of neuronal branches labelled with the specific inhibitory presynaptic marker vGAT (green) and BIII-tubulin (blue) to highlight neuronal processes. c-d) Quantitative analysis of average size (c) and mean intensity (d) of vGAT positive puncta in AZD-treated neurons with respect to controls. e-f) Quantitative analysis of average size (e) and mean intensity (f) of gephyrin positive puncta in AZD-treated neurons with respect to controls.”
- **Figure 14: results – pag. 62;** “a) Scheme of the experimental time line of AZD treatment and related electrophysiological experiments. b) Quantification of E/I ratio in 21 DIV hippocampal neurons upon AZD6738 chronic treatment. c) Electrophysiological analysis of mEPSCs frequency and amplitude in 21 DIV hippocampal neurons, treated or not with AZD6738. d) Representative electrophysiological traces of excitatory miniature post-synaptic currents measured in 21 DIV neurons. e) Electrophysiological analysis of mIPSCs frequency and amplitude in 21 DIV hippocampal neurons, treated or not with AZD6738. f) Representative electrophysiological traces of excitatory miniature post-synaptic currents measured in 21 DIV neurons.

- **Figure 15: results – pag. 63;** “a) Quantitative analysis of vGlut1+PSD95 colocalizing puncta (complete excitatory synapse) density in 21 DIV hippocampal neurons upon AZD6738 chronic treatment. b) Quantitative analysis of vGAT+gephyrin colocalizing puncta (complete inhibitory synapse) density in 21 DIV hippocampal neurons upon AZD6738 chronic treatment.”
- **Figure 16: results – pag. 64;** “a) Quantitative analysis of vGlut1 puncta density in 21 DIV hippocampal neurons upon AZD6738 chronic treatment. b) Quantitative analysis of average size and mean intensity of vGlut1 positive puncta in AZD-treated neurons with respect to controls. c) Quantitative analysis of PSD95 puncta density in 21 DIV hippocampal neurons upon AZD6738 chronic treatment. d) Quantitative analysis of average size and mean intensity of PSD95 positive puncta in AZD-treated neurons with respect to controls. e) Representative immunofluorescence images of neuronal branches labelled with the specific excitatory marker vGlut1 (green - presynaptic), PSD95 (red – postsynaptic) and BIII-tubulin (blue) to highlight neuronal processes.
- **Figure 17: results – pag. 65;** “a) Quantitative analysis of vGAT puncta density in 21 DIV hippocampal neurons upon AZD6738 chronic treatment. b) Quantitative analysis of average size and mean intensity of vGAT positive puncta in AZD-treated neurons with respect to controls. c) Quantitative analysis of gephyrin puncta density in 21 DIV hippocampal neurons upon AZD6738 chronic treatment. d) Quantitative analysis of average size and mean intensity of gephyrin positive puncta in AZD-treated neurons with respect to controls. e) Representative immunofluorescence images of neuronal branches labelled with the specific excitatory marker vGAT (green - presynaptic), gephyrin (red – postsynaptic) and BIII-tubulin (blue) to highlight neuronal processes.”
- **Figure 18: results – pag. 66;** “a) Quantification of Multi Unit activity upon AZD6738 chronic treatment. b) Representative electrophysiological traces of spiking events recorded in control and AZD-treated hippocampal neurons.
- **Figure 19: results – pag. 68;** “a) Normalized analysis of excitatory events amplitude before and after LTP promotion in control and AZD-treated neurons. b) Graphical representation of amplitude variation during the experimental procedures. c) Representative electrophysiological traces of



excitatory events recorded in control and AZD-treated hippocampal neurons, before and after LTP chemical induction.”

- **Figure 20: results – pag. 69;** “a) Normalized analysis of excitatory events amplitude before and after LTD promotion in control and AZD-treated neurons. b) Graphical representation of amplitude variation during the experimental procedures. c) Representative electrophysiological traces of excitatory events recorded in control and AZD-treated hippocampal neurons, before and after LTP chemical induction.”
- **Figure 21: results – pag. 70;** “a) Quantitative analysis of PSD95 puncta density in control hippocampal neurons upon chemical induction of LTP and LTD. b) Quantitative analysis of PSD95 puncta density in AZD-treated hippocampal neurons upon chemical induction of LTP and LTD. c) Representative immunofluorescence images of CTRL neuronal branches labelled with PSD95 (green) and B<sub>III</sub>-tubulin (red). d) Representative immunofluorescence images of AZD neuronal branches labelled with PSD95 (green) and B<sub>III</sub>-tubulin (red).”
- **Figure 22: results – pag. 71;** “a) Western Blotting analysis of AZD6738 duration of action in hippocampal tissues collected from P90 wild type mice treated with kainic acid (25 mg/kg) or kainic acid (25 mg/kg) plus AZD6738 20 mg/kg. The graph shows that the ATR inhibitor action persists for at about 48 hours. b) Representative image of Western Blotting experiments carried out on P90 hippocampal tissues.”
- **Figure 23: results – pag. 73;** “RNA profiling performed in hippocampi of DMSO- and AZD-treated mice revealed that the ATR blocker acts as a master downregulator. Vulcano Plot representing the deregulated genes: 778 downregulated and 174 upregulated.”
- **Figure 24: results – pag. 74;** “Bioinformatic analysis performed in both “Cellular Component” (a) and “Molecular Function” (b) repositories from GEO revealed that AZD treatment is responsible for a significant downregulation of terms belonging to the synaptic transmission, such as glutamatergic synapses, modulation of synaptic transmission, postsynaptic specialization and regulation of synaptic plasticity.”
- **Figure 25: results – pag. 75;** “Bioinformatic analysis investigated several transcriptional factors (TF) repositories. Here are reported the five most significant deregulated factors for each repository of origin. The most

deregulated TF belong to the category “Genome Browser PWMs” and among them it is highlighted Egr1.”

- **Figure 26: results – pag. 77;** “a) Scheme of the experimental time line of AZD treatment and related Real Time PCR experiments. b) Legend depicting all the experimental condition. c) Quantification of Egr1, Fos, Egr4 and Npas4 basal mRNA levels by Real Time PCR experiments in hippocampal cultured neurons treated chronically with AZD6738. d) Quantification of Egr1, Fos, Egr4 and Npas4 mRNA levels upon KCl 50mM application by Real Time PCR experiments in hippocampal cultured neurons treated chronically with AZD6738.”
- **Figure 27: results – pag. 79;** “a) Scheme of the experimental time line of in vivo AZD treatment and KA-induced seizures monitoring. b) Quantification of time latency to the first seizure event in control and AZD-pretreated animals. c) Graphical representation of seizure severity during the behavioral monitoring. d) Quantification of the maximum seizure score for each animal, pretreated or not with AZD6738. e) Quantification of the mean seizure score for each animal, pretreated or not with AZD6738. f) Percentage of time spent in active epileptic activity of each animal, pretreated or not with AZD6738.”
- **Figure 28: results – pag. 80;** “a) Quantitative analysis of Egr1 protein expression in hippocampal tissues collected from P90 wild type mice upon seizure induction. b) Representative image of Western Blotting experiments carried out on P90 hippocampal tissues.”
- **Figure 29: results – pag. 82;** “a) Quantitative analysis of CACNA1H protein expression in hippocampal tissues collected from P90 wild type mice upon seizure induction. b) Quantitative analysis of CACNA2D4 protein expression in hippocampal tissues collected from P90 wild type mice upon seizure induction. c-d) Representative images of Western Blotting experiments carried out on P90 hippocampal tissues.”
- **Figure 30: results – pag. 83;** “a) Quantification of calcium channels CACNA1H, CACNA2D4 and CACNA1G basal mRNA levels by Real Time PCR experiments in hippocampal cultured neurons treated chronically with AZD6738. b) Quantification of CACNA1H, CACNA2D4 and CACNA1G mRNA levels upon KCl 50mM application by Real Time PCR experiments in hippocampal cultured neurons treated chronically with AZD6738.”

- **Figure 31: results – pag. 85;** “a) Representative image of Western Blotting experiments carried out on hippocampal tissues collected from young, adult and aged wild type male and female mice. b) Representative image of Western Blotting experiments carried out on hippocampal tissues collected from young, adult and aged male mice. c) Quantitative analysis of ATR protein expression. d) Quantitative analysis of pATR/ATR ratio. e-f) Quantitative analysis of pATR/ATR ratio in male (e) or female (f) mice.”
- **Figure 32: results – pag. 86;** “a) Representative image of Western Blotting experiments carried out on hippocampal human tissues collected from young, adult and aged individuals. b) Quantitative analysis of ATR protein expression. c) Quantitative analysis of ATR expression in male individuals.”

## **DISSEMINATION OF RESULTS**

The project described in this thesis has already been disseminated during my PhD training, both as oral communication and as poster presentation, at several workshops and congresses. In addition, a paper regarding this subject is in preparation and we are planning to submit it in the course of the next year. Importantly, the novel pharmacological application of the ATR inhibitor here presented has been patented during the last summer.

Lay summary:

The ATR protein is mostly known for its essential nuclear role played as DNA damage repairer, but more recently it has been found that it plays different functions also into the neuronal cytoplasm. Mutations of ATR are indeed responsible for the onset of the neurodevelopmental disorder called Seckel Syndrome. In this project, we decided to investigate the effect of a pharmacological ATR inhibition on the neuronal transmission. The results here presented demonstrate that ATR does not take part in the development of the GABAergic inhibitory system, whereas it is essential for the maintenance of a correct synaptic transmission in mature neurons. Absence of the protein activity is responsible for the establishment of a strong imbalance between the excitatory and the inhibitory activity, strengthening the inhibitory one. Coherently, we tested the effect of the ATR inhibitor in vivo and we found that it displays a good anticonvulsant effect, suggesting its usage as an innovative therapeutic tool in neurological disorders characterized by increased excitability, such as epilepsy.

La proteina ATR è principalmente nota per il suo ruolo nucleare di riparatrice del danno al DNA, ma più di recente è stato dimostrato come sia coinvolta anche in altri processi cellulari ed in particolare a livello del citoplasma neurale. Infatti, mutazioni di ATR sono responsabili dell'insorgenza della Sindrome di Seckel, un disordine del neurosviluppo. In questo progetto abbiamo deciso di investigare l'effetto generato dall'inibizione farmacologica di ATR sulla trasmissione nervosa. I risultati qui presentati dimostrano come ATR non sia coinvolta nello sviluppo del sistema inibitorio GABAergico e che invece svolga un ruolo essenziale per il mantenimento della corretta trasmissione sinaptica nei neuroni maturi. L'assenza dell'attività della proteina è responsabile di un forte sbilanciamento tra attività eccitatoria ed inibitoria, favorendo un più sviluppato tono inibitorio. Coerentemente,

abbiamo testato l'effetto dell'inibitore di ATR in vivo, mettendo in evidenza il suo caratteristico effetto anticonvulsivante e suggerendo quindi il suo utilizzo come strumento terapeutico innovativo in disordini neurologici caratterizzati da un'aumentata eccitabilità, come ad esempio l'epilessia.